Aalto University
School of Engineering

Prabilson Khadka

Joining Polymer to Aluminium by Through Hole Extruded Friction Stir Spot Welding

School of Engineering

Dissertation for the Degree of Master of Science in Mechanical Engineering

Espoo

November 2017

Supervisor and Advisor: Professor Pedro Vilaça

Aalto University
School of Engineering

Abstract

Author Prabilson Khadka

Title of thesis Joining Polymer to Aluminium by Through Hole Extruded Friction Stir Spot Welding

Degree programme Master of Science Mechanical Engineering

Major/minor Mechanical Engineering **Code** IA3027

Thesis supervisor Professor Pedro Vilaça

Thesis advisor(s) Professor Pedro Vilaça

Date 27.11.2017 **Number of pages** 102+11 **Language** English

Abstract

The demand of joining dissimilar materials is increasing in several industries with growing need for light-weight design solutions. The increasing environmental concerns, cost reduction and low fuel consumption requirement in transport industries are pushing the need for optimized structural components integrating multiple materials, where polymer-based components and aluminium alloys play an important role. With the limitations that exist, with the currently available joining processes, to join polymers and composite to metals, the work presented here aims at introducing the development and evaluation of a new efficient solution for joining these materials.

Two new dissimilar material joining process, Through Hole Extruded – Friction Spot Welding (THE-FSpW) and Through Hole Extruded – Friction Stir Spot Welding (THE-FSSpW), are implemented and tested in joining polymer to aluminium alloy. These two processes share the same concept. The concept is the utilization of a rigid thin extrusion die plate positioned in the middle an overlapped joint formed by aluminium alloy plate over the polymer. This extrusion die plate has at least one through-hole (or slot). The metallic component will be pushed through the hole in THE-FSpW (or slot, in THE-FSSpW) into the polymer component, by a non-consumable, rigid rotating tool. The stirred visco plasticized aluminium that is forced to pass through the hole in the extrusion die plate will flow into the polymer forming a hook. Mechanical locking and adhesive bonding mechanism are achieved in between these dissimilar materials forming the joint. This new solution has distinct benefits in comparison with the existent alternatives and arrives in a moment when the perceived need, and market, for these metal-to-polymer joints is growing. The tested metals are AA5754-H111 and AA2024-T351 with 6 mm thick. The polymers are plates with a thickness of 10 mm, made of PEEK and Polyamide 6. The rigid thin extrusion die plate is AISI316 with 1 mm thick.

The implementation of these two solid-state joining process involved: tool design, development of experimental setup and process parameters. Tool design and development of experimental setup have a critical role in the application of any solid-state joining process. The influence of process parameters on joint hook geometry is studied, and a set of optimal parameters is established for the tested base materials. To analyze the joint, mechanical, microstructural and geometrical tests are conducted. For both processes, the joint formation was repeatable and controllable. From the analysis of both joining processes the THE-FSSpW process shown better joint hook geometry with an average thickness of 1.9 mm, delivering a tensile shear load bearing capacity of 7.3 kN. The hook from THE-FSpW process presented an average thickness of 1.4 mm, and the joint reached a tensile shear load bearing capacity of 2.3 kN.

Keywords Dissimilar Materials, Light-Weight Structure, Aluminium Alloy, polymer, Friction Stir Welding, Through Hole Extruded – Friction Spot Welding (THE-FSpW), Through Hole Extruded – Friction Stir Spot Welding (THE-FSSpW), Joint Hook

Acknowledgments

Thank you:

To Aalto university for granting me the study right and introducing me to such a beautiful world of engineering.

To my supervisor professor, Pedro Vilaça for introducing and allowing me to work on such a noble project and guiding me through ought the time. His immense support always encouraged me to try things beyond the ordinary which made it possible to reach a point where this project is now. His passion towards the development of new technologies is tremendous and inspiring.

To Xu Xiaoyan, Lecturer, Tongji University, for her guidance during the project. Her support is precious to this project.

To colleagues at workplace especially, Arju, Goncalo, and Hekki, for their precious help during various phases of the project.

To the staff at the workplace specially Samuli, Kim, Seppo and Teemu for their assistance during the development and testing phases of the project.

To my family for their patience, love and continuous support and keeping me positive throughout. To my uncle and aunt in Finland for their support and my two little cousin sister Sudhi and Selena for making my life a lot easier in Finland. To my friends for their support and for those never-ending discussion on engineering field which has always help me to stay inspired and motivated.

To everyone who is associated directly or indirectly with this project. The project would not have been possible without you guys.

Contents

1 INTRODUCTION 0

1.1 Scope 0
1.2 Objectives. 0
1.3 Organization of Thesis 1

2 STATE OF THE ART 2

2.1 Introduction 2
2.2 Dissimilar Material (Metal/Polymer) Joining techniques 2
2.2.1 Mechanical Fastening. 3
2.2.2 Adhesive Bonding. 5
2.2.3 Welding 7
2.3 Frictional Heating Based Metal/Polymer Joining Process 8
2.3.1 Friction Spot Joining 8
2.3.2 Friction Riveting. 9
2.3.3 Friction Lap Welding 10
2.4 Mechanical Test Analysis 11
2.4.1 Tensile-Shear Test 11
2.4.2 Cross-Tension Test 11

3 FUNDAMENTALS OF THE-FSPW AND THE-FSSPW 12

3.1 Introduction 12
3.2 THE-FSpW Process 12
3.2.1 Joining Procedure for THE-FSpW 13
3.3 THE-FSSpW Process 13
3.3.1 Joining Procedure for THE-FSSpW 14

4 MATERIALS AND METHODS 15

4.1 Introduction 15
4.2 Base Materials 15
4.2.1 AA5754-H111 15
4.2.2 AA2024-T351 16
4.2.3 Stainless Steel (AISI 316) 17
4.2.4 Ployaryletherketones (PEEK) 17
4.2.5 Polyamide (PA6) 18
4.3 Welding Equipment 19
4.4 Testing Equipment 20
4.4.1 MTS Landmark 810 Material Testing System 20
4.4.2 Optical Microscope 21
4.5 Testing Method 22
4.5.1 Tensile-Shear Test 22
4.5.2 Cross-Tension Test 24
4.5.3 Microscopic Characterization 25

5 DESIGN OF TOOL. 26

5.1 Introduction 26
5.2 Tool Material 26
5.3 Designing and Producing New Tool 27

5.4 Tool Components 27
5.4.1 Tool Body 27
5.4.2 Shoulder 28
5.4.3 Probe 28
5.5 Tool Assembly 30
5.6 THE-FSpW and THE-FSSpW Tool 30

6 DEVELOPMENT OF THE-FSPW 32

6.1 Introduction 32
6.2 Development of Experimental Conditions 33
6.2.1 Test Pieces 33
6.2.2 Stainless steel Plate and Plate Geometry. 34
6.2.3 Clamping System 35
6.3 Performance Assessment Parameters 37
6.4 Process Parameters 37
6.5 Process Variables 38
6.6 Experimental Approach 38
6.6.1 Feasibility Study of THE-FSpW Process. 38
6.6.2 Material Geometry Development 40
6.6.3 Process Parameters Development 44
6.6.4 Set of Optimal Parameters 46
6.7 Optimization of Process Parameters for Selected Base Materials 47
6.7.1 Joining of AA5754-H111 and PEEK 47
6.7.2 Joining of AA5754-H111 and PA6 47
6.7.3 Joining of AA2024-T351 and PEEK 47
6.7.4 Joining of AA2024-T351 and PA6 47

7 DEVELOPMENT OF THE-FSSPW 48

7.1 Introduction 48
7.2 Joining of AA5754-H111 to PEEK. 48
7.3 Selection of Weld Length Parameter 49
7.4 Optimization of Weld Depth to Probe Length 50
7.5 Set of Optimal Parameters 52

8 MICROSCOPIC CHARACTERIZATION 53

8.1 Introduction 53
8.2 Macrostructure Analysis of THE-FSpW 54
8.2.1 Before Etching 55
8.2.2 After Etching 56
8.3 Macrostructure Analysis of THE-FSSpW 57
8.3.1 Before Etching 57
8.3.2 After Etching 63
8.4 Microstructure Analysis 66
8.4.1 Microstructure of THE-FSpW Sample 66
8.4.2 Microstructure of The-FSSpW Sample 70
8.5 Geometrical Parameterization of Joint Hook 76
8.5.1 THE-FSpW Sample 76
8.5.2 THE-FSSpW Sample 76

9 MECHANICAL TESTING 78

9.1 Introduction 78
9.2 Mechanical Test of THE-FSpW Joint 78
9.2.1 Tensile Shear Test of AA5754-H111/PA6 Joint 78
9.2.2 Tensile Shear Test of AA5754-H111/PEEK Joint 79
9.2.3 Tensile Shear Test of AA2024-T351/PA6 Joint 80
9.2.4 Tensile Shear Test of AA2024-T351/PEEK Joint 82
9.2.5 Cross-Tension Test of AA5754-H111/PA6 Joint 83
9.2.6 Cross-Tension Test of AA5754-H111/PEEK Joint 84
9.2.7 Analysis of Results for THE-FSpW 85
9.3 Mechanical testing of THE-FSSpW Joint 86
9.3.1 Tensile Shear Test of AA5754-H111/PEEK Joint 86
9.3.2 Cross-Tension Test of AA5754-H111/ PEEK Joint 88
9.3.3 Analysis of Results for THE-FSSpW 91
10 SUMMARY 92
10.1 Discussion and Conclusion 92
10.2 Future Work 95
11 REFERENCES 97
12 APPENDIX 103

Symbols and abbreviations

Abbreviations

AA	Aluminium Alloy
AISI	American Iron and Steel Institute
CT	Cross Tension
DT	Dwell Time
FSW	Friction Stir Welding
FSpJ	Friction Spot Joining
HAZ	Heat Affected Zone
HF	Hydrofluoric
ISO	International Organization for Standardization
OT	Offset Travel
OM	Optical Microscopy
PEEK	Ployaryletherketones
PA6	Polyamide 6
RS	Rotational Speed
SZ	Stirred Zone
TS	tensile Shear
THE-FSpW	Through Hole Extruded - Friction Spot welding
THE-FSSpW	Through Hole Extruded - Friction Stir Spot welding
TMAZ	Thermo-Mechanically Affected Zone
WP	Weld Position

1 Introduction

1.1 Scope

The Through Hole Extruded – Friction Spot Welding (THE-FSpW) and the Through Hole Extruded – Friction Stir Spot Welding (THE-FSSpW) are new methods for joining metal to the polymer. These processes are friction stir based solutions, processing the materials in solid state physical domain with heat generated at the interfaces, by frictional dissipation, and internally, by bulk plastic deformation. Both processes are supported by the same operational concept. The concept supporting THE-FSpW and THE-FSSpW processes is pending on a patent issued by Aalto University. The concept is to join metal to the polymer by extruding the viscoplasticized processed part of the metal through a hole in a rigid plate (at the processing domain temperatures) and pushing it into the polymer to create an efficient joint supported by multiple joining mechanisms.

The operational concept of these processes developed for joining metal to the polymer is different from any other existing process that is used for joining these materials. The THE-FSpW and the THE-FSSpW are processes developed with aiming at producing efficient joints which can be optimized for joining various metal polymer combinations. In this work aluminium alloys, AA5754-H111 and AA2024-T351 plates are used as metal to be extruded; the stainless steel plate AISI316 is used as rigid thin extrusion die plate with the through-hole used for extrusion of the aluminium alloys into the polymer plates made of PEEK and polyamide 6. The initial testing of this new processes also involved Polycarbonate.

The extrusion die plate has at least one through-hole, in THE-FSpW (or slot, in THE-FSSpW). The metallic component will be pushed through the hole (or slot) into the polymer component, by a non-consumable, rigid rotating tool. The stirred visco plasticized aluminium that is forced to pass through the hole in the extrusion die plate will flow into the polymer forming a hook. Mechanical locking and adhesive bonding mechanism are achieved in between these dissimilar materials forming the joint. Unlike the THE-FSpW which is a spot weld, in the THE-FSSpW process tool stirs over a short weld length to form a joint hook.

There are very few joining processes currently available for joining aluminium alloys to polymer-based materials (simply addressed as polymer throughout the report). With the limitation that exists, with the currently available joining processes, the work presented here aims at introducing the development and evaluation of a new efficient solution for joining these type of dissimilar materials. This new solution has distinct benefits in comparison with the existent alternatives and arrives in a moment when the perceived need, and market, for these metal-to-polymer joints is growing.

1.2 Objectives.

This research aims at the development and evaluation of a new efficient solution for joining aluminium alloy to the polymer. The objectives of this work are listed below. To accomplish these objectives, will enable a new joining process to join aluminium alloy to the polymer. The objectives are:

- To develop and demonstrate the feasibility of a new concept for joining aluminium alloy to polymer based components.

- To develop the necessary experimental conditions to implement the processes, such as, design and development of new tools, clamping system, material geometry and set of process parameters.
- To investigate the effect of process parameters on the joining performance, microstructure and mechanical properties.
- To study the possible joining mechanism activated from the processes.
- To obtain a set of optimal parameters for the selected base materials.
- To perform mechanical and metallographic characterization.

1.3 Organization of Thesis

The dissertation is divided into ten chapters:

After the introduction, the second chapter of the thesis is state of the art, which encompasses the literature review on the existing and developing joining techniques for joining metal to polymer, with focus on the friction stir based methods.

Chapter 3 describes the fundamentals of the THE-FSpW and the THE-FSSpW processes, with typical experimental procedure listed.

Chapter 4 lists the selected base material applied in the development of both the process, welding equipment, as well as, testing equipment and experimental methods.

Chapter 5 describes the design, development, and manufacturing of the tool for the joining processes and selection of best tool for both the process.

Chapter 6 and 7 discuss the development phase of the joining processes. Chapter 6 discuss developing phases of the THE-FSpW process and Chapter 7 discuss developing phases of the THE-FSSpW process.

Chapter 8 discuss the microscopic characterization of the joints produced by both the joining process. This chapter also includes geometrical parameterization of the joint hook.

Chapter 9 presents the mechanical tests that were carried out on the joints. Tensile shear test and cross tension test were carried out on samples made as per European testing standard, produced from both processes.

Chapter 10 summarizes the overall work with analysis, conclusions, and recommendations for further work in this area.

2 State of the Art

2.1 Introduction

Material science has a long history; it has a profound impact on the evolution of human civilization. From stone age to the modern age there has been a significant development in the material science field.[1] There is the continuous introduction of various new materials, now and then to suffice the material requirements of the rapidly developing automobile, aerospace, and other industries. In the 21st century, the key to successful product in many industries is to have a good customer value and minimum environmental impact [2]. One of the approaches used by industries to reduce environmental impact is by reducing the weight of the product. Weight reduction can be achieved by use of a material having a low material density such as lightweight alloys and polymers. For example, in aerospace industries weight reduction can improve fuel consumption, reduce maintenance frequencies and increase range. The use of advanced material or combination of several dissimilar materials can enhance the overall mechanical properties, which have given rise to the synthetic material age with materials of superior performance characteristics [1, 3].

Lightweight metal and the polymer have excellent mechanical properties for structural applications. Some polymeric materials are even stronger than the metals, with high mechanical, chemical and corrosion performance properties. Although the use of lightweight material and polymer are separately used extensively in various applications, the combination of both materials to further optimize the weight and to enhance the performance of the overall structure is an area to be explored [4]. The use of multi-material structures is extensive in various transport industries such as automotive, aerospace and shipbuilding [3, 5].

With the evolution of multi-material structure, the need of joining several dissimilar materials together is a vast area to explore. Although several methods are available to join, the dissimilar metal but the process for joining the metal to the polymer are very few. To build a complex engineering component, by joining the various dissimilar material has developed various new joining method in the field of material joining [5, 6].

Due to the possibility of exploiting the peculiarities of each material, the area of the dissimilar material structure has a high potential. For this suitable wielding methods are necessary to join this dissimilar material and integrate it into engineering structures. Currently available joining methods for polymer-metal structures (adhesive bonding, mechanical fastening, ultrasonic spot welding, induction welding, injection clinching joining, friction riveting and laser heating) are usually application-specific with limited performance properties.

2.2 Dissimilar Material (Metal/Polymer) Joining techniques

There are very few methods developed for joining of dissimilar material (polymer and metal) in automotive and aerospace industry. Although many studies have been carried out on reviewing available joining techniques for thermoplastic and thermoplastic matrix composites, little information is available on joining of polymer to metal [1]. The common joining methods currently used for dissimilar materials are mechanical fastening, adhesive bonding, and some welding processes [2, 3, 6]. The other techniques are hybrid joining method (adhesive bonding combined with mechanical fastening or welding) and plastic injection molding in

perforated metallic parts which are currently being explored [4]. The latest process developed to join the polymer to metal is the Friction Riveting [4, 7, 8]. The various techniques widely used for joining polymer to metal are discussed in detail in the coming sections.

2.2.1 **Mechanical Fastening.**

Mechanical fastening is the widely used technique to join dissimilar material due to its strength, appearance, and reusability. This technique allows joining of two dissimilar material structure, independent of their material properties. [4]. It uses an additional integral component such as a screw, rivet to form a joint between two or more materials. These integral components are termed as 'fastener.' 'Fasteners' (Figure 1) are the hardware device that mechanically joins two or more component together without fusing the joint surfaces. It can be permanent, semi-permanent and non-permanent [9]. It is used because of their high holding strength, appearance, and reusability in the multi-material assembly [10].

The industrial fastener market has a confounding variety of fasteners design. The typical general categories of fasteners are tension fasteners- designed to take the tensile load (pan head, truss head, Hex head, socket screws, etc.), compression fasteners- designed to take compression load (set screws, washers) and shear fasteners- designed to take loads in perpendicular axis (dowel pins). The other way to categories fasteners is into metallic and non-metallic fasteners [11].

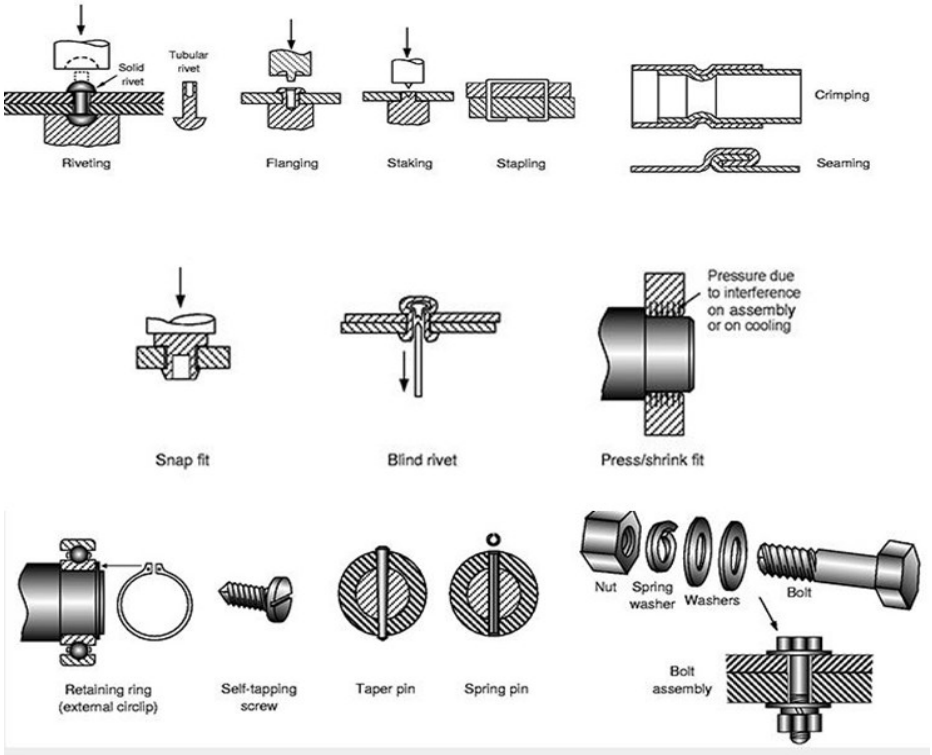

Figure 1: Various Mechanical Fastening Systems [12]

Stress due to eccentricities, stress concentration, slippage of connectors and excessive deflection, etc. are the primary cause of failure in mechanical fastening. Failure modes are similar to those observed in metallic joints (shear-out, net-tension, bearing, cleavage, bolt pulling through the coupons and bolt failure). They show higher susceptibility to hole stress concentration because of the higher polymer notch sensitivity. Fiber reinforced joints even display lower joint efficiency (about 50 % of the weaker joining partner) [4, 13].

There are various advantages of mechanical fastening; some of the key advantages are [4, 11] Ability to disassemble, controllable volume capability, joint of dissimilar material [9]. accessible technology and machinery, easy joint inspection, structural integrity assurance by suitable prediction method and analysis, minimum surface cleaning and preparation and modular replacement of pieces are possible. Some disadvantages of mechanical fastening are, some fastening process requires heating of rivet before the process, pre-processing requirement such as drilling of hole, making of screw thread, etc. [4].

There are many mechanical fastening methods for joining the metal-polymer, multi-material structures. The widely used method is the press-in-fastening, self-tapping screws, press-on fasteners, boss caps and panel fasteners. Some other way of mechanical fastening techniques are clinching (Figure 2) and collar joining method (Figure 3)**.** In collar joining method a metal is punched and projected to form a collar which is later cold pressed into the plastic piece forming a mechanical interlocking that creates a strong joint between metal and polymer. However, the joining process is, unsuitable for brittle polymer and suffer stress concentration due to cold pressing [4]. Although for polymer-metal joining by mechanical fastening is one of the reliable joining processes, it comes with limitation such as increased component weight, stress concertation inducing the strength degradation and eventually creating corrosion related problem [9]. The detail information on the theory and technology aspects of mechanical fastening and mechanical fastening of polymer-metal structure is available in [11].

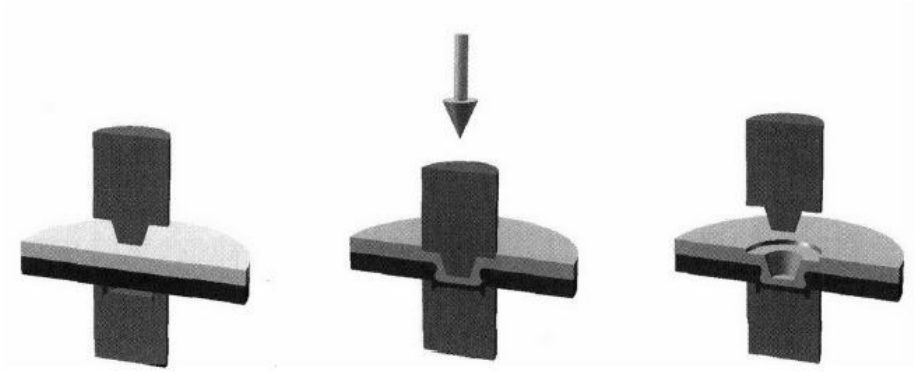

Figure 2: Schematic Representation of Clinching Joining Process [10]

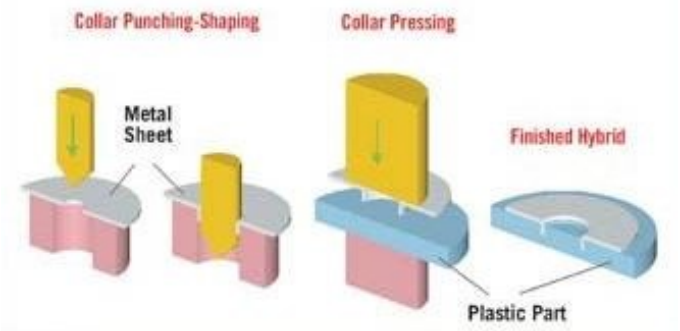

Figure 3: Schematic Representation of Collar Joining Process [14]

2.2.2 **Adhesive Bonding.**

Adhesive bonding is the process of joining two or more surface using an adhesive material (Figure 4). This joining technology offers maximum design flexibility and broad applicability in various areas. The advantage of adhesive bonding over other joining technology is that it requires little or no heat while joining such that the joined materials do not undergo any microstructural changes, deformation or internal stress [15]. Adhesive bonding has proven to be one of the useful methods for joining dissimilar materials. The primary function of an adhesively bonded joint is to transfer load from one structural member to another through interfacial shear [16]. Adhesive joining has a significant role in modern technology, with its range of application from toys and table tops to supersonic transports. It has been increasingly used in the construction and repair of aircraft [17-20], in automobile [20-22], shipbuilding and railway manufacturing [20].

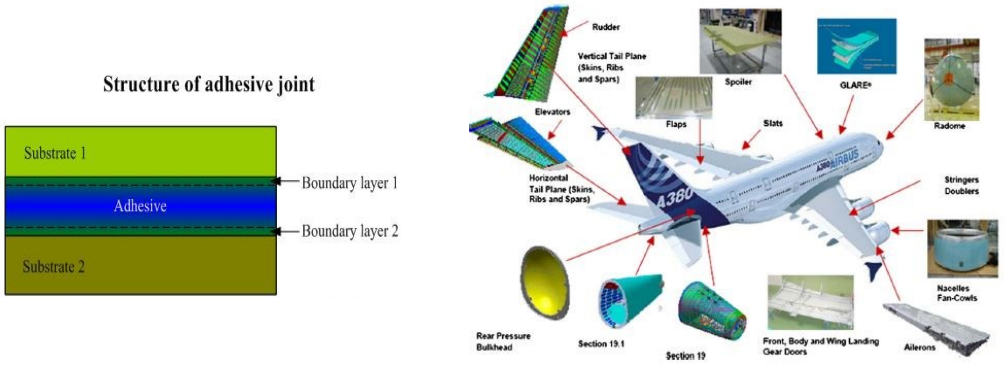

Figure 4: Structure of Adhesive Joint [23]and Adhesive Bonding Application on Aircraft [24]

Adhesive bonding is obtained by the application of a substance called 'Adhesive.' The adhesive is polymeric substances with viscoelastic behavior, which when applied to the surface of the material can join them together and resist separation due to higher shear strength. Adhesives can be natural, semi-synthetic, synthetic and inorganic. Its different types are chemical reactive type's thermoplastic types, evaporation types, and diffusion types. For further reading [25].

Adhesive bonding can be understood by the theory of adhesion and cohesion phenomenon. 'Adhesion' is a phenomenon, which allows the adhesive to transfer a load from the adherent to the adhesive joint, or energy required to separate the interface between two surfaces. 'Cohesion' is a phenomenon in which the internal force of the body or structure keeps it together. The various adhesion mechanism theories (Figure 5) are adsorption, electrostatic, diffusion, chemical bonding, and mechanical interlocking and viscoelastic properties of the coating materials [26].

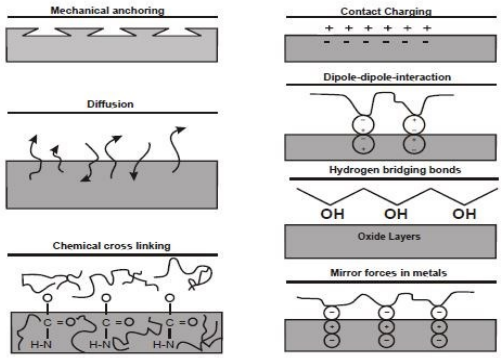

Figure 5: Various Adhesion Mechanism [26]

Although the whole adhesive bonding is joining technology based on adhesion mechanism, the long-term behaviors of adhesives are still a big area to explore. The determination of adhesive joint strength is complex primarily by the nature of the polymeric material itself. Therefore, to obtain required adhesion the subsequent wetting by the coating adhesive material is essential such that the surface tension of the coating material should be lower or equal to the substrate [15, 26]. Since these problems are mainly mechanical nature, stress analysis is required to understand how the force loads are distributed along the adherents and the adhesive layer. Most structural engineers consider the durability or stability of a joint to be fatigue related. However, is only partly right for adhesive bonds as most durability issues driven by environmental resistance rather than fatigue loads. The environmental resistance of an adhesive bond is determined by the chemical bonds formed during cure of the adhesive and the resistance of the chemical bonds to environmental degradation [16]. A comparative study on the stress of adhesive bond joints with weld-bonded and spot-welded joint can be found here [27].

Although the use of adhesive bonding is increasing rapidly, there are still significant issues which need to be addressed in joint analysis, design, durability, and performance considerations. Such as joint geometries, materials (i.e., adhesives and adherents), loading conditions (i.e., static and dynamic loadings), failure modes (i.e., cohesive, adhesive or mixed failure modes), and temperature and moisture or environmental effects (humidity, solvents, corrosion, temperature extremes, thermal cycling etc.) [16, 26, 28].

The various advantages of adhesive bonding are: high resistance to fatigue, uniform stress distribution, Joining of large surfaces, joining of dissimilar materials, proper sealing (gas proof and liquid tight), corrosion resistive, good dynamic strength and damping properties, lower or no stress concentration, excellent surface finish, repairability, weight reduction, low curing temperature and ability to join heat sensitive material. The various disadvantages are as follows: cleaning and surface preparations are required, specific production requirement, resistance only for shear loading, low engineering design confidence, and less predictable failure, stability changes with temperature- many adhesives is not stable above 180 celsius, limitation on assembly rate- high assembling and preparation time, special handling care required due to involvement of chemicals and solvents, no universal adhesive present- different joint may require different adhesive, high strength adhesive is brittle- deficient impact properties, susceptible to creep failure, not easily disassembled, limitation on thickness of joint design, nondestructive testing is not applicable for quality check, joint degradation may occur in hostile environment, and residual thermal stress can be induced

[4, 15, 16, 29]. The more detail information on adhesive bonding material, as a technology and its field of application [20].

2.2.3 **Welding**

Welding of similar and dissimilar metal is already a well-known research area. Some conventional welding processes such as gas tungsten arc welding, gas metal arc welding, submerged arc welding and shielded metal arc welding has been widely used to weld the two dissimilar metals. These welding processes involve high- heat energy, which affects the material microstructure. This limits their use to weld dissimilar materials. However, other welding processes such as laser welding, ultrasonic welding, friction spot welding and friction stir welding are more suitable for joining dissimilar materials [9].

There has been some development in welding techniques for joining polymer material, but their applications are limited to some polymer grades and joint configuration [30]. There have been a constant research and development in this field to make welding process more applicable and versatile. Some of the new welding process developed is infrared welding [31], forced mixed extrusion technique and the friction stir welding [30].

Joining of metal to polymeric material is a complicated process because of the remarkably different nature of the materials. Polymer materials have structural macromolecules formed by thousands of covalently bonded units, held together by the van der Walls forces, while metal; consist of the densely packed crystalline structure with high cohesive energy. The solubility of metal with polymers is very low such that when welded together the metal form clusters instead of mixing. The other aspect is the requirement of high temperature for plasticizing the metallic material are extreme as compare to the polymeric material. The direct welding of dissimilar polymer to the metal structure is not possible without joint design modifications, due to the degradation of the polymer before the melting temperature of the metal is achieved. Welding is limited to the thermoplastic polymeric material. Thermosets, when heated, has an irreversible crosslinking reaction resulting in degradation, which makes it impossible to reshape. Thermosets are adhesively bonded and mechanically fastened not welded [9, 30].

The various welding process for joining polymer and related material, which are classified as follows (Figure 6), based on the mode of heat generation and source, they are electromagnetic, conductive and frictional welding processes [4].

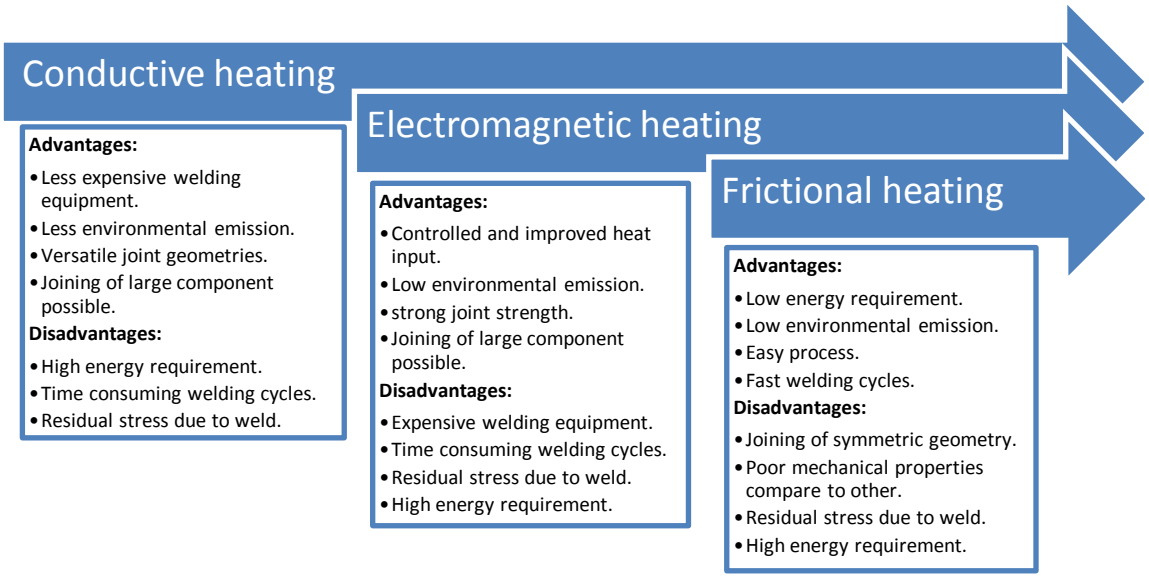

- **Figure 6: Welding Techniques for Polymers with its Advantages and Disadvantages**

The various welding technology for joining dissimilar material with some reference for further reading are below. All process is not discussed in the literature review, to limit the review more to the newly developed FSW based method for joining the metal to polymer

- Ultrasonic Welding. [32-36]
- Laser Welding.[36-42]
- Friction Spot Welding.[43-46]
- Friction Lap Welding.[47-49]
- Friction Riveting.[4-8, 50-52]

2.3 Frictional Heating Based Metal/Polymer Joining Process

Some of the newly developed joining method based on frictional heating are further discussed below:

2.3.1 Friction Spot Joining

Friction spot joining (FSpJ) is a solid state joining method for lightweight metal to polymeric material developed at Helmholtz Zentrum Geesthacht by Sergio T. Amancio-Filho. This process joins two dissimilar material with the application of heat using a non-consumable rotating tool. The bonding mechanism of two dissimilar material is a combination of adhesiveness and mechanical force between two-joined materials (Figure 7b).

FSpJ uses a non-consumable tool (Figure 7a) which is a three-piece tool system which consists of a pin, shoulder and clamping ring. The three components mounted coaxially, which makes it able to rotate and move independently. The joining process can be carried out in two variations, i.e., sleeve plunge and pin plunge. The joining of the process starts with the clamping of the pieces to be joined with a metal piece on the top of the polymer. The tool with modular sleeve and pin arrangement starts to rotate in the same direction. First, the sleeve touches the metal surface creating frictional heat enough to plasticize it and penetrates into the metal, the plasticized metal is squeezed into the created reservoir. After this,

the sleeve retracts to the metal surface and the pin plunge to push the plasticized material collected in the reservoir refilling the keyhole created during the sleeve plunging. The plunge depth is limited to the metal surface thickness to prevent the fiber damage and degradation of the polymer. However, the joint is created with the formation of metallic nub in the polymer surface due to the deformation of plasticized metal during the tool plunging. Also, the localized melting of a thin layer of polymer at metal-polymer interface creates some adhesive bonding. Similarly, in pin plunge method, all the process are similar but unlike the sleeve plunge to the metal surface first in sleeve plunge method her pin plunge to the metal surface first [53]. Further reading on various studies carried out to find out the applicability of the process on different material in [43-46].

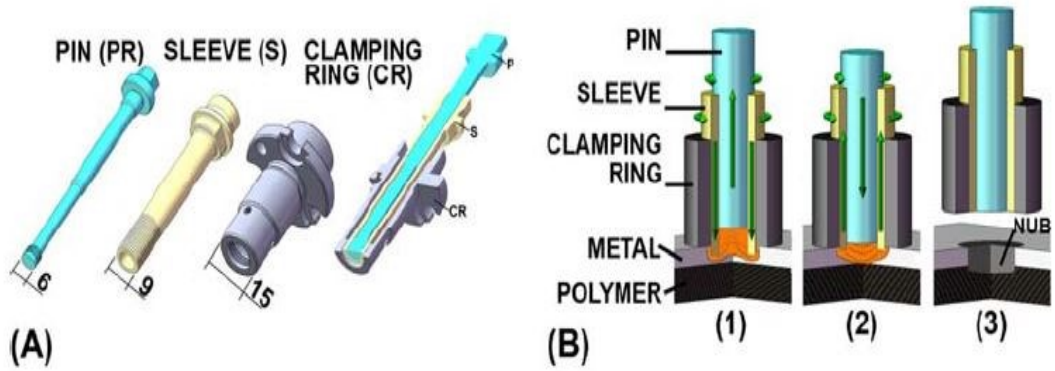

Figure 7: (a)Schematic Description of the FSpJ Tool;(b) FSpJ Joining Process [53]

2.3.2 Friction Riveting.

Friction riveting is a friction based joining technique for joining similar and dissimilar materials invented and developed by, S. Amanico, patented by Helmholtz Zentrum Geesthacht, Germany (US 7,575,149B2, EP 1 790 462 B1CA 2 568 278 C, JP 5129476[4, 5]. The process was developed to reduce the limitation related to mechanical fastening and adhesive bonding method. The process involves joining two base material, which can be a polymer or metallic alloys or both, by using metallic rivet. The rivet can be of different geometries as shown in (Figure 8a). The friction riveting can be used for a point on plate insert joint, overlap joint and sandwich type joint (Figure 8b).

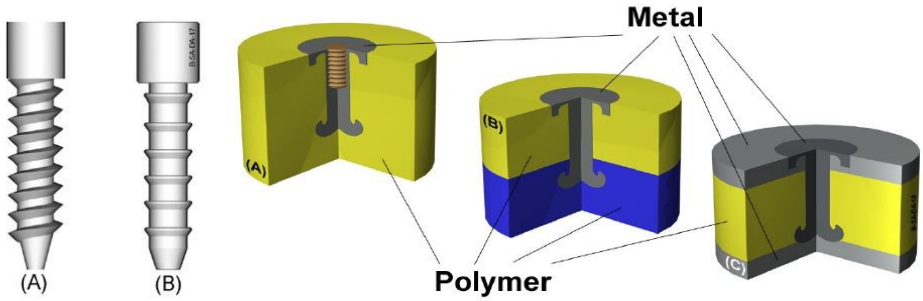

Figure 8: (a) Rivet Geometries; (b) Joint Geometries from Friction Riveting Process [4]

(Figure 9a) Illustrates the process for point to plate joint. The process includes the positioning and clamping of joining partners (A), insertion of rotating rivet into the polymeric base plate(B), rotation braking and subsequent rivet forging(C) and lastly cooling and joint consolidation(D).[4]. The actual process is shown on (Figure 9b). When the rivet is rotated and pressed against the surface of the polymeric component, the high rotation and axial force create heat which makes localized melting of the polymer and the tip of the rivet. When the rivet is pressed into the polymer, the excess amount of polymer is expelled out as flash. Due to the high temperature and low thermal conductivity of polymer the thermoplastic, the local temperature at the tip of the rivet rises significantly. When the temperature at the tip of rivet reaches near to its plasticizing temperature, the rotational speed is decreased, and the axial force is increased. The plasticized rivet tip deforms locally and creates a mushroom-like structure having a larger area of contact at the tip with the polymer. After cooling, the joint is consolidated [7].

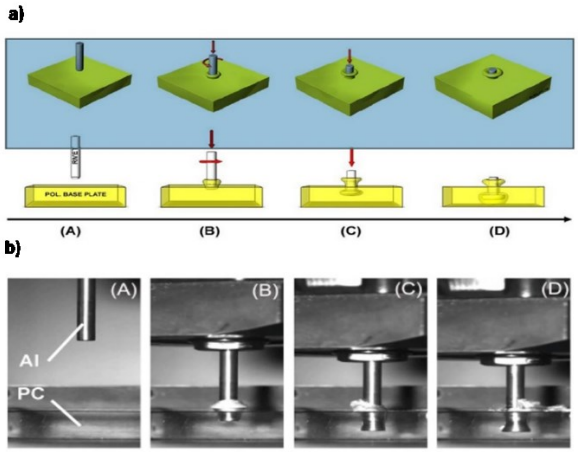

Figure 9: Schematic; (b) Actual Friction Riveting Process Steps for Metallic Insert Type Joints. [4, 7]

The various study is available to understand the applicability of friction riveting. Some studies carried out in this field are friction riveting of titanium alloy on short fiber-reinforced thermoplastic polymers [50], aluminium AA2024-T351 and polycarbonate[6], Force controlled friction riveting of glass fiber reinforced polyamide 6 and aluminium alloy 6065 hybrid joints [52], Ti-6Al-4V and glass fiber reinforced polymer [8] and aluminium AA2024-T351 and polyetherimide (PEI)[4, 7].

2.3.3 Friction Lap Welding

Friction lap joining is the new concepts of direct joining method for metal to polymer developed by joining and welding research institute (JWRI), Osaka University. The process of joining (Figure 10) looks similar to friction stir welding which uses a rotating non-consumable tool, but the difference between the friction lap is joining, and friction stir welding is that the non-consumable rotating tool used in friction lap joining does not use stir pin. Therefore, unlike the friction stir welding where material flow is achieved around stir pin, here in friction lap joining the primary function of the rotating tool is to press and heat up the metal workpiece. The heat generated in metal is transferred to polymeric material through conduction, which melts the polymer in the metal-polymer interface. The bonding is achieved when the molten metal solidifies in the metal-polymer interface, under pressure from the tool. Further reading on the process and its application on several dissimilar material combinations can be found in [47-49].

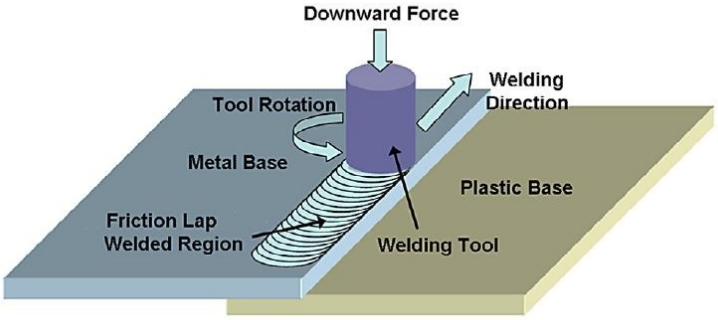

Figure 10: Friction Lap Joining Process [49]

2.4 Mechanical Test Analysis

The mechanical test is carried out to assess the joints produced by the THE-FSpW and the THE-FSSpW process. The testing result of the joint will prove the efficiency of the joint and possible implementation of the process in the commercial label. The detail information on some of the standard destructive test carried out on the joint is discussed in coming sections.

2.4.1 Tensile-Shear Test

The tensile shear test is a standard testing process for spot welding in which a test specimen is subjected to traction until fails. The specimen deforms at the spot joint and fails mostly due to shearing. In this test, samples are made as per the European Standard and joined with a spot weld located at the center of the overlapped region. The sample is then pulled in tension, failure load and fracture morphology from the test are examined to assess the performance of the weld. Two types of weld fractures can be observed during the tensile shear test. They are full button pull out such that fracture occurs around the weld button in the interface by leaving the entire button intact or the fracture occurs through the weld nugget at the interface between two material joined. It is also possible to get a combination of both failure modes such that a part of the nugget is pulled out and the rest of the nugget shears at the interface [54].

2.4.2 Cross-Tension Test

In cross-tension tests, according to the European Standard, two test pieces measuring150 mm long × 50 mm wide are positioned normal to each other such that an overlap of 50 mm is maintained. A spot weld is made at the center of the overlapping section. During the cross-tension test, a tensile load is applied to the weld in a direction normal to the weld until failure occurred. Failure load and fracture morphology from the test are examined to assess the performance of the weld. In cross tension test the button pull type of fracture mode is observed in most failure cases. However, in some exceptional cases, an interfacial tensile failure is observed [54].

3 Fundamentals of THE-FSpW and THE-FSSpW

3.1 Introduction

This chapter discusses the fundamentals of the two new processes that were developed for joining the aluminium to the polymer, which are the THE-FSpW (Through Hole Extruded – Friction Spot Welding) and the THE-FSSpW (Through Hole Extruded –Friction Stir Spot Welding).

In section3.2, the fundamental of the THE-FSpW is presented. The section gives an introduction to the process with the schematic and actual representation of the process. The subsection 3.2.1, the typical procedure followed during the THE-FSpW process is listed.

Similarly, in section3.3 the fundamentals of the THE-FSSpW is presented. The section gives an introduction to the process with the schematic and actual representation of the process. In subsection 3.3.1, the typical procedure followed during the THE-FSSpW process is listed.

3.2 THE-FSpW Process

'Through Hole Extruded – Friction Spot Welding' (THE-FSpW) process (Figure 11) is a new concept developed to join aluminium to the polymer material (PEEK and Polyamide 6), using friction spot welding process. This new joining process involves three layers of material. The concept is the utilization of a rigid thin extrusion die plate positioned in the middle an overlapped joint formed by aluminium alloy plate over the polymer. This extrusion die plate has at least one through-hole. The metallic component will be pushed through the hole into the polymer component, by a non-consumable, rigid rotating tool. The stirred visco plasticized aluminium that is forced to pass through the hole in the extrusion die plate will flow into the polymer forming a hook. Mechanical locking and adhesive bonding mechanism are achieved in between these dissimilar materials forming the joint.

The weld depth is set in such a way that the tool travels through the stainless steel plate hole pushing the visco-plastic aluminium to deposit into the polymer creating a hook-like structure termed as 'joint hook.' An offset travel of 0.5 mm to 1 mm is used to maintain the thickness of the hook. The THE-FSpW process is repeatable, controllable and this process does not require any consumables or chemicals.

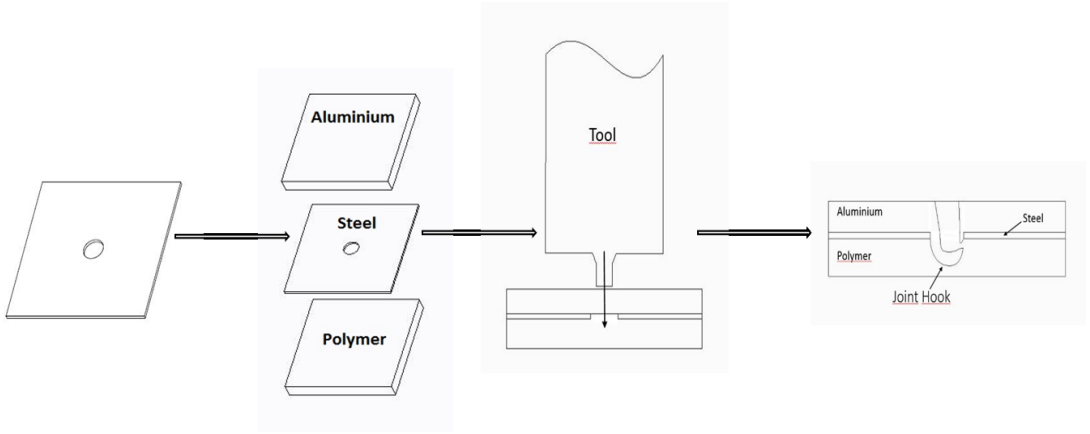

Figure 11: Schematic Representation of THE-FSpW Process Concept

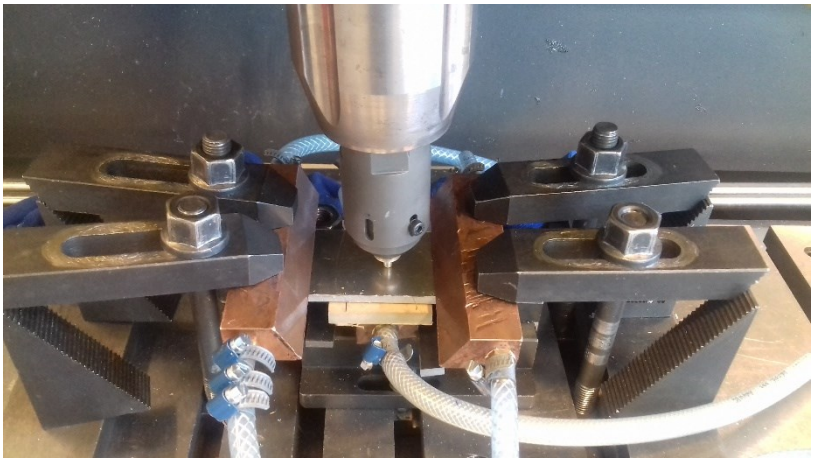

Figure 12: THE-FSpW Setup

3.2.1 Joining Procedure for THE-FSpW

The procedure followed during the typical THE-FSpW joining process is described in several steps below:

- The base materials are prepared as per the required geometry for the test.
- The polymer and stainless steel plate is clamped in the table vice clamp, to make a through a hole in the stainless steel plate and a groove in PEEK plate of required depth. The ESAB LEGIO FSW 5UT machine used to make hole using a drill tool. The position of the hole is saved in the machine, which is later used as a plunging point during friction spot welding.
- The aluminium plate is placed on top of the stainless steel plate and clamped using a clamp with a cooling arrangement.
- The drilling tool is replaced with friction spot welding tool.
- The joining process parameters are set on the ESAB LEGIO FSW 5UT machine through its user interface. After setting all parameters, the machine is automated to friction spot weld at the same position saved earlier.
- The test starts and joining of the metal to polymer is achieved.
- After the test, the three-layer material joint is retrieved out of the clamp, when the specimen is cooled to room temperature.

3.3 THE-FSSpW Process

'Through Hole Extruded – Friction Stir Spot Welding' (THE-FSSpW) process (Figure 13) is an improved version of the THE-FSpW concept developed to join aluminium to the polymer material, using friction stir spot welding process. This improved joining process also has three layers of material. The concept is the utilization of a rigid thin extrusion die plate positioned in the middle an overlapped joint formed by aluminium alloy plate over the polymer. This extrusion die plate has at least one through 'slot' of a length. The metallic component will be pushed through the 'slot' into the polymer component, by a non-consumable, rigid rotating tool. The stirred visco plasticized aluminium that is forced to pass through the hole in the extrusion die plate will flow into the polymer forming a hook. Mechanical locking

and adhesive bonding mechanism are achieved in between these dissimilar materials forming the joint. Unlike, the THE-FSpW in this process, the stainless steel plate has a through 'slot' over a length on its surface through which the visco-plasticized aluminium flow through and deposits into the polymer forming a longer 'joint hook' throughout the 'weld length.'

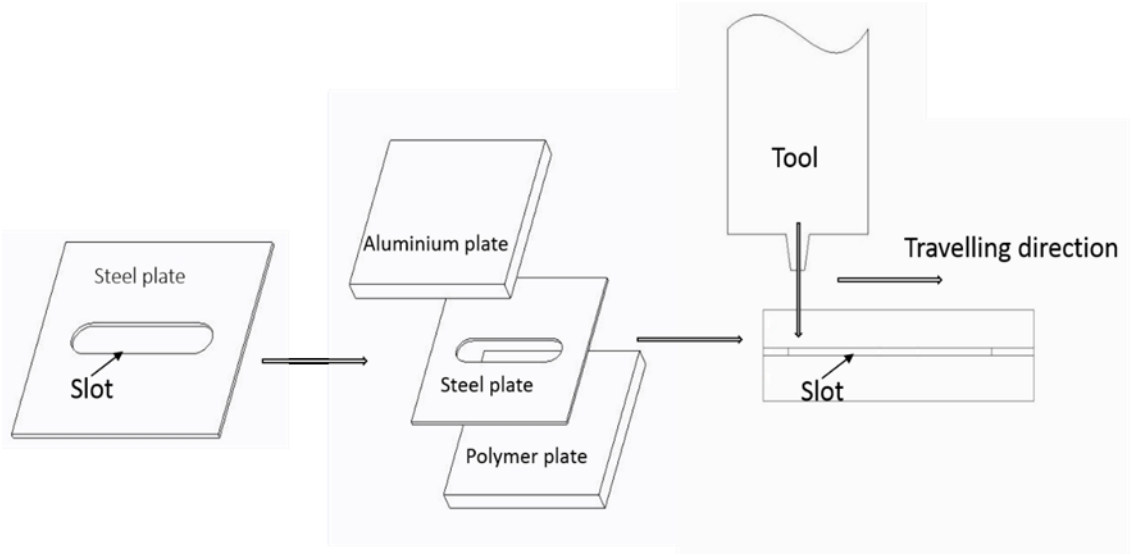

Figure 13: Schematic Diagram of THE-FSSpW Process

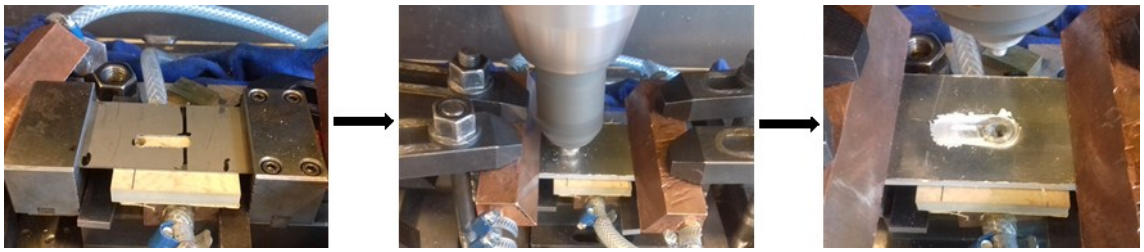

Figure 14: THE-FSSpW Process

3.3.1 Joining Procedure for THE-FSSpW

The procedure followed during a typical THE-FSSpW joining process is described in several steps below:

- The base materials are prepared as per the required geometry for the test.
- The slot on the stainless steel plate is made beforehand using a milling machine.
- The polymer and stainless steel plate with slot are clamped in the table vice clamp.
- The initial penetration position is set manually set using the tool and machine and the position saved in the machine.
- The aluminium plate is placed on top of the stainless steel plate and clamped using a clamp with a cooling arrangement.
- The joining process parameters are set on the ESAB LEGIO FSW 5UT machine through its user interface.
- The test starts and joining of the metal to polymer is achieved.

After the test, the three-layer material joint is retrieved out of the clamp, when the specimen is cooled to room temperature.

4 Materials and Methods

4.1 Introduction

In this chapter the materials, welding equipment's and Test analysis method that was utilized during the development of the THE-FSpW process and the THE-FSSpW process are presented.

In section 4.2, the essential information on the properties of the base materials that were used in this work are presented.

In section 4.3, the welding equipment utilized during the development process are presented. The friction stir welding machine ESAB LEGIO FSW 5UT was used for this work.

In section 4.4, the testing equipment utilized during the mechanical test and metallography analysis of joint is presented. The MTS Landmark 810 material testing system was used to perform the tensile shear test and cross tension test. An optical microscope was used for metallography.

In section 4.5, the method used for carrying out various analysis of joint is presented. Tensile –shear test and cross-tension test was performed as a part of the destructive test, and optical microscopy was performed as a part of the metallographic analysis.

4.2 Base Materials

The various base material used during the development of the THE-FSpW process and the THE-FSSpW process are discussed in coming sections. The physical, chemical and mechanical properties are tabulated for all the materials.

4.2.1 AA5754-H111

AA5754-H111 is the wrought aluminium which belongs to 5000 series- magnesium family. The H111 designation refers to, H1- strain hardened only, and Hx11 explains that it has gone sufficient strain hardening after final annealing to fail to qualify as 0 temper but not enough tempered to call as Hx1 temper. In general, the 5000 series family has enhanced work hardening characteristics due to the significant solubility of magnesium in the aluminium which imparts the substantial solid solution strengthening. Alloy in these series possesses good welding characteristics, mechanical properties, and excellent corrosion resistance. However, there is some limitation for higher magnesium-containing alloy, for the amount of cold work and safe operating temperature to avoid susceptibility to stress corrosion cracking. Due to its excellent properties, it is widely used as structural material in aerospace, shipbuilding and automotive industries [55]. This alloy was used as one of the base material for investigating the THE-FSpW process and the THE-FSSpW process. It was selected due to its extensive commercial application. The material obtained from the supplier was the 6mm thick plate. The chemical composition, mechanical and thermal properties are in (Table 1) and (Table 2).

Table 1: Chemical Composition of AA5754-H111 [56]

Wt%	Si	Fe	Cu	Mn	Mg	Cr	Zn	Ti	Others	Al
AA5754	0.4	0.4	0.1	0.5-2,6	3.6	0.3	0.2	0.15	0.15	Bal.

Table 2: Mechanical Properties of AA5754-H111. [56, 57]

Properties	Range
Temper	H111
Density	2,68 e3 kg/m3
Tensile Strength	190-240 MPa
0,2% Proof Stress	80 MPa
Elongation	18 %
Brinell Hardness	52 HB
Thermal Conductivity	132 W/mºK
Melting Point	595 ºC

4.2.2 **AA2024-T351**

AA2024-T351 also known as aerospace alloy belongs to aluminium 2000 series family. The T351 temper gives the information that alloy was solution heat-treated, cold worked, naturally aged to the stable condition and stress relieved. In general, 2000 series family have copper as principal alloying element and magnesium as a secondary alloying element. These alloying elements are solution heat treated to get required properties. Although, compared to other aluminium family series it has low corrosion resistance and weldability. However, it is known for its high strength and excellent fatigue resistance properties which make its applicable on structure requiring high strength to weight ratio such as in automotive and aircraft industries [55]. This alloy was used as one of the base material for investigating the THE-FSpW process. It was selected due to its extensive commercial application. The material obtained from the supplier was the 8mm thick plate which was later milled into 6 mm thickness using the milling machine available in Aalto university facility**.** The chemical composition, mechanical and thermal properties are listed in (Table 3) and (Table 4).

Table 3: Chemical Composition of AA2024-T351 [58]

Wt.%	Cu	Mn	Mg	Fe	Si	Zn	Cr	Ti	Al
AA2024	3.8-4.9	0.30-0.90	1.2-1.8	0.50	0.50	0.25	0.10	0.15	Bal.

Table 4: Physical, Mechanical and Thermal Properties of AA2024-T351. [57, 58]

Properties	Range
Temper	T351
Density	2,75-278 e3 kg/m3
Tensile Strength	460-480 MPa
0.2 % Proof Stress	330-420 MPa
Elongation	7-20 %
Hardness	137 HV
Thermal Conductivity	121-131 W/mºK
Melting Point	500-600ºC

4.2.3 Stainless Steel (AISI 316)

AISI 316 is an austenitic chromium-nickel stainless steel containing molybdenum, which makes it corrosion resistance and increased strength at elevated temperature. It also has good weldability and lowers thermal conductivity [59]. The 1mm thick plate is one of the base material used for investigating the THE-FSpW process. It was chosen mainly for its lower thermal conductivity, which was one of the constraints for selection of stainless steel base material to be used in THE-FSpW. The stainless steel with lower thermal conductivity was chosen, to prevent a significant amount of heat transfer during the joining process of aluminium alloy to the polymer material The chemical composition, mechanical and thermal properties of the stainless steel material used are listed in (Table 5) and (Table 6).

Table 5: Composition Details of AISI 316 [57, 59]

Compo-sition	C	Cr	Fe	Mn	Mo	Ni	P	S	Si
%	0,08	18	72	2	3	14	0,045	0,03	1

Table 6: Physical, Mechanical and Thermal properties of AISI 316[57, 59]

Properties	Range
Young's Modulus	205 GPa
Yield Strength (elastic limit)	310 MPa
Tensile Strength	515 MPa
Elongation	50 %strain
Compressive Strength	310 MPa
Flexural Strength	310 MPa
Shear Modulus	82 GPa
Hardness-Vickers	220 HV
Density	8,07e3 kg/m^3
Melting Point	1400°C
Thermal Conductivity	13 W/m.°C
Specific Heat Capacity	490 J/kg.°C
Thermal Expansion Coefficient	15 µstrain/°C

4.2.4 Ployaryletherketones (PEEK)

The ployaryletherketones (PEEK) is a high-performance thermoplastic. It is a high service temperature engineering polymer which is semi-crystalline, poorly soluble and robust. The chemical structure of PEEK is shown in fig (). It is produced by the condensation of 4, 4'-diflurodiphenyl ketone ($(FC_6H_4)_2C=O$) with the potassium salt of hydroquinone(KOC_6H_4OK). The ether linkage in the structure give it a high process ability and the ketone group gives stiffness resulting in strength and high modulus [60, 61].

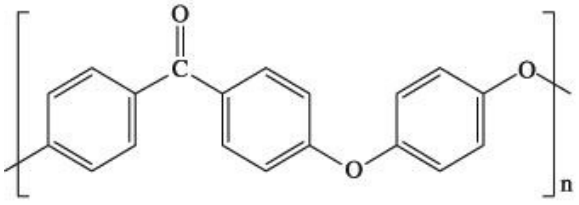

Figure 15: Chemical Structure of PEEK [62]

PEEK was designed by Rose in 1970, after recognizing the structure-property relationship of the presence of carbonyl group which was temperature resistant and robust as well as flexible due to the presence of ether groups in the polymer chain. It was also found to have a high degree of oxidation stability, radiation resistance, solvent resistance and flame resistance. It was marketed in 1978 with the trade name of victrex PEEK [60, 62]. PEEK has high strength and rigidity compared to other thermoplastic polymeric material even at a wide range of elevated temperature. Due to its good physical, mechanical and chemical properties, its application is found in wide range of engineering areas. The processing of PEEK is complicated due to its resistance to chemical and solvent, and also due to its high temperature [60, 62].

Due to its broad engineering application and commercial viability, the material was chosen as one of the base material for THE-FSpW. The mechanical, physical and thermal properties of PEEK from the manufacturer is listed in (Table 7).

Table 7: Mechanical, Physical and Thermal Properties of PEEK [63]

Group	Condition	Methods	Unit	PEEK450G 100 % PEEK
Density	23ºC	ISO 1183	g/cm3	1.3
Friction Coefficient			µ	0.35
Rockwell Hardness	23ºC	ASTM D785		99
Tensile Elongation	23ºC	ISO 527	%	45
Tensile Modulus	23ºC	ISO 527	GPa	3.7
Bending Modulus	23ºC	ISO 178	GPa	4.1
Melting Point		ISO 3146	ºC	343
Glass Transition Temperature(Tg)	Initial temperature	ISO 3146	ºC	143
Distortion Temperature	1.8Mpa	ISO 75A-f	ºC	152
Pyro-conductivity	23ºC	ASTM C177	W/mºC	0.29
Dielectric Strength	2.5mm Thickness	IEC 60243-1	KV/mm	16

4.2.5 **Polyamide (PA6)**

Polyamide (PA6) is an engineering polymer. The monomer of PA6 is ε-Caprolactam. PA6 is easy to synthesized by open-cycling polymerization from ε-Caprolactam. This type of nylon was designed for its low cost and availability of monomers. The six carbon segment gives nylon 6 a good toughness and yet to be stiff, stronger and crystalline. PA6 is widely used in almost all industries such as automotive, biomedical and aerospace [60].

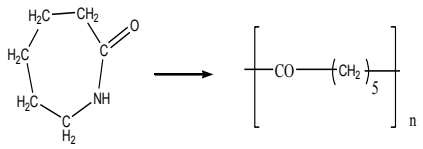

Figure 16: Chemical Structure of Polyamide 6 (PA6)

Due to its broad engineering application and commercial viability, the material was chosen as one of the base material for THE-FSpW. The mechanical, physical and thermal properties of PEEK from the manufacturer are listed in (Table 8).

Table 8: Mechanical, Physical and Thermal Properties of PA6 from Manufacturer. [64]

Properties	Test standard	Values/unit
Density	ISO 1183	1,13 g/cm³
Tensile Modulus	ISO 527-2	3200 MPa
Tensile Stress (yield)	ISO 527-2	83 MPa
Elongation (yield)	ISO 527-2	4%
Elongation at Break	ISO 527-2	>30 %
Flexural Modulus	ISO 178	3200 MPa
Flexural Strength	ISO 178	120MPa
Melting Point	DIN EN 11357-1	222 °C
Flammability	UL 94	V2 class

4.3 Welding Equipment

Friction Stir Welding (FSW) machine, ESAB LEGIO FSW 5UT (Figure 17) was the Welding equipment used for both the THE-FSpW process and the THE-FSSpW process. This machine is modular and designed explicitly for the friction stir welding. The machine is well equipped with a rigid base frame for strength and high-performance operation during heavy loading which was perfect for the development of both the joining process.

AC motor drives the spindle of the machine. There is a liquid cooling setup on the spindle components and pin tool to minimize the wear. The machine is controlled by PLC technology and high accuracy drives which make the control of axis position and speed precisely. The Z axis can be used in either position control or force control mode. The FSW machine is also equipped with a user interface, which can be accessed through 15-inch touch screen HMI interface or conventional keyboard and mouse. The interface can be used to input the set of process parameters for the test. It also provides monitoring capabilities of the process parameters, alarm, and system status. The machine table also has a series of grooves and holes, which are used for mounting the clamping arrangements [65].

The specification of the FSW machine according to the ESAB LEGIO FSW 5UT friction stir welding equipment are as listed below:

- Maximum Torque: 200(Nm).
- Maximum Rotational Speed: 3000 (rpm).
- Maximum Forging force: 100(kN).
- Maximum welding travel speed: 4(m/min).
- Work Envelope Dimensions: 2000*400*300(XX,YY,ZZ)(mm).
- Welding control(Z-Axis):
  - Force
  - Position
  - Speed
- Welding Angle: 0 degrees to 5 degree.

- Monitoring parameters
  - Spindle speed and Torque.
  - Position, Speed and Force in XX, YY and ZZ axes.

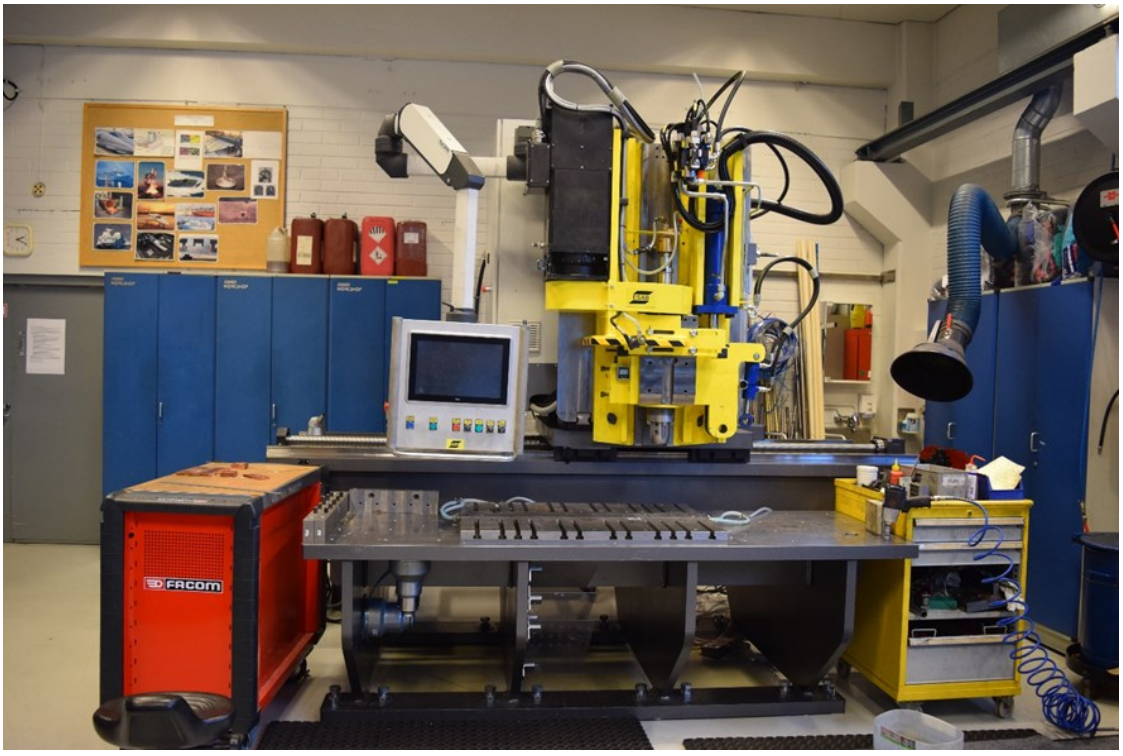

Figure 17: ESAB LEGIO FSW 5UT Friction Stir Welding Machine

4.4 Testing Equipment

4.4.1 MTS Landmark 810 Material Testing System

MTS Landmark 810 material testing system (Figure 18) was used for both tensile shear test and cross-tension test. The machine is available at engineering material department lab, school of engineering, Aalto University. It is a versatile, multipurpose, high-performance machine with servo-hydraulic testing technology, for static and dynamic material and component testing. Different jig and clamp were used to fix the test specimen on the machine. Some of the specification of the MTS 810, floor-standing model are as listed below: [66, 67]

- Force range: 25 KN-500 KN.
- The materials that can be tested: plastics, elastomers, aluminium, composites, steel, and superalloys.
- Specimen sizes compatibility - subsidized, standard, medium and large.
- Multipurpose- various test: tensile test, cross tension test, torsion test and the shear test can be done using the machine, with proper jigs, fixtures, and clamps.

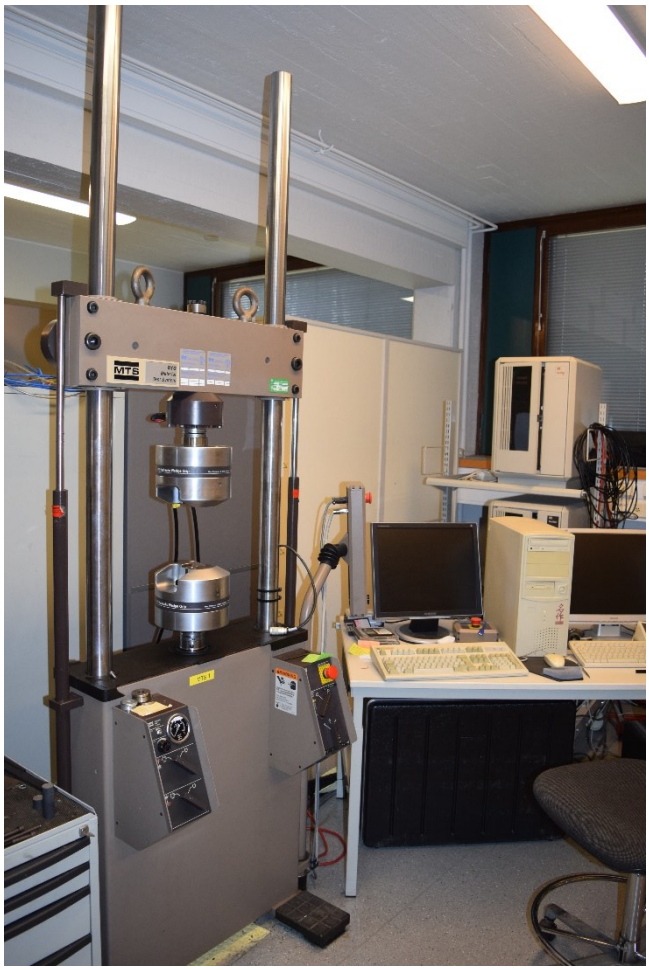

Figure 18: MTS Landmark 810 Material Testing System

4.4.2 Optical Microscope

NIKON Epiphot 200 (Figure 19), Optical microscope, available at engineering material department lab, school of engineering, Aalto University was used for the Microscopic characterization of the sample. The Nikon Epiphot 200 is a compact inverted metallographic microscope with lower stage design and ergonomic control. It is a versatile instrument with CF infinity-corrected optical system, which let it is to combine NIKON CF optics with an infinity-corrected design for greater system flexibility. It has five objectives of 5x, 10x, 20x, 50x and 100x. With the use of NIS-Elements F2.30. Software, the result can be viewed, captured and saved in computer [68].

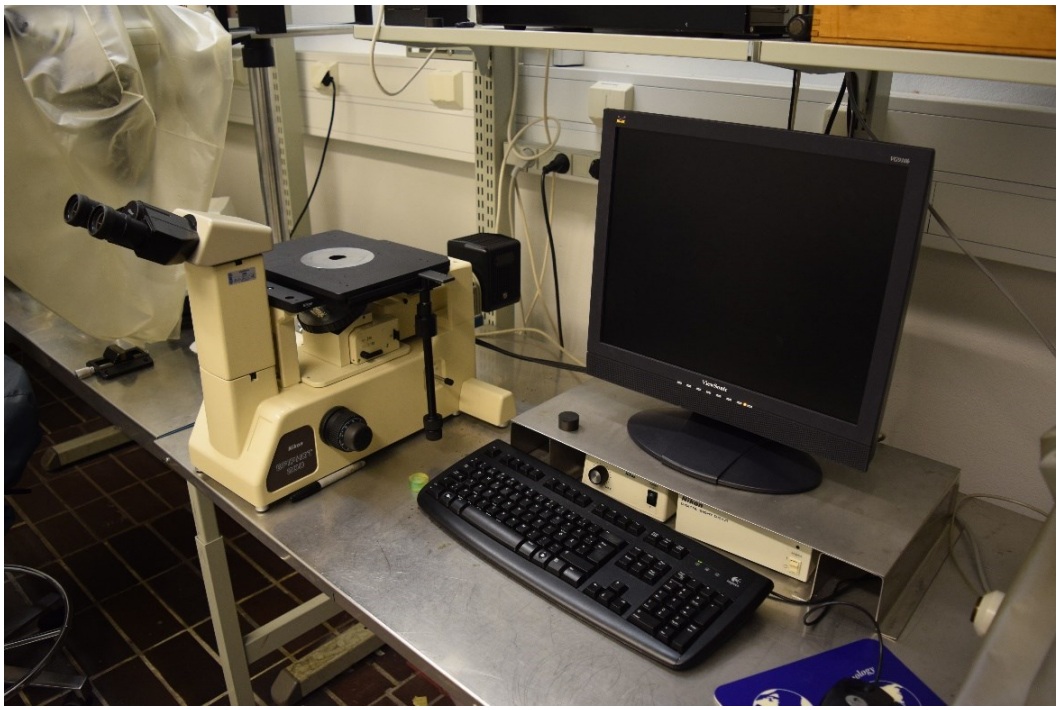

Figure 19: Optical Microscope Setup

4.5 Testing Method

4.5.1 Tensile-Shear Test

Tensile shear testing was carried out in MTS landmark 810 material testing machine system. The machine is available in the Aalto University, engineering material facility. All the test were performed in the laboratory at room temperature. The traverse speed used for the test was 1mm/min. The force-displacement plot was obtained from the computer simultaneously during the testing.

The test specimen is according to the European Standard EN ISO 14273:2016"Resistance welding, Destructive testing of welds. Specimen dimensions and procedure for tensile shear testing resistance spot and embossed projection welds (ISO 14273:2016)" [69]**.** The European Standard EN ISO 14272:2016 has the status of a Finnish national standard. All test specimen produced using the THE-FSpW, and the THE-FSSpW process uses the same standard. The schematic figure of the general test specimen (Figure 20).

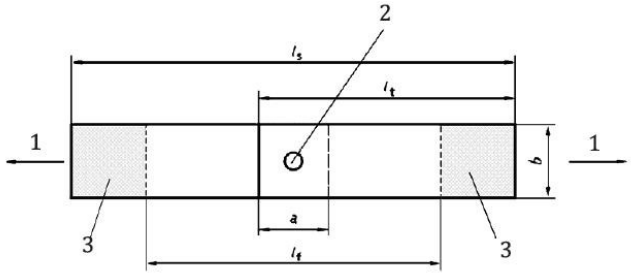

Key

1 direction of test load
2 weld
3 clamping zone

Figure 20: Schematic Diagram of Tensile Shear Test Specimen [69]

The test specimen dimension used for testing the joint strength produced by the THE-FSpW process are in (Table 9).

Table 9: Test Specimen Dimension for Tensile-Shear Test of the THE-FSpW Produced Joint

S.N		For THE-FSpW
1.	Length of Individual Test Specimen (l_t)	110 mm
2.	Free Length Between Clamps (l_f)	95 mm
3.	Specimen Length(l_s)	185 mm
4.	Specimen Width (b)	45 mm
5.	Overlap (a)	35 mm

The dimension is similar for all tensile shear test, for joint made using different material combinations. (Figure 21a), shows one of the typical test specimen and (Figure 21b) during the testing process.

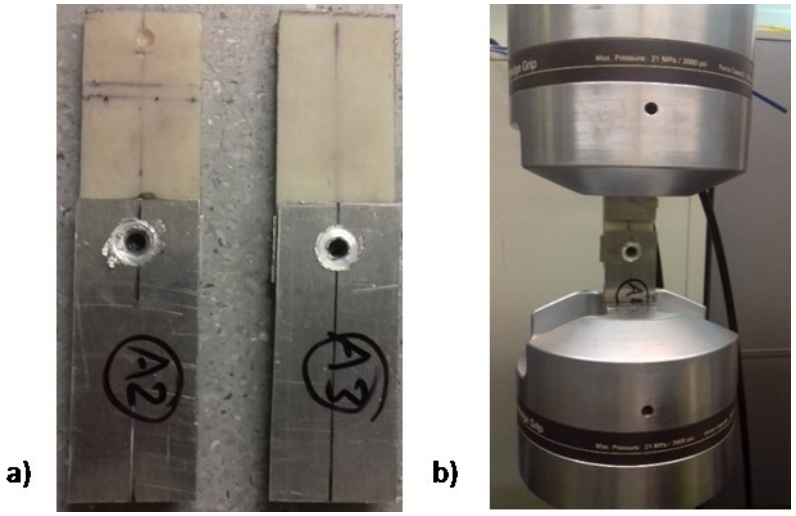

Figure 21: a) Tensile-Shear Test Specimen, b) Test Specimen in the MTS 810 Landmark Machine

For the THE-FSSpW test specimen, weld in both longitudinal and transverse direction with reference to aluminium alloy plate was made for testing. To understand the weld behavior in multiple directions and the failure modes in a better way, they were tested in both the direction. The test specimen dimension used for the test differs depending on the weld direction. The test specimen dimension used for testing the joint produced by the THE-FSSpW process are in (Table 10).

Table 10: Test Specimen Dimension for Tensile-Shear Test of the THE-FSSpW Produced Joint

S.N		For FSW- (longitudinal weld)	For FSW- (Transverse weld)
1.	Length of Individual Test Specimen (l_t)	160 mm	160 mm

2.	Free Length Between Clamps (l_f)	120 mm	120 mm
3.	Specimen Length(l_s)	260 mm	260
4.	Specimen Width (b)	50 mm	80 mm
5.	Overlap (a)	60 mm	50 mm

(Figure 22a) shows test specimen having transverse weld and (Figure 22b) test specimen having longitudinal weld produced from the THE-FSSpW process during the testing process.

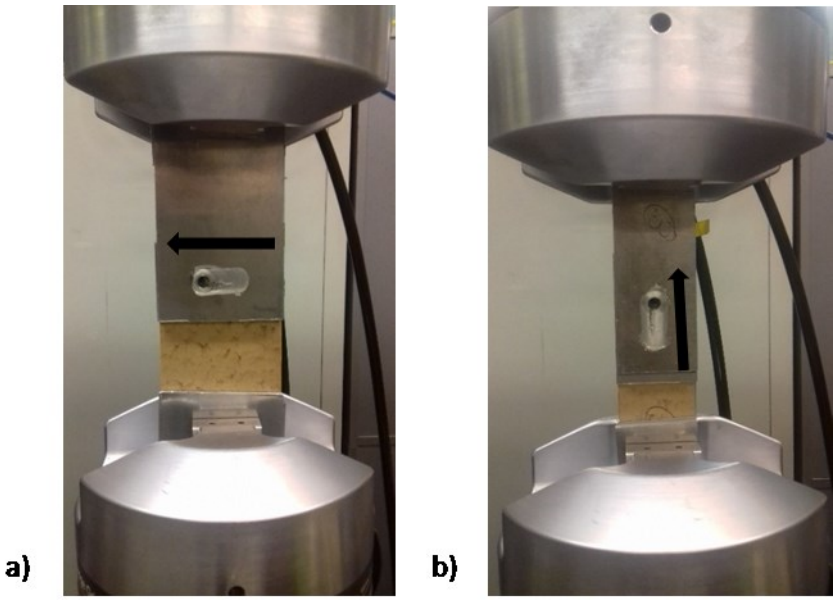

Figure 22: Tensile-Shear test a) Transverse Direction Weld, b) Longitudinal Direction Weld

4.5.2 Cross-Tension Test

Tensile shear testing was carried out in MTS landmark 810 material testing machine system. The machine is available in the Aalto University, engineering material facility. All the test were performed at laboratory room temperature. The traverse speed used for the test was 1mm/min. The force-displacement plot was obtained from the computer simultaneously during the testing.

The test specimen was made according to the European Standard EN ISO 14272:2016"Resistance welding, Destructive testing of welds. Specimen dimensions and procedure for cross tension testing of resistance spot and embossed projection welds (ISO 14272:2016)"[70] The European Standard EN ISO 14272:2016 has the status of a Finnish national standard. All test specimen produced for THE-FSpW and THE-FSSpW process use the same standard. The schematic figure of the general test specimen is as shown in (Figure 23).

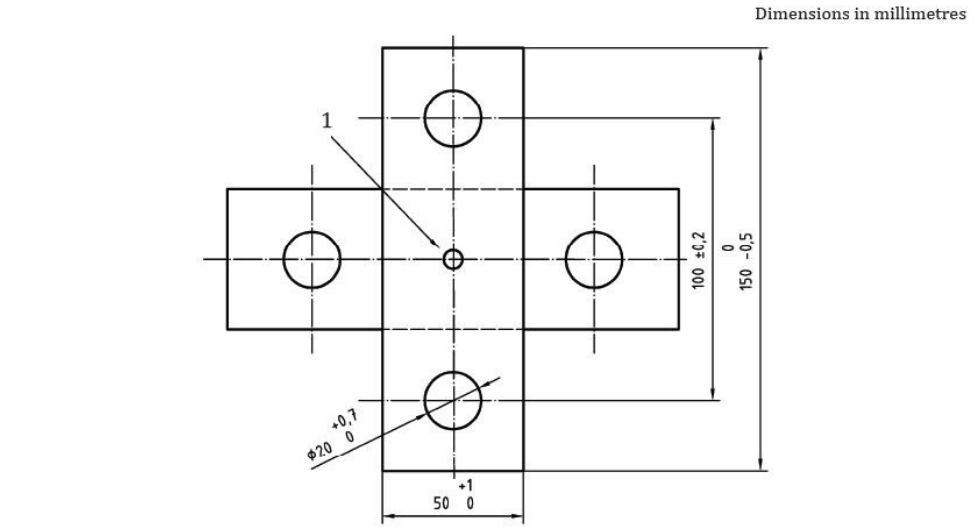

Figure 23: Schematic Diagram of Cross-Tension Test Specimen [70]

The cross-tension test specimen (Figure 24a) having transverse weld and (Figure 24) having longitudinal weld produced from the THE-FSSpW process (Figure 24c) during the testing process.

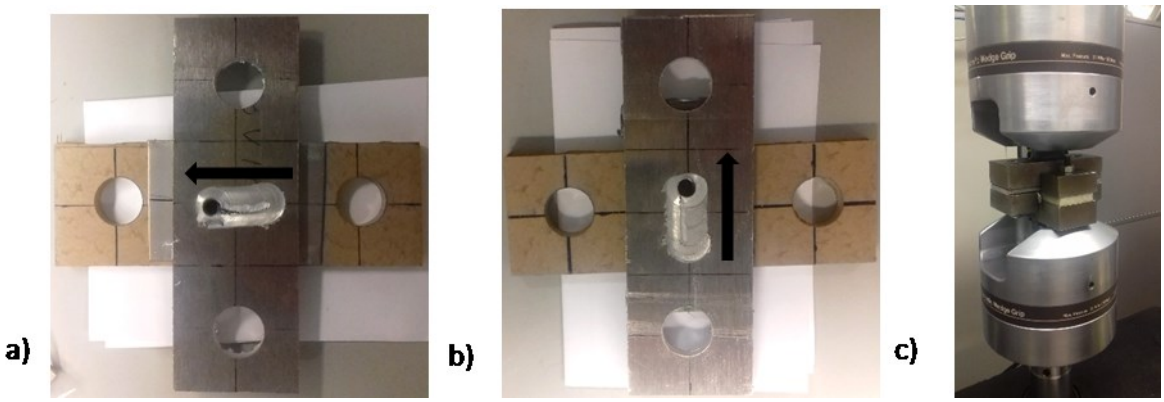

Figure 24: Cross-Tension Test Specimen a) Transverse Weld, b) Longitudinal Weld, c) Specimen in the Test Machine

4.5.3 Microscopic Characterization

To carry out the microscopic analysis of the sample, they were cut using the Beka-MaK BMSY 32CGL saw in the appropriate section. Samples are mounted in resin – Struers DuroCit Kit, cold mounting, acrylic resin. Samples were then grinded and polished form 46 micron to 1 micron. The samples are studied before and after etching. First optical microscopy analysis was done before etching. After that, the sample was etched with 10% hydrofluoric acid for approximately 20-30 seconds, and microscopy analysis was done. All the samples used for the characterization were prepared using the best optimal parameters. Nikon Epiphot 200 microscope with Nikon DS-2Mv camera was used for optically characterizing the samples. Samples for Both macrostructure and microstructure characterization were prepared using same steps.

5 Design of Tool.

5.1 Introduction

This chapter discusses tool design and development**.** During the early phase development of the THE-FSpW process: old tool was used for the joining process of polymer based material to the aluminium alloy plates. The existing tools used for the THE-FSpW process have problems such as the excess loss of material during initial penetration of the probe and squeezing out of material, i.e., not enough pressure to push the material to the direction of transverse movement of the tool. This was due to the tool geometry so, the requirement of new tools was realized. The tool geometry has a significant role to play in the joining process. The probe and shoulder control the material flow that results in the shape of the joint hook geometry and also inducing of the adhesive bond between the polymer and the aluminium alloy plates. The inadequacy of the old tool and its problems were eliminated to a greater extent by a new improved set of tools. The modular tool has three different parts such as tool body, shoulder, and probe.

In section 5.2, the material and properties that are used for the tool manufacturing are presented. Tool steel H13 was used, which is a widely used material for tool manufacturing. In section5.3, designing and production of the new tool is presented followed by section5.4 where several components of the tool are described. In section 5.5, the method for assembling various tool component into a single tool is presented. Moreover, in section 5.6, the most used tool for THE-FSpW and THE-FSSpW is presented.

5.2 Tool Material

All the parts of the tool used for the THE-FSpW process and the THE-FSSpW process were manufactured from tool steel H13.The tool steel H13 is a chromium-molybdenum-vanadium hot worked steel classified to group H by AISI, has the suitable mechanical properties required for the tool. The excellent resistance to abrasion at both low and high temperatures, high ductility, machinability, high-temperature strength and resistance to thermal fatigue made it suitable as a tool material. (Table 11) and (Table 12) list the chemical and mechanical composition of the tool steel listed [71]. All parts were heat treated (quenching + tempering) surface hardening by ionic nitration (avoiding threaded zones).

Table 11: Chemical Composition of H13 Tool Steel

Element	Content (%)
Chromium, Cr	4.75-5.50
Molybdenum, Mo	1.10-1.75
Silicon, Si	0.80-1.20
Vanadium, V	0.80-1.20
Carbon, C	0.32-0.45
Nickel, Ni	0.3
Copper, Cu	0.25
Manganese, Mn	0.20-0.50
Phosphorus, P	0.03
Sulfur, S	0.03

Table 12: Mechanical Properties of H13 Tool Steel

Properties	Metric
Tensile Strength, (ultimate)	1200 - 1590 MPa
Tensile Strength, (yield)	1000 - 1380 MPa
Reduction of Area	50.00%
Modulus of Elasticity	215 GPa
Poisson's Ratio	0.27-0.30

5.3 Designing and Producing New Tool

During the development of the THE-FSpW process, new tools especially probes of various geometry were designed and developed. The tool body is an improved prototype of the existing tool used for the initial test. The significant changes were made in the shoulder and probe. Probe design with eight different variations such as conical, cylindrical and hybrid (combination of both cylindrical and conical) was developed. All probe has left-hand threads.

The hybrid probe enhanced and improved the joining quality for the THE-FSpW process and was used further for development and optimization of the process parameters. The result obtained from the newly designed hybrid probe was significantly better than the conical and cylindrical threaded probe. Similarly, for the THE-FSSpW process conical left hand threaded probe was used for development and optimization of the process parameters. The modeling of the probe was done using PTC Creo parametric 3.0.

5.4 Tool Components

5.4.1 Tool Body

The tool body holds the shoulder and probe, which is then mounted to the FSW machine. The torque and forces are transferred from FSW machine to the probe and shoulder through tool body due to which it requires withstanding mechanical stresses. (Figure 25) is a schematic of tool body used for the THE-FSpW process and the THE-FSSpW process. The detail drawing of the tool body is attached in the appendix.

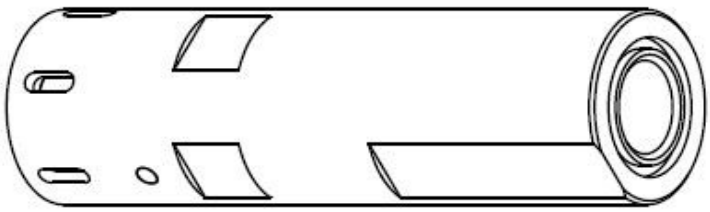

Figure 25: Tool Body

5.4.2 **Shoulder**

The shoulder in the THE-FSpW process is responsible for the application of adequate pressure on the plates which is required to obtain adhesive bond between aluminium plate and polymeric material surface and make a tight joint. The 5-degree concavity on the shoulder helps to squeeze in the aluminium towards the weld point by preventing the flash to escape. (Figure 26) Shows the schematic of shoulder used in the THE-FSpW process. During the initial test for the THE-FSpW process, a flat shoulder was used for the test during which there was excessive loss of the material as flash which was eliminated by the use of the new shoulder. The detail drawing of the shoulder is attached in the appendix.

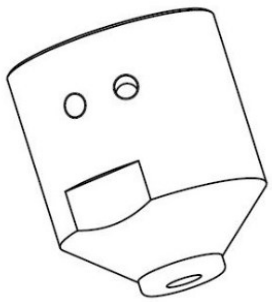

Figure 26: Shoulder

5.4.3 **Probe**

The probe designed plays a vital role in the THE-FSpW process. The probe is responsible for the shear deformation and deposition of the visco-plastic material into the polymer. During the initial test of the THE-FSpW development, the conical and cylindrical probe was used which had the problem of, the excess loss of material during penetration of the probe and less deposition of visco-plasticized material. The existing probe designs were not equipped for producing joint. The problems while using the conical probe were different to that occurred using the cylindrical probe. Moreover, some of the problems occurred during the use of conical probe was eliminated while using the cylindrical probe and vice versa which made us design a hybrid probe which is the combination of the conical and cylindrical probe. A series of 4 different conical probes (Figure 27) and hybrid probe (Figure 28) were designed. from the testing, the hybrid probe produced a good joint with the elimination of the existing problem. The further test was carried out using the selected hybrid probe in (Figure 29). The detail drawing of probes is attached in the appendix.

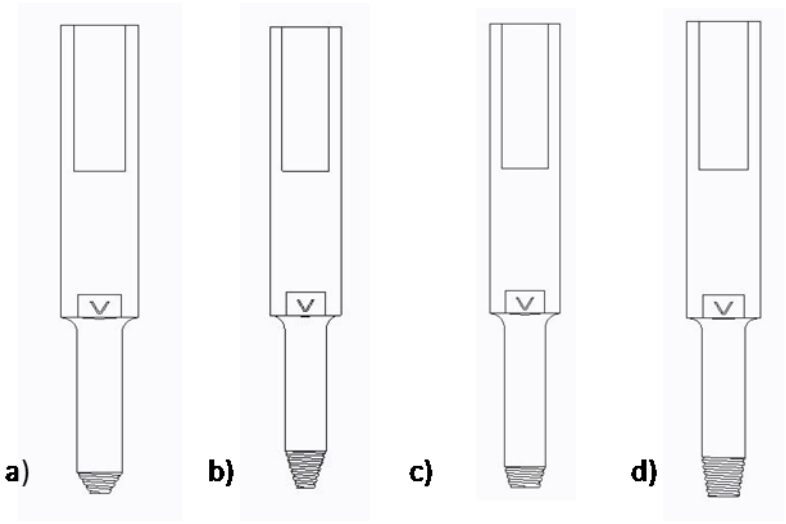

Figure 27: Four Different Set of Conical Probe

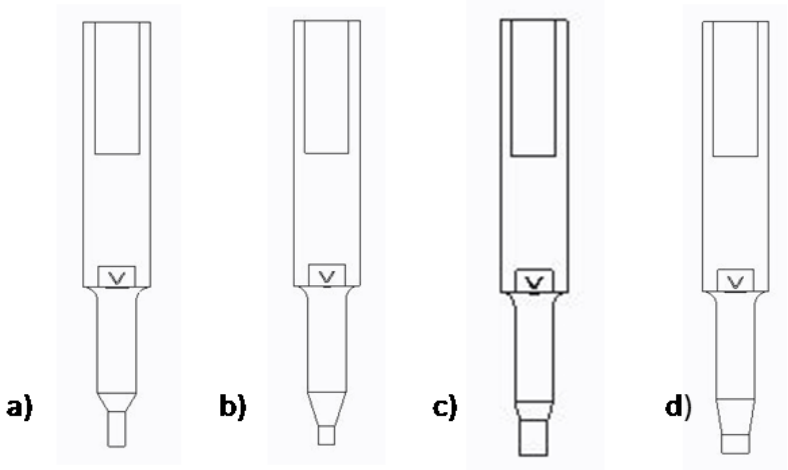

Figure 28: Four Different Sets of Hybrid (Conical + Cylindrical) Probes

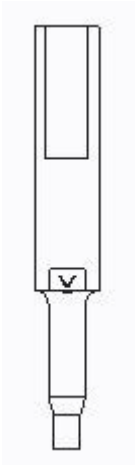

Figure 29: Selected Hybrid Probe Used for Further Development of THE-FSpW Process

5.5 Tool Assembly

The tool has three modular parts, tool body, shoulder and probe (Figure 30a). Initially, the probe is fastened to the tool body which has a slot with helical threads for the probe. The probe is fixed using the screws to prevent its rotation. Similarly, the shoulder is fastened to the tool body, which also has a slot with helical threads for shoulder and fixed using screws to prevent its rotation. The probe and shoulder can be adjusted as per the probe length requirement. The final assembly of a tool resembles (Figure 30b).

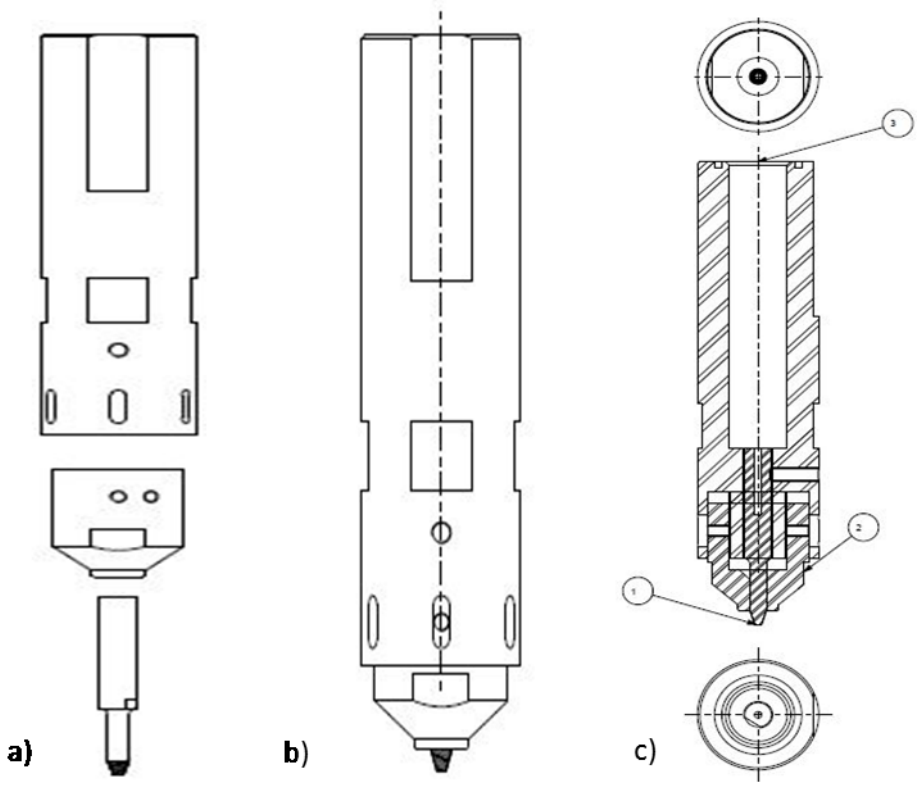

Figure 30: THE-FSpW Tool (a) Exploded View; (b) Assembled View (c) Sectioned View

5.6 THE-FSpW and THE-FSSpW Tool

The tool (Figure 31) is used for joining polymer to aluminium alloy plate for the THE-FSpW process, and the THE-FSSpW process. The tool holder and shoulder were similar for both the processes, but the probe used was different.

Figure 31: THE-FSpW and THE-FSSpW tool

A set of the tool was used for drilling hole and slot on the steel plate. A collet chuck holder was used to drill the hole in the stainless steel plate using FSW machine, and the hole position was later used as the plunging point for the THE-FSpW tool. The tool consists of components, i.e., collet holder, collet, drill bit (Figure 32). The same set of tool was also used to make slot on the stainless steel plate for THE-FSSpW process using the milling machine.

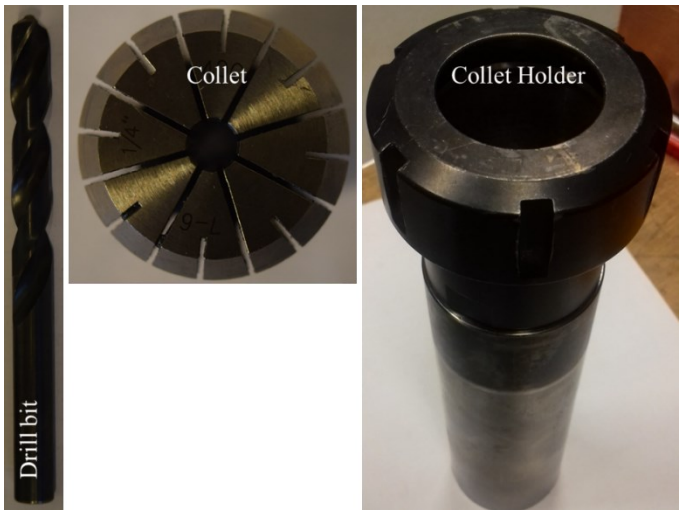

Figure 32: collet holder, collet, drill bit

Both the tool are inserted into the FSW machine spindle which has a tool cooling system. A set of O-ring and Teflon tape is used during tool assembly, to prevent coolant leakage.

6 Development of THE-FSpW

6.1 Introduction

The chapter presents the development of the THE-FSpW process. The overall strategy behind this work was to explore the feasibility and then develop the new polymer to aluminium alloy joining process termed as THE-FSpW. The various development phases of the joining process are discussed.

In section 6.2 development of experimental conditions are presented which include the preparation of test pieces, theory behind the use of the stainless steel plate with a hole in between the aluminium alloy plate and the polymer and the development of the new clamping system.

In section 6.3 the various performance assessment parameters that were set to assess the joining process is presented, and in section 6.4, the various process parameters involved in the joining process is presented. In section 6.5 the various process variables involved in the joining process is presented.

In section 6.6, the experimental approach for the development of the THE-FSpW process is presented. In section6.6.1 feasibility test carried out on several different combinations of material is presented. The initial tests were done to explore area such as material properties requirement, process parameters and variables, experimental conditions, tool design and clamping arrangement required for the joining process.

In section 6.6.2, the effect of the tool design and the materials physical geometry on the joining process were explored. The selection of material to be joined and process parameters used at this stage were selected on the basis of findings from the feasibility tests. This phase sums as the heart of development phase and most critical findings for the THE-FSpW process was in this phase.

In section 6.6.3, the influence of each process parameter was individually studied and optimized to get a set of optimal parameters. The primary parameters were the rotational speed, weld position, dwell time and offset travel. The minor parameter- depth of the hole in the polymer which also has some effect in the joint is explored. All the parameters were individually studied and varied by manual inspection and analysis. The change in parameters was made after assessing the joint made on the previous test. All the process parameter were explored similarly.

In section 6.7, the optimization of the process parameter for the selected base material is presented. The material chosen was based on its commercial use and also with physical, mechanical, thermal and optical properties suitable for the THE-FSpW process. The selection was made to define the newly developed process the THE-FSpW as a good option for commercial application.

The next step was to characterize the joint through metallographic analysis, and mechanical testing explained separately in details in chapter 8 and chapter 9. Finally, with the results obtained from the joint characterization of the joint produced by the THE-FSpW process, a new process was developed to improve the result. The process is termed as THE-FSSpW

(Through Hole Extruded-Friction Stir Spot Welding) which development is presented in chapter 7.

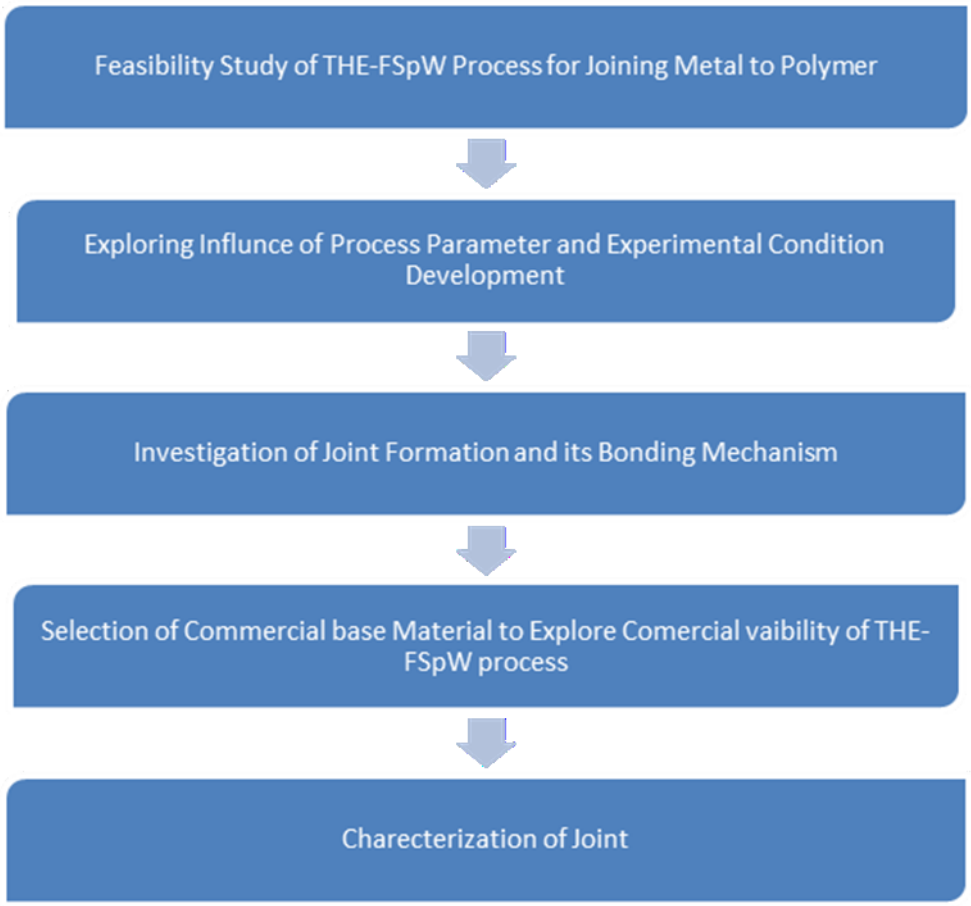

Figure 33: Flow Chart of Development Phase of THE-FSpW Process

6.2 Development of Experimental Conditions

6.2.1 Test Pieces

The test piece used was commercially used aluminium grades (AA5754 and AA AA2024), stainless steel plate (AISI 316) and engineering polymers (PEEK and Polyamide). Detail description of the material is done in chapter 4.

During the initial test, the dimension of test pieces was variable depending on the test requirement. One of the primary dimension used for the development process were 50mm*50mm*6mm for the aluminium plate (55mm*55mm*1mm for stainless steel plate with a 7mm diameter through a hole in the center and 25mm*25mm*10mm for the polymer. The test specimen dimension was changing continuously as per the requirement during the development of the THE-FSpW process.

The test pieces are to be arranged in the form of sandwich structure, such that, in the bottom lies the polymer, stainless steel plate in the middle and the aluminium on the top. A through hole is required to be made in the stainless steel plate through which the visco-plasticized aluminium pass through into the polymer and form the joint hook. The typical arrangement of the test piece is as shown in (Figure 34).

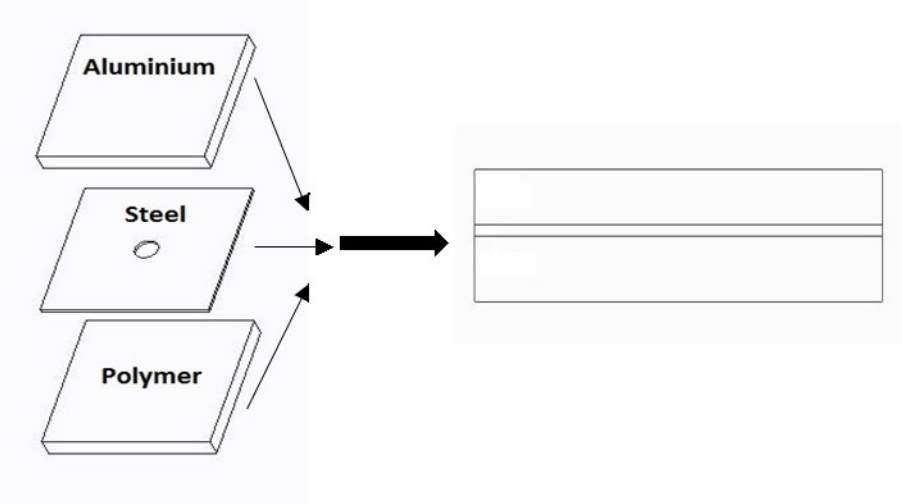

Figure 34: Test Pieces Arrangement

6.2.2 Stainless steel Plate and Plate Geometry.

In general, the concept of whole joining process is based on extruding the viscoplastic metal to the polymer surface. The rigid material and its geometry, which is used as a medium for extruding should have melting point temperature higher than the material that is to be extruded through it. The hole geometry on the material acts as die for extrusion process involves the joining process.

In these work, the material used for the development of the joining process is aluminium and polymers. Therefore stainless steel plate (Figure 35) was chosen as a material that is kept in between and used as an extrusion die. The stainless steel plate has a critical part of both the THE-FSpW process and the THE-FSSpW process. The use of stainless steel plate has a significant role to play to create joint hook between the polymer and aluminium alloy. The various reason for using the stainless steel plate are:

- The hole geometry on the stainless steel plate is a crucial aspect of the whole work. The guided extrusion of the visco-plasticized aluminium into the polymer creates a control deposition of aluminium and create a hook geometry to anchor the aluminium alloy plate to the polymer, i.e., a proper joint is formed between two material.
- To create a thermal barrier between aluminium alloy and the polymer, i.e., there is a minimum transfer of heat generated due to frictional heating during the process from aluminium to polymer. Due to this a stainless steel material with lower thermal conductivity was selected for the application.
- To also acquire the material properties of stainless steel which can enhance overall properties of the multi-material structure.

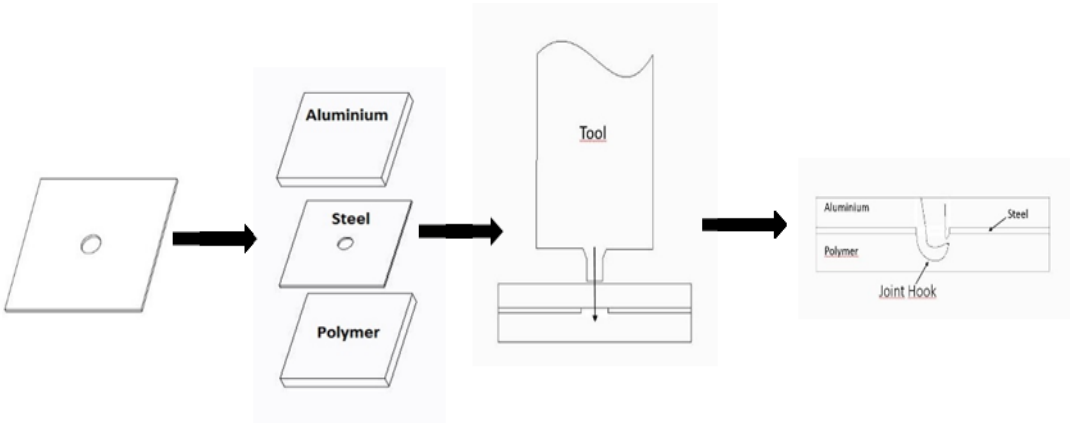

Figure 35: Schematic Diagram for the Use of Stainless steel Plate in THE-FSpW Process

The Stainless steel material with lower thermal conductivity was a criterion in the selection of a stainless steel material. AISI 316 was chosen as a rigid plate material for whole work. Description and properties of a stainless steel material are discussed in chapter 4.

6.2.3 Clamping System

A new clamping arrangement was developed during the development of the THE-FSpW process. THE-FSpW process involves clamping of three layers of materials (i.e., aluminium plate, stainless steel plate and polymer plate) with a proper alignment. The stainless steel plate has a through hole of a required diameter, and the polymer to have a blind hole of similar diameter and depth. The test specimen is positioned in order (Figure 35) such that in the bottom lies the polymer, stainless steel plate in between, and aluminium alloy plate on the top. The position at which the tool penetrates in the aluminium plate should be parallel and aligned with the hole on the stainless steel plate below it so that the viscous-plasticized aluminium and the probe can go through the hole and deposit it into the polymer. The plasticized aluminium form a hook shape that anchors aluminium alloy plate to the polymer. An offset of 0.5-1.0 mm was used to generate a joint hook thickness.

During the initial test, the three-layer specimen alignments were done manually, and the joining process was carried out. The specimen was clamped using stationary copper blocks with the cooling arrangement and fixed on the table using the nut and bolts (Figure 36). The joint produced were acceptable, but the joint hook thickness was inconsistent.

Figure 36: Old Clamping System

Since the offset traveling of the tool by 0.5 to 1.0 mm controlled the joint hook thickness, the manual positioning and alignment of the test specimen were not accurate enough to get consistent hook thickness. This led to the idea of positioning the plunging point on the aluminium alloy plate by using the FSW machine, for which a new clamping arrangement was made. The other reason to develop a new clamping system was also to incorporate various cooling arrangement to minimize the temperature during the joining process and prevent degradation of the polymer due to high temperature.

The various component of the clamping system is shown in (Figure 37a) table vice and (Figure 37) copper blocks.

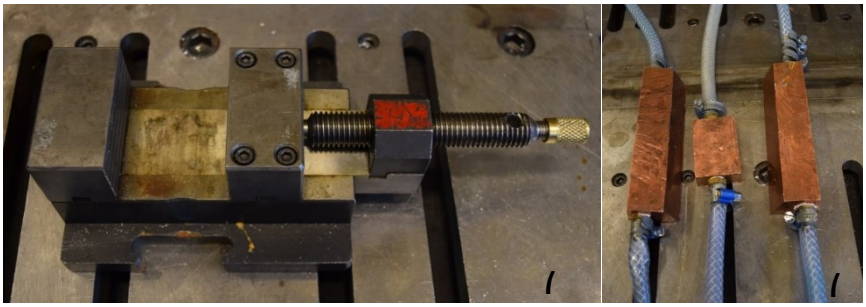

Figure 37: (a)Table Vice and (b) Cooling Arrangements

The new clamping system has the control over consistency and repeatability of joint hook geometry for the THE-FSpW process. In the new clamping system arrangement (Figure 38) the material is clamped using procedure listed below:

- A table vice clamp was used to clamp the stainless steel plate and the polymeric material. A copper base block equipped with the cooling arrangements was used on which the polymeric material rest.
- The FSW machine drills the hole using a drill tool (Figure 32), on the stainless steel plate and polymeric material together and the position of the hole was saved on the machine.
- The aluminium plate is clamped on the top using the two copper block equipped for cooling and fixed using the nut and bolts. THE-FSpW tool is used to join the aluminium alloy plate to the polymer using the previously saved position.

Figure 38: New Clamping Arrangement

6.3 Performance Assessment Parameters

A set of performance assessment parameters was set to assess the joint produced by the THE-FSpW process. For this Geometrical analysis of the joint hook and joining mechanism were taken into consideration. The geometrical analysis includes the factor such as the shape of the joint hook (thickness, volume, and orientation of hook) and depth of the hook into the polymer. Joining mechanism involves mechanical locking (joint hook), bonding (adhesive bonding from the melted polymer) and chemical bonding (bonding between metal and polymer in the joint interface). The joint, having a joint hook which has a proper thickness, the maximum volume of metal deposition, anchor-like shape and higher penetration to the polymer were considered good joint regarding 'geometrical factor.' The joint with minimum degradation of the polymer, a minimum flow of molten polymer out of the joint area towards the side or upwards, and a good overlapping mixture of metal and polymer were considered as the good joint regarding 'joining mechanism.' The whole work is a new process developed. The evaluation of joint was done by manual observation of the hook with the performance assessment guidelines as mentioned above.

6.4 Process Parameters

Initially, the process parameters and variables were adopted from the set of parameters that were used for the typical friction spot welding process. Then, necessary process parameters that could be important for the joining process is selected. The process parameter selected are as follows:

- **Rotational Speed**: The rotational speed of the friction spot welding tool, which is used to join the metal to the polymer. The rotational speed of the tool is utilized to create friction heat when it plunges into the aluminium metal surface. The heat generated at the interfaces by frictional dissipation and internally by bulk plastic deformation visco-plasticize the aluminium. The rotational speed has a direct influence on the amount of heat generation by friction. It also has an indirect effect on the joint hook geometry.

- **Weld Position**: The weld position has the direct effect on the joint hook formation into the polymer which is further explained in detail in the material geometry development section 6.6.2.

- **Dwell Time**: The dwell time has a direct effect on the joint hook stability. Minimum dwell time can have an adverse effect on the geometry of the mechanical joint hook. Higher dwell time can create defect on polymer due to thermal degradation.

- **Offset Travel**- It affects the geometry of the joint hook directly. The thickness of the joint hook depends on the offset value.

The indirect process parameters such as reference force, plunging speed, pre and post cooling time and depth of hole on polymer was selected and investigated briefly. Initially, the various test was done to find out the minimum and maximum value for the selected process parameter. The detail explanation on the selection of parameters ranges is experimental approach section 6.6.

6.5 Process Variables

The primary process variables that were investigated are:

- **Temperature**: The temperature were directly associated with the process parameters. Since the process involves two material with a huge difference in there melting temperature, the temperature was related to the material with low melting point (in this case polymer). The temperature was assessed with the amount of thermal degradation, burning of the polymer, molten polymer on the interface and outside the joining area. The different set of process parameters induces different temperature related defects. The optimization of the process parameter to minimize the thermally induced defect was a major challenge of the work.

- **Heating Time**: this variable was associated with the process parameters, rotational speed and the dwell time. The variable has a direct influence on the visco-plasticizing of aluminium, the formation of joint hook and thermal degradation of the polymer.

There are other various variables that can influence the process are related to the mechanical and physical properties of the base material used for joining, is not explored in this work.

6.6 Experimental Approach

6.6.1 Feasibility Study of THE-FSpW Process.

Initially, the selection of the material to be joined were random. The test was carried out to verify the concept of the THE-FSpW and also its feasibility and joinability of the metal to the polymer. The aluminium alloy mostly 5000 series, AISI316 stainless steel plate and different polymer material such as polycarbonate, polyamide, and PEEK were used. The approach was to join the aluminium alloy to the polymer utilizing various process parameters and different joining conditions. The repeated testing with various parameters and joining conditions were done. For each tests analysis of joint was done based on performance assessment parameters. From the findings, a further set of process parameters and the variables involved in the THE-FSpW process were refined.

The test involves the joining of aluminium alloy to the polymer; the initial process parameter was chosen in such a way that, they were enough to form a visco-plastic aluminium with less heat generation, to prevent the polymer surface degradation due to the heat. The initial test was done mostly on the polycarbonate (Figure 39). The temperature during the test exceeds the melting point of the polymer which results in burning and melting of the polycarbonate surface because the heat generated during the visco-plasticizing of the aluminium was very high. The primary objective of the initial test was to create a good flow of visco-plasticized aluminium and deposit it into the polymer so that, it forms a joint hook-like structure inside the polymer that can anchors aluminium and the polymer.

From the result obtained on a different test and its analysis concluded that, due to the low melting point of the polycarbonate, the deposition of visco-plasticized aluminium into it resulted in the formation of very inconsistent hook regarding its geometry and direction. The inconsistent volume of the hook is also due to the loss of visco-plastic aluminium in the form of flash. The inconsistent direction of the hook is due to the softening of the polymer which

let the visco-plastic aluminium to flow in the direction which is more susceptible to the heat transferred from the aluminium flow. These findings lead us to choose a polymeric material with higher melting point than the polycarbonate such as PEEK and Polyamide 6.

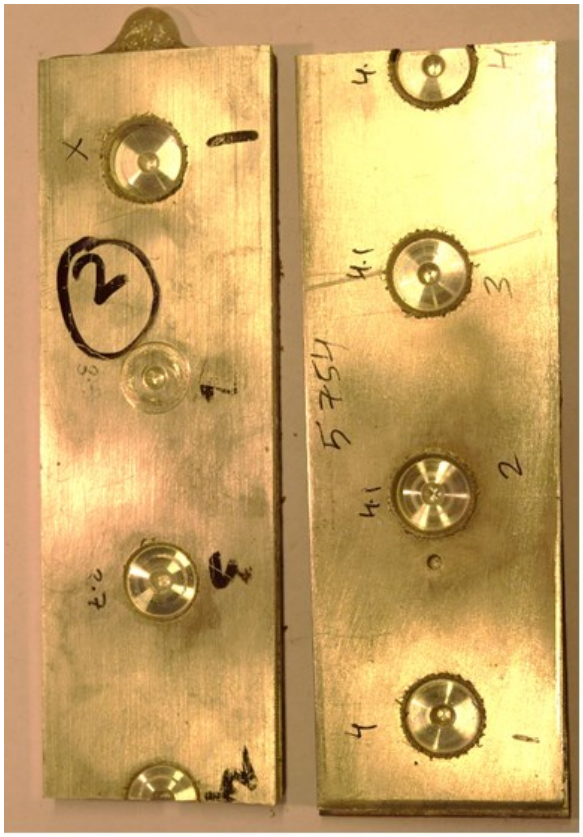

Top View

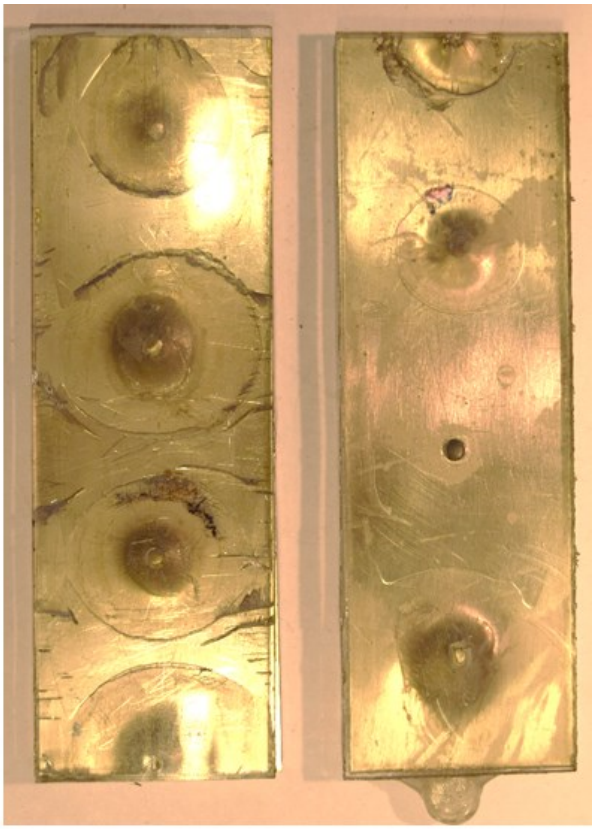

Bottom View

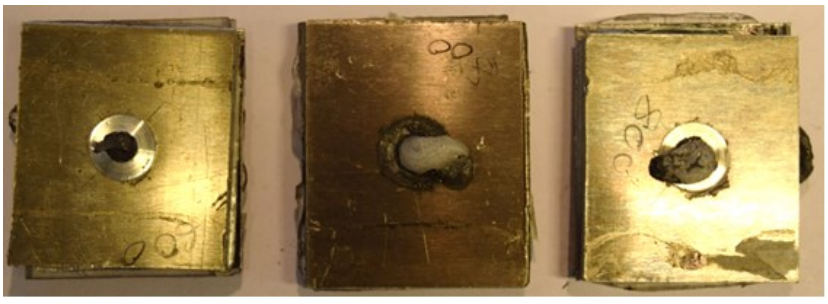

Top View

Bottom View

Figure 39: Feasibility Test Carried out with Aluminium and Polycarbonate

6.6.2 **Material Geometry Development**

The development of the THE-FSpW process involves various test piece geometry (aluminium alloy plate, stainless steel plate and polymer). The geometry of test piece was evolving by findings from the continuous test and their analysis based on performance assessment parameters. In all the conditions discussed below, the process parameters was also optimized parallelly to get a set of the optimal process parameters. The changes were made on the basis of the result obtained from the preceding test analysis. There were several iterations of the changes that were made on the material geometry, the only changes that have significant changes in the result are discussed below.

- **Condition 1**
  - Aluminium plate- No hole.
  - Stainless steel plate- Through the hole of diameter equal to the minimum diameter of the probe.
  - Polymer plate- No hole.
  - The probe used- cylindrical threaded probe and conical threaded probe (Depth of probe travel is less or equal to the thickness of the aluminium).

A number of the test was carried out using the above condition (Figure 40), and with its analysis based on performance assessment parameters, further changes were made. The test was carried out with aluminium AA5754, AISI316 stainless steel plate and polymeric material (PEEK and polyamide).

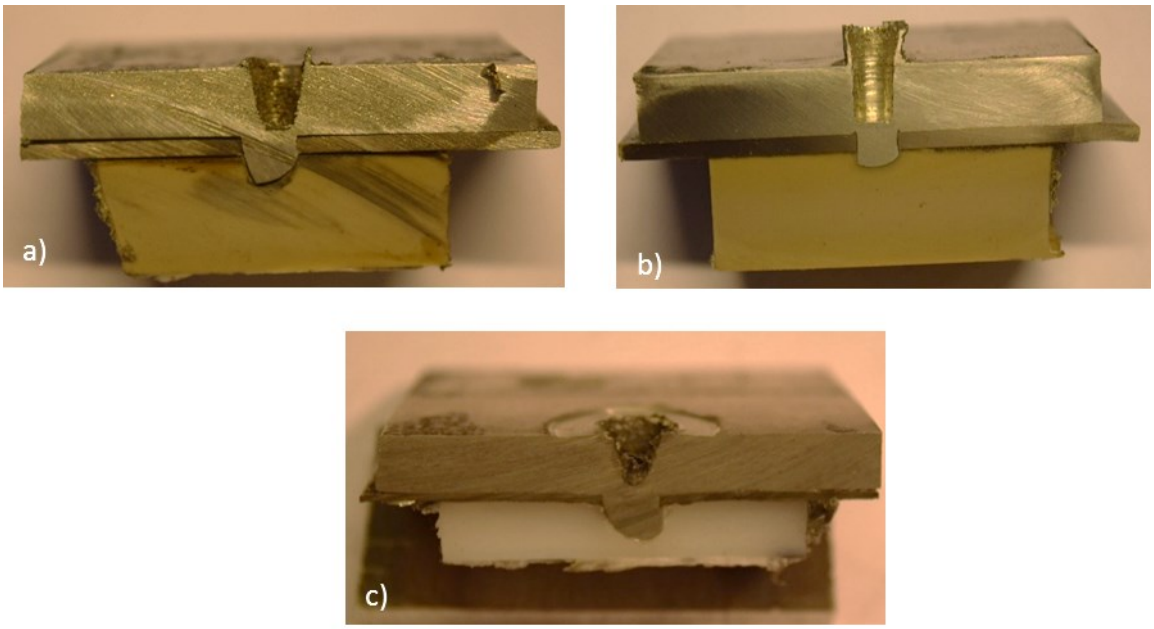

Figure 40: Test Sample Produced Using Condition 1- a) Test Specimen with PEEK Polymer, b)Test Specimen With Polyamide 6

Observation: The experimental test done with the test piece having above conditions have significant polymer surface deterioration, squeezing of the molten polymer outwards, loss of material as a flash generation, low deposition of visco-plastic aluminium on the polymer surface, poor hook formation.

Analysis: The polymer surface deterioration was due to the high temperature. The squeezing of polymeric material outward is because, to deposit the aluminium on the polymeric surface a part of it needs to be removed to accommodate it, due to which the excessive polymer whether vaporize or squeeze out. The loss of flash and low deposition of aluminium is due to the difference in the rate of the production of visco-plastic aluminium and its deposition on polymeric surface and due to the upward force from squeezing out of the molten polymer. The probe geometry is also not equipped to push the visco-plastic aluminium into the polymer. Poor joint hook formation is due to the not enough deposition of the aluminium which can form a hook on the polymer.

Changes: The hole on the stainless steel plate was increased and made equal to the maximum diameter of the probe to increase and ease the flow of visco-plastic aluminium. The analysis result was considered, and changes were made in the test piece geometries. In the polymer, a hole of 2.5-3mm deep and diameter equal to the hole on the stainless steel plate was made to increase the deposition of the aluminium and prevent the squeezing of the polymer. In aluminium, a hole 3mm deep and diameter equal to the minimum diameter of the probe was made to decrease the heat generation and minimize the polymer degradation due to excessive heat and decrease the loss of aluminium as flash. These changes are made in following condition 2.

- **Condition 2**
  - Aluminium plate- Hole 3mm deep with a diameter equal to the minimum diameter of the probe.
  - Stainless steel plate- Through the hole of diameter equal to the minimum diameter of the probe.
  - Polymer plate- 2.5 - 3mm deep hole equal to the diameter of the hole on the stainless steel plate.
  - The probe used: - conical threaded probe. (Depth of probe travel is approximately equal to the thickness of the aluminium).

A number of the test was carried out using the above condition (Figure 41) and its analysis based on performance assessment parameters further changes were made. The test was carried out with aluminium AA5754, AISI316 stainless steel plate and polymeric material (PEEK and polyamide).

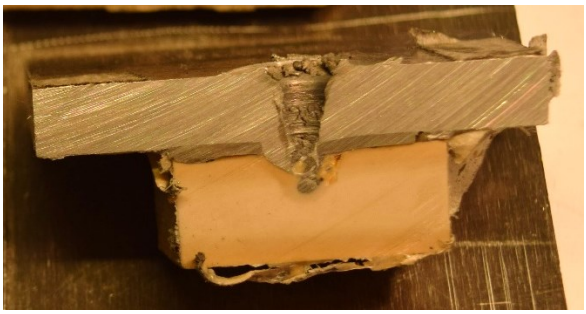

Figure 41: Test Sample with PEEK Polymer Produced Using Condition 2

Observation: The experimental test done with above conditions have reduced polymer surface deterioration but there was still significant, squeezing of the molten polymer outwards and reduction in loss of material as a flash, increased deposition of visco-

plasticized aluminium on polymer surface but not enough due to the pre-removal of aluminium, improved hook formation.

Analysis: The polymer surface deterioration was still due to the high temperature which is required to visco- plasticized the aluminium. Still some squeeze of polymer outward but was considered good because it acts as an adhesive and increases the joint strength. Still significant loss as flash which is likely due to the probe geometry.

Changes: The hole in the aluminium plate is to remove to have enough viscoelastic material to deposit on the polymer surface. Changes in the probe geometry were made, based on the observation. A new hybrid probe was designed which is a combination of the cylindrical and conical probe. More detail description on the probe can be found on tool design section of this work. A hole of diameter equal to the maximum diameter of the probe was made on stainless steel plate so that the probe can travel through the hole and deposit aluminium into the polymer. These changes are made in following condition 3.

- **Condition 3**
  - Aluminium plate- No hole.
  - Stainless steel plate- Through the hole of diameter equal to the maximum diameter of the probe.
  - Polymer plate- 2.5 - 3mm deep hole equal to the diameter of the hole on the stainless steel plate.
  - The probe used: - Hybrid probe (probe travel is into the polymeric surface, position at polymer were varied).

A number of the test was carried out using the above condition (Figure 42) and its analysis based on performance assessment parameters; further changes were made. The test was carried out with aluminium AA5754, AISI316 stainless steel plate and polymeric material (PEEK and polyamide).

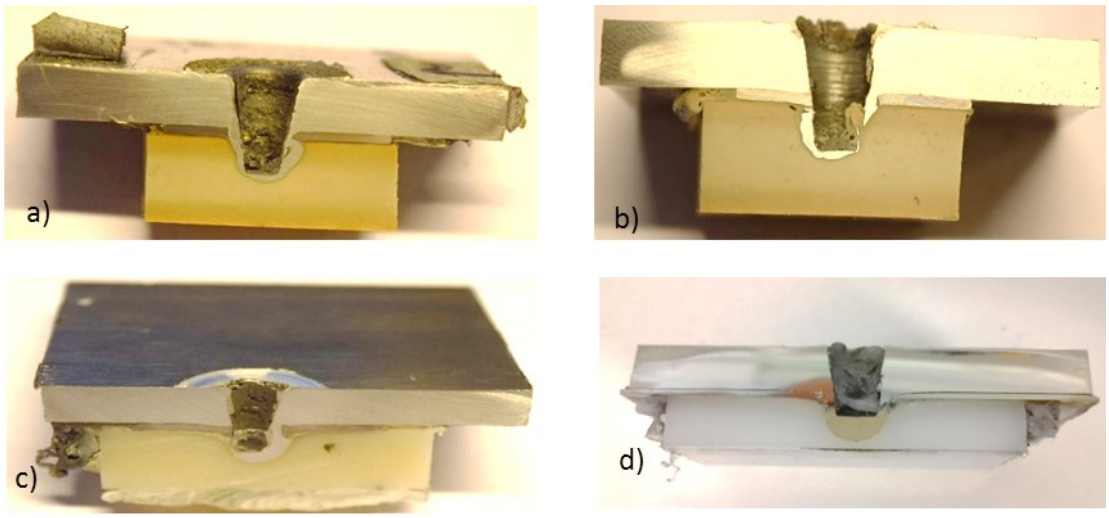

Figure 42: Test Sample Produced Using Condition 3, (a-b) PEEK Sample; (c-d)- Polyamide 6 Sample

Observation: The experimental test done with the test piece having above conditions have still significant polymer surface deterioration, reduction in squeezing of the molten polymer

outwards and reduction in loss of material as flash generation, increased deposition of visco-plastic aluminium on polymer surface, improved joint hook formation.

Analysis: The polymer surface deterioration was still due to the high temperature which was still uncontrollable but was less compare to above conditions. Still some squeeze of polymer outward, considered as good because it acts as an adhesive and increases the joint strength. Significant reduction in the loss of flash compared to the previous test, which is likely due to the improved probe geometry. The hook formation and joint strength were still not good enough due to the very minimum bonding between the polymer and aluminium, the aluminium deposited on the surface of the polymer have minimum contact and no mixture of polymer and aluminium.

Changes: To increase the hook thickness and make it consistent offset travel and new clamping system was introduced. These changes are made in upcoming condition.

- **Condition 4**
  - Aluminium plate- No hole.
  - Steel plate- Through the hole of diameter equal to the maximum diameter of the probe.
  - Polymer plate- up to 3mm deep hole equal to the diameter of the hole on the steel plate.
  - The probe used: - Hybrid probe. (Depth of probe travel is through the steel plate into the polymer. a penetration of 4mm into polymer surface was used from the findings from condition 3).
  - Offset travel of 0.5-1mm.

A number of the test was carried out using the above condition (Figure 43), and its analysis based on performance assessment parameters, further changes were made. The test was carried out with aluminium AA5754, AISI316 stainless steel plate and polymeric material (PEEK and Polyamide).

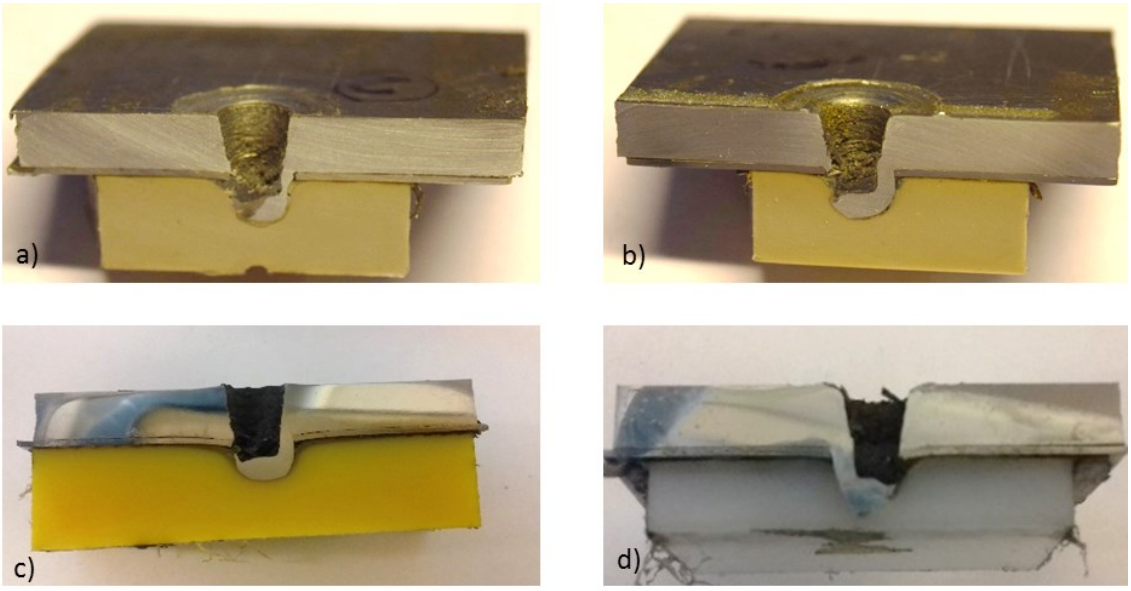

Figure 43: Test Sample Produced Using Condition 4 (a-b)-PEEK Sample ; (c-d)-Polyamide Sample

Observation: The polymer surface deterioration was still due to the high temperature which was minimized compared to above conditions. Still some aluminium material loss as flash but were decidedly less compare to above conditions. A right hook shape formation resulting in good joint strength compare to above conditions.

Analysis: The good joint strength is due to Mixture of polymer and aluminium create an overlapping of aluminium and polymer with each other in the polymer surface. The reason for inconsistent hook geometry is due to the inaccuracy in setting the plunging point for the tool. The problem was solved with the design of new clamping system.

Changes: No further major changes were made and the condition 4 was further used for development and optimization of the parameter to reduce the polymer surface degradation, reduce the loss due to flash and improve joint hook geometry.

6.6.3 Process Parameters Development

The THE-FSpW process parameters were developed and optimized by making joints on AA5754, AISI316, PEEK and Polyamide 6. The selected process parameters that were used for optimization are Rotational speed (RS), Weld position (WP), Dwell Time (DT), Offset travel (OT). All of this different process parameter was varied, and the test was carried out. The working parameters envelope for RS was between 500 rpm to 1000 rpm, for WP from 5mm to 13 mm, for DT from 0sec to 3 sec, OT from 0mm to 1 mm.

A detailed study of various parameters and its effect in joint hook formation were studied and are described below. The parameter was investigated on by one, i.e., a variation of one parameter with other process parameters kept constant. Based on the joint analysis for defect and joint efficiency the process parameter investigated were varied and optimized.

1. **Rotational Speed**

The rotational speed was varied in between 500 to 1000 rpm to obtain the optimum rational speed. At some point, a rotation speed up to 1800 rpm was used to see the effect of rotational speed on joint hook formation. The upper limit of 1000 rpm was set because rotational speed above that does not yield right joint and increase in degradation of the polymeric surface due to high heat generation.

2. **Weld Position**

Various weld position was used to find the possible optimum weld position to get the proper hook shape flow of aluminium into the polymeric surface. The range from negative 5 mm to 13 mm was used to understand its influence in the joint formation. The initial test was done with the weld position above the stainless steel plate, such that within the thickness of aluminium plate used for joining. Eventually, it was increased to obtain proper joint hook. From weld depth starting above the stainless steel plate at 5 mm to the weld depth of 13 mm such that 6mm into the polymer was studied and the best maximum weld depth was chosen.

(Figure 44) moreover, (Figure 45) shows some example of the evolution of hook by varying the weld depth.

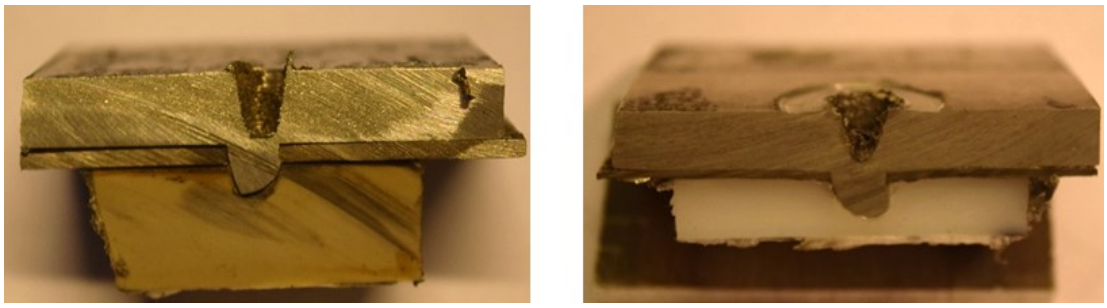

Figure 44: Sample with weld depth less or equal to the thickness of the aluminium plate.

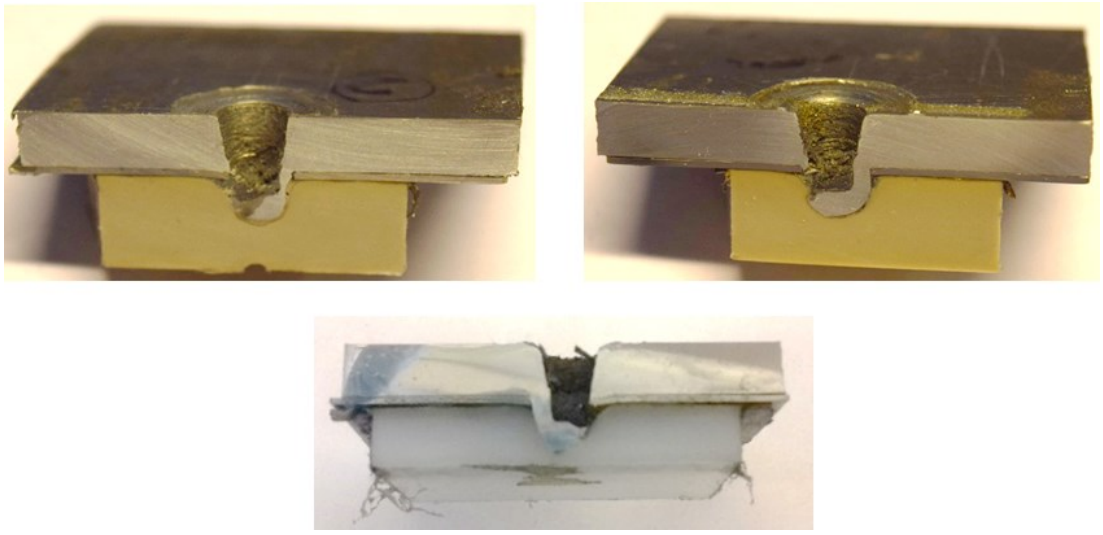

Figure 45: Sample with Weld Depth Between (9-13) mm

3. Dwell Time

The dwell time was used from zero seconds to 3 seconds. The upper limit of 3 seconds was set after studying the test result where the degradation and burning of the polymer were higher in dwell time higher than 3 sec. There was considerable degradation of the polymer when 3 sec dwell time was used.

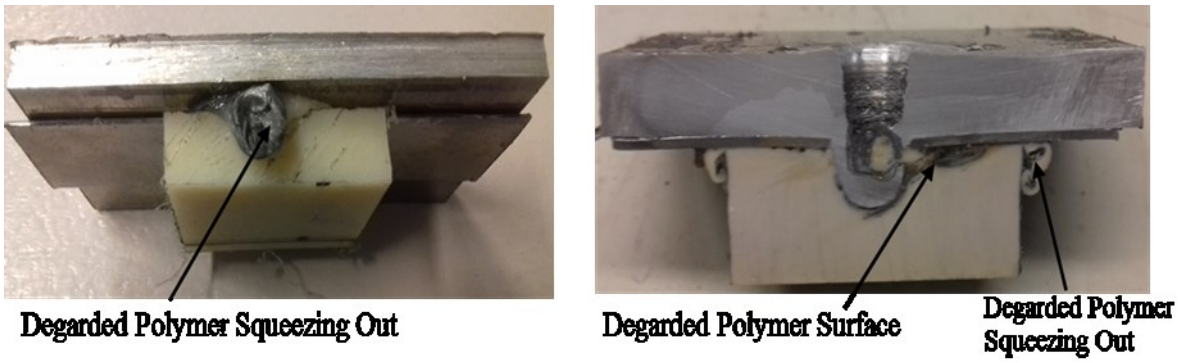

Figure 46: Polymer Degradation Due to Excessive Heat

4. Offset Travel

Initially, the test was done without offset. With the development of the process, the requirement of offset was realized and introduced as a process parameter. Offset were used to increase the thickness of the joint hook by deposition of more visco plasticized aluminium into polymer surface. The use of offset increases the thickness of joint hook and also increase the joint hook volume. An offset of 0.5 mm to1 mm was investigated.

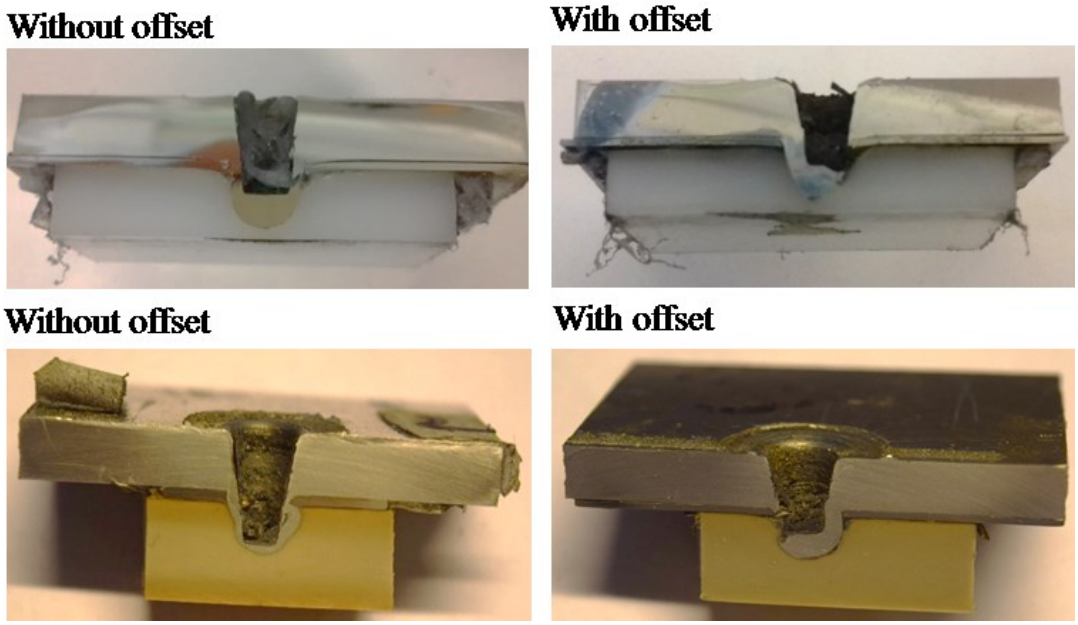

Figure 47: Joint Hook Thickness Geometry Without and With Offset

6.6.4 Set of Optimal Parameters

Table 13: Process Parameters for Both Aluminium AA5754-H111 and Aluminium AA2024-T351

Parameters	For Peek width -10mm	For PA6 width-10mm
Rotational Speed(rpm)	900	600
Weld Position(mm)	-11	-11
Tool Plunge (mm/s)	0,2	0,2
Reference Force (kN)	8	8
Control	Position	Position
Dwell Time (sec)	2	2
Offset Travel (mm)	0.5	1.0
Diameter of Hole in Stainless steel Plate	Diameter- 7mm Through Hole	Diameter - 7mm Through Hole
Diameter and Depth of Hole in PEEK Plate	Diameter -7mm and Depth -3mm	Diameter -7mm and Depth -3mm

6.7 Optimization of Process Parameters for Selected Base Materials

This phase of the THE-FSpW development proceeded with the systematic selection of engineering materials that are commercially used. The selection was made to define the newly developed process of joining the aluminium alloy to the polymer as a good option for commercial use.

The two aluminium grades AA5754-H111 and AA2024-T351, both commercially used in automobile and aerospace industries were chosen. AISI316 stainless steel grade was chosen based on its physical and thermal properties. Polymer (PEEK and PA6) were chosen because they are commercially used and have higher melting point compare to other polymers. The further test was done to optimize the process parameter for each combination of the selected material to produce controllable and repeatable joint. The test piece used for optimizing parameters for the test follow the condition 4. All the test were carried out using the same test conditions. The different material combination selection and the description of the optimized parameter are discussed in sections below.

6.7.1 Joining of AA5754-H111 and PEEK

The test was carried out using the material geometry (condition 4), new clamping system. The parameters were optimized by carrying out various tests and its analysis based on performance assessment parameters; further changes were made.The sets of optimized process parameter for joining the AA5754-H111 to PEEK are tabulated in (Table 13).The primary parameters further optimized from the value obtained from (Table 13) was the rotational speed and the offset travel. They were further optimized to have a good flow of visco-plastic aluminium and to increase the thickness and overall geometry of joint hook.

6.7.2 Joining of AA5754-H111 and PA6

The test was carried out using the material geometry (condition 4), new clamping system. The parameters were optimized by carrying out various tests and its analysis based on performance assessment parameters, further changes were made The set of optimized process parameter for joining the AA5754-H111 to PA6 are tabulated in (Table 13).The primary parameter was further optimized from the value obtained from the (Table 13) were the rotational speed and the offset travel length. The rotational speed was decreased to prevent burning of PA6 which has low melting point compared to PEEK. The loss of PA6 by burning are very significant at higher rotational speed losing the joint hook integrity with the polymer surface. The offset travel length was further increased to improve the joint hook geometry.

6.7.3 Joining of AA2024-T351 and PEEK

The same parameter (Table 13) used for joining the AA5754 and PEEK were used for joining the AA2024-T351 and PEEK as well. The joint obtain and the hook geometry were similar to that obtained for the AA5754-H111.

6.7.4 Joining of AA2024-T351 and PA6

The same parameter (Table 13) used for joining the Aluminium5754 and PA6 were used for joining the AA2024-T351 and PEEK as well. However, the joint obtain and the hook geometry were improved compared to that obtained for the AA5754-H111.

7 Development of THE-FSSpW

7.1 Introduction

This chapter presents the development of the THE-FSSpW process which was developed to improve the failure load result obtained from the THE-FSpW process tests. The two findings that were made during the characterization of the THE-FSpW test sample were the insufficient joint hook geometry regarding thickness and volume and the insufficient overlapping area between the polymer and aluminium at the joint hook intersection. This problem was overcome with the development of the THE-FSSpW process.

In section 7.2, the feasibility test of AA5754-H111 to PEEK is presented. All the process parameter were similar to THE-FSpW process with additional process parameter 'weld length' In section 7.3, the systematic selection of weld length parameter is presented. In section 7.4, optimization of weld depth to probe length is presented. Moreover, in section 7.5, the optimal parameter are tabulated.

7.2 Joining of AA5754-H111 to PEEK.

The process parameter and experimental condition developed For the THE-FSpW process was used for the THE-FSSpW process for few initial test to join aluminium alloy to the polymer. The test was done with AA5754-H111, AISI 316 and PEEK. A slot in the stainless steel plate, a slot blind hole on PEEK were pre-made using the milling machine. (Figure 48) show one of the first joints made.

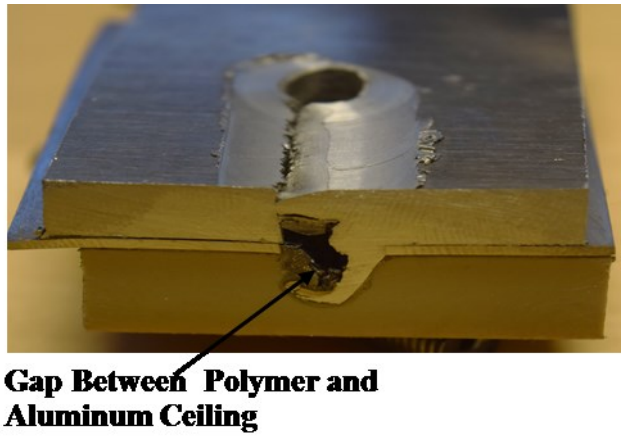

Figure 48: THE-FSSpW Sample with Gap Between the Polymer Surface and Aluminium Ceiling

In (Figure 48) there is a gap between the aluminium and polymer in the joined area. To fill the gap for further test the slot blind hole was eliminated from the PEEK surface. It filled the gap observed initially and also increased the overlapping area which increases multi-material contact. Several tests were carried out to see the feasibility of the process (Figure 49).

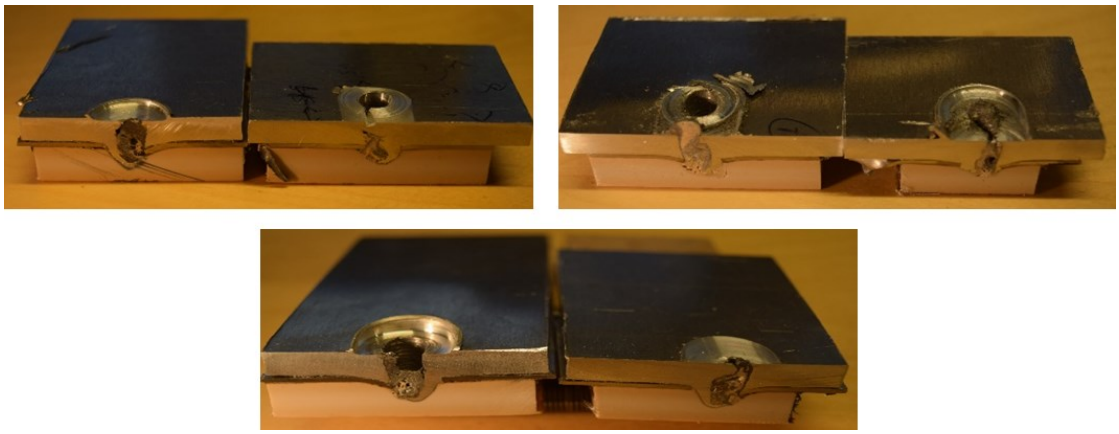

Figure 49: Feasibility Test of THE-FSSpW Process

The pressurized outward flow of the polymer was observed at the plunging point (Figure 50). A hole similar to the THE-FSpW process was made at the point where the tool initially plunges to minimize the pressurized outward flow of polymer.

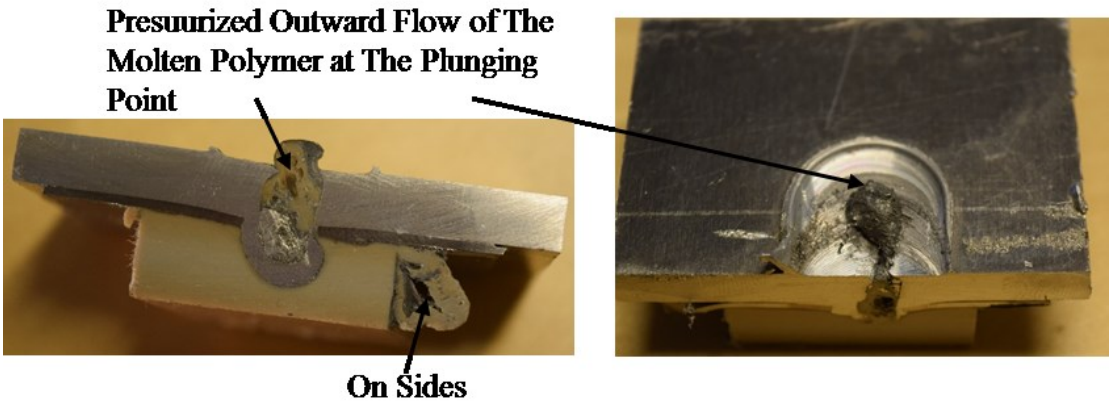

Figure 50: Pressurized Outward Flow of the Polymer at The Plunging Point

7.3 Selection of Weld Length Parameter

The weld length was determined by the probe diameter and shoulder diameter of the tool used for the joining process. The relation between the tool dimension and weld length was established for a systematic evaluation of weld length effect on the joint strength in future work. Three possible combinations of weld length discussed are in (Table 14).

Table 14: Different Weld Length

Combination	Probe Diameter (7mm)	Shoulder Diameter (17mm)	Total Length
1	2xProbe Diameter	-	14mm
2	1xProbe Diameter	1xShoulder Diameter	24mm
3	-	2xShoulder Diameter	34mm

Out of the three possible combinations, the combination 2 which is the sum of probe diameter and shoulder diameter was chosen for the further test and development of the THE-FSSpW process on this work.

7.4 Optimization of Weld Depth to Probe Length

A small design of experiment was made to optimize the weld depth process parameter (Table 15). In addition to weld length, all the process parameter similar to the THE-FSpW process was used. Only the weld depth concerning probe length was varied. A machine tilt angle of 2.5 degrees was used for all the test.

The optimization of the probe length to the weld depth was done to find out the optimum combination that can yield a joint with minimum surface flash, entirely closed weld surface and the acceptable joint hook into the polymer surface.

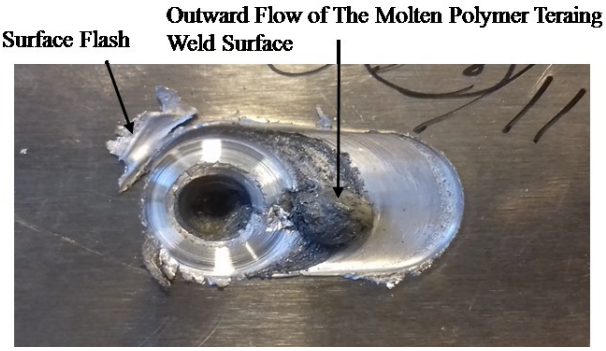

Figure 51: Problem in Weld Before Weld depth to Probe Length Optimization

Table 15: Design of Experiment for Probe Length to Weld Depth Ratio(varying probe length and weld depth)

Probe length:10mm	Weld depth:9.4mm		Probe length:10mm	Weld depth:9.8mm
				

Probe length:11mm	Weld depth:9.4mm		Probe length:11mm	Weld depth:9.8mm
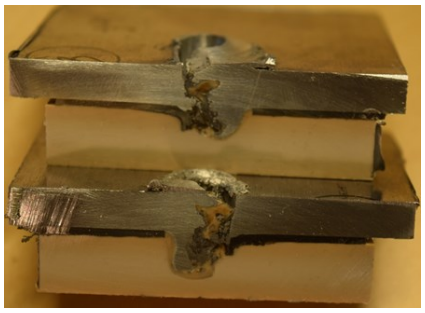				

The lower limit and higher limit for both the probe length (10 mm -11 mm) and for weld depth (9.4 mm - 9.8mm) were set beforehand and test were carried out. Form the experimental test the weld depth to probe length combination of 9.4/10 and 9.8/10 resulted in better result regarding joint hook geometry, the low pressurized outward flow of polymer and less surface flash.

The range between the 9.4/10 and 9.8/10 was further explored to optimize the weld depth to probe length ratio. Several tests with a fixed probe length of 10mm and the weld depth of range from 9.4 to 9.8 were explored to find out the optimum combination. The several tests carried out are shown in (Table 16).

Table 16: Design of Experiment for Probe Length to Weld Depth Ratio(fixed probe length and varying weld depth)

Probe length:10mm	Weld depth:9.4mm	Probe length:10mm	Weld depth:9.5mm
			
Probe length:10mm	Weld depth:9.6mm	Probe length:10mm	Weld depth:9.7mm
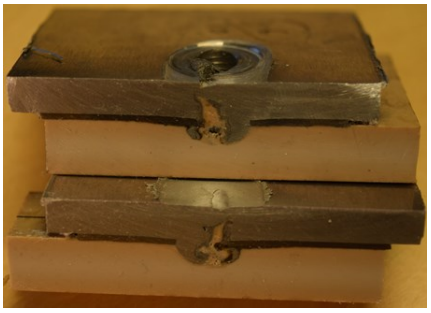			
Probe length:10mm	Weld depth:9.8mm		
			

From the above test result, the weld depth to probe length ratio of 9.7/10 was chosen since it had the acceptable joint hook geometry, less surface flash and closed weld surface (Figure 52). All the further test were carried out using the same ratio.

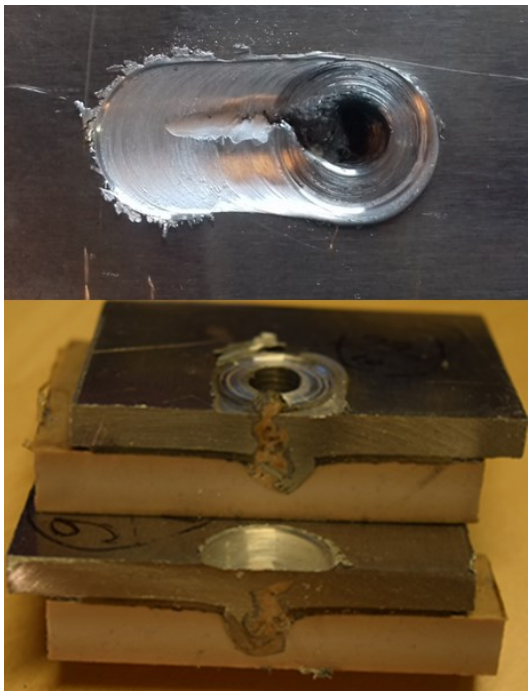

Figure 52: Test Weld Sample with the 9.7/10 Ratio of Weld Depth to Probe Length

7.5 Set of Optimal Parameters

The optimal parameter set is listed in the table: All the further test and test specimen were prepared using the tabulated set of parameters in (Table 17).

Table 17: Optimal Set of Parameter's for THE-FSSpW Process

Parameters	For PEEK Width -10mm
Rotational Speed(rpm)	900
Probe length(mm)	10
Weld position(mm)	-9.7
Welding speed(mm/min)	175
Tool plunge (mm/s)	0.2
Reference force (kN)	8
Control	position
Dwell time (sec)	1(at plunging point)
Offset length in Y Direction (mm)	1mm (from the center)
Weld Length (mm)	22-24
Diameter of Hole in Stainless steel Plate	Diameter- 8mm Through Slot of 26mm

8 Microscopic Characterization

8.1 Introduction

To understand the microscopic features of the joint produced from both THE-FSpW and THE-FSSpW process, they were characterized by optical microscopy. The primary objective of this study was to characterize the joint hook geometry, possible bonding mechanism, polymer degradation at the metal-polymer interface and the difference in material characteristic between the processed area and base material. The detailed metallographic analysis was conducted on a sample prepared using the set of optimal parameters.

In this chapter, microscopic characterization of both the THE-FSpW and the THE-FSSpW sample are presented. In section 8.2 macrostructure analysis of the THE-FSpW sample is presented and in section8.3, macrostructure analysis of the THE-FSSpW sample is presented. In section 8.4 the microstructure analysis of both the THE-FSpW and the THE-FSSpW is presented. Finally in chapter 8.5 geometrical parameterization is presented.

AA5754, AISI316 and PEEK polymer are the material involved in the sample used for microscopic characterization of the joint hook for both the joining processes.

For the THE-FSpW samples, the metallographic analysis was done at the center of the spot weld. Sample was cut as shown in (Figure 53).

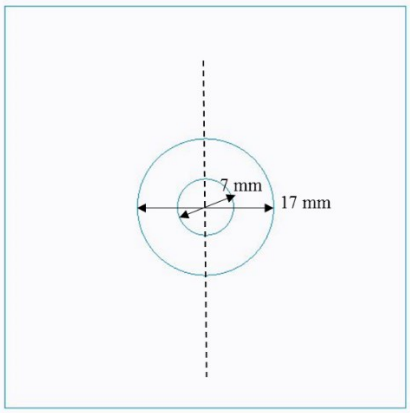

Figure 53: Sample Cutting Position for THE-FSpW

For the THE-FSSpW metallographic analysis was done at the five various section along weld length in transverse direction (Figure 54) and one sample in the longitudinal direction. (Figure 55).

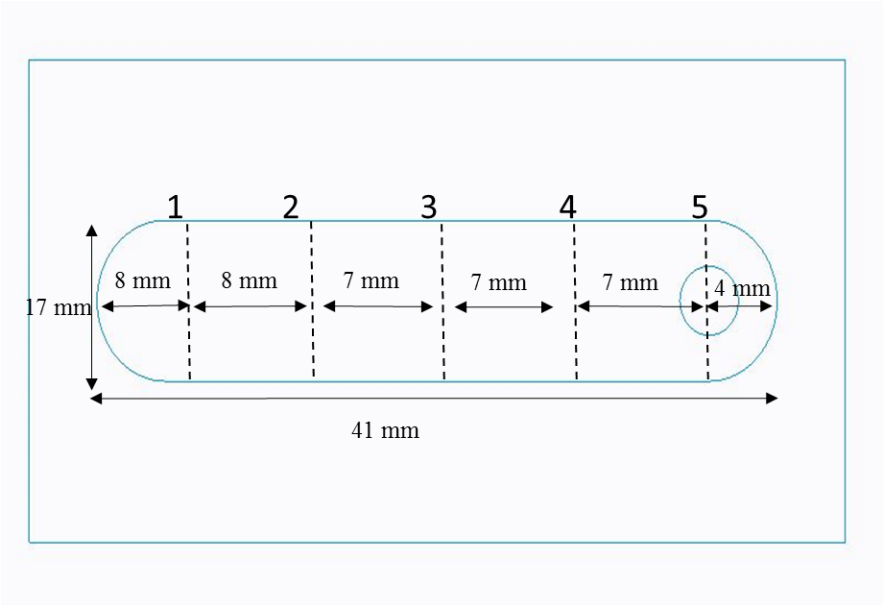

Figure 54: Sample Cutting Position for THE-FSSpW (Transverse Direction)

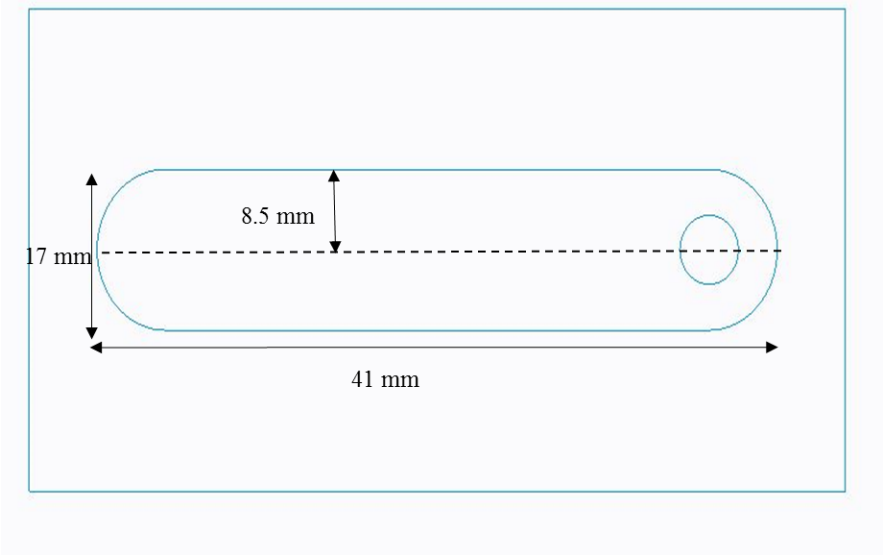

Figure 55: Sample Cutting Position for THE-FSSpW (Longitudinal Direction

8.2 Macrostructure Analysis of THE-FSpW

The macrostructure analysis was done on specimen produced from the THE-FSpW process using optimal parameters. It was carried out to understand the geometry of the joint hook, to assess the polymer surface condition at the metal and polymer material interface. The specimen was cut approximately in the center and studied (Figure 53). The sample for micrograph analysis was prepared as described in section 4.5.3. Since the sample has three different material involved, they were studied before etching and after etching to prevent the degradation of the polymer surface with the etchant used for aluminium alloy. The etchant used was explicitly for aluminium alloy. Three sets of the picture were taken for all the sample, i.e., before etching (aluminium focused (Figure 56) and polymer focused (Figure 57)) and after etching (aluminium focused (Figure 58)). Only one set of pictures were taken after etching with aluminium focused since the etchant used was aluminium specific.

8.2.1 **Before Etching**

- **Aluminium Focused**

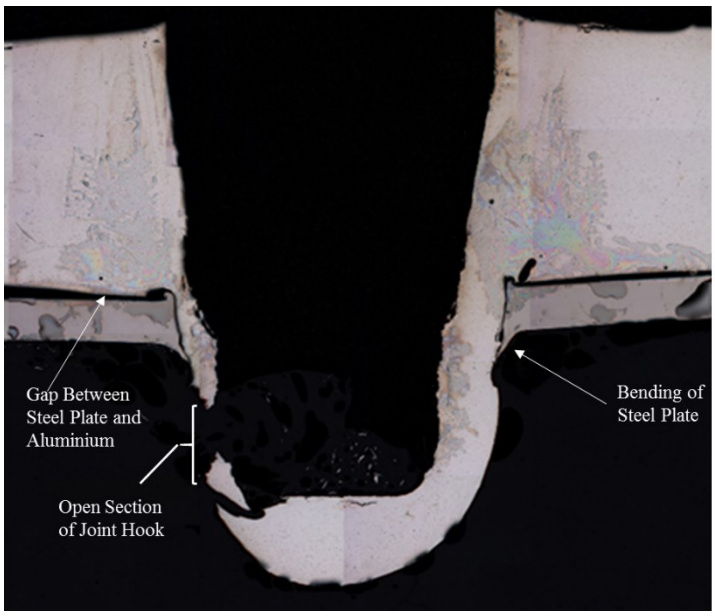

Figure 56: Geometry of the Joint Hook While Aluminium Focused

The first sets of micrograph were taken with aluminium in focused. In (Figure 56) is the geometry of the joint hook produced by the THE-FSpW process. The open section of the joint hook is the result of offset travel of (0.5mm-1 mm) used to increase the thickness of the joint hook and to create the aluminium/polymer overlap around the joint hook geometry (Figure 57). The bending of stainless steel plate is due to its movement during the joining process when the polymer surface where it rests, soften due to the high temperature. The gap between the aluminium and stainless steel plate interface is due to the bending of stainless steel plate and due to the squeezing of the polymer in between the two plate interfaces. There are also visible aluminium particles suspended in the polymer creating an aluminium/polymer mixture.

- **Polymer Focused**

The second sets of micrograph were taken with the polymer in focus to see the polymer condition, and polymer degradation due to high temperature at the overlap area and the aluminium/polymer interface. The squeezing of the polymer over the joint hook is due to the offset travel used during the process. The black dots (Figure 57) are the voids that are introduced their due to the vaporization of the polymer by the high-temperature condition during the joining process. The sponge-like structure over the top of the joint hook is a combination of voids and polymer (molten during the joining process and solidified after at room temperature). The polymer surface degradation can be seen throughout the area where the metal surface is in contact with the polymer surface. There are also visible aluminium particles suspended in polymer creating an aluminium/polymer mixture.

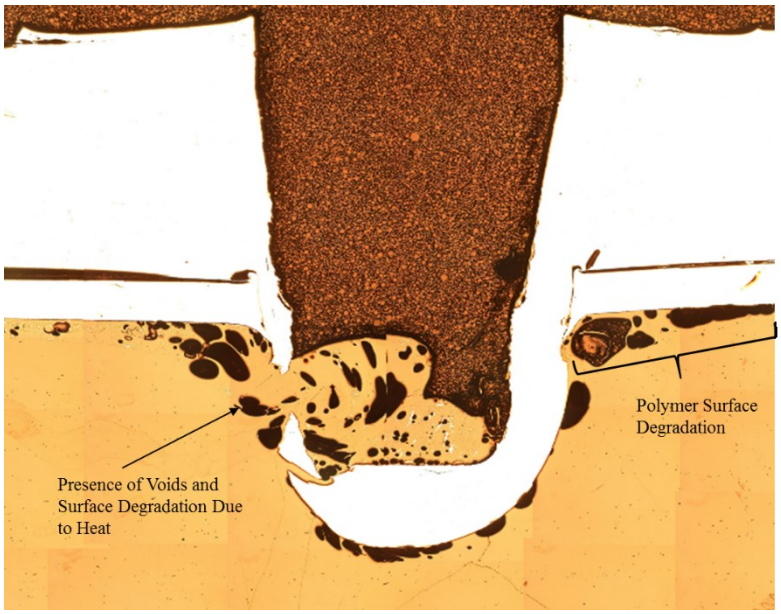

Figure 57: Geometry of the Joint Hook and Polymer Surface Condition While PEEK Focused

8.2.2 After Etching

The above sample (Figure 56) was then etched using the 10% hydrofluoric acid for about 25-30 seconds to see the material grain structure and flow direction on aluminium. Since the etchant used is specific for aluminium material, the third set of micrograph was taken with aluminium in focus only. In (Figure 58) the grain structure orientation and flow direction can be observed which reveals significant recrystallization and grain refinement at SZ and visible TMAZ, which is discussed in detail in section 8.4.1 microscopic analysis.

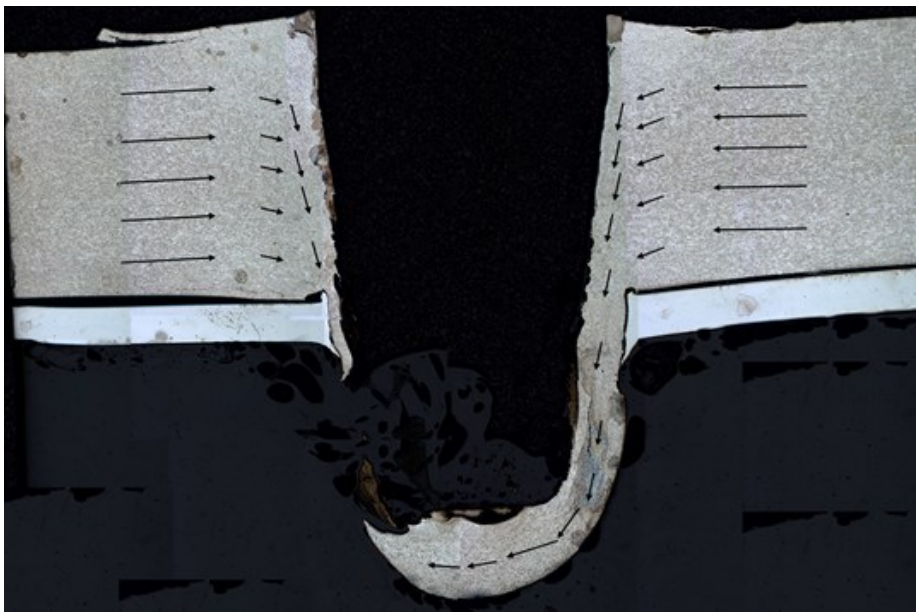

Figure 58: Etched THE-FSpW Sample

8.3 Macrostructure Analysis of THE-FSSpW

The macrostructure analysis of the specimen produced from the THE-FSSpW process using the optimal parameters. It was done on five different sections extracted from the same sample over the weld length. Various micrograph was taken and later merged to form a single picture which resembles the joint hook at various sections. Three sets of the picture were taken for all the sample, i.e., before etching (aluminium focused, and polymer focused) and after etching (aluminium focused).

The six sample (five in transverse direction over a weld length and one in the longitudinal direction) was prepared to observe the consistency of the joint hook geometry throughout the weld length. From the study, it was found that the joint hook geometry is consistent approximately to over 35% of total weld length (Figure 60). in the remaining 65% of weld length, the joint hook geometry starts to reduce, with no aluminium hook shape at the end of weld length (Figure 59) and (Figure 60) (aluminium focused). Similarly, the micrograph was also taken with polymer focused (Figure 61) and (Figure 62).

The inconsistency of the joint hook geometry is due to the insufficient visco- plasticized aluminium flowing to the polymer when the tool travels over the weld length and due to the pressurized outward flow of the molten polymer (as temperature increases when tool travel over the weld length) creating an upward thrust which opposes the deposition of visco – plasticized aluminium into the polymer.

8.3.1 Before Etching

- **Aluminium Focused**

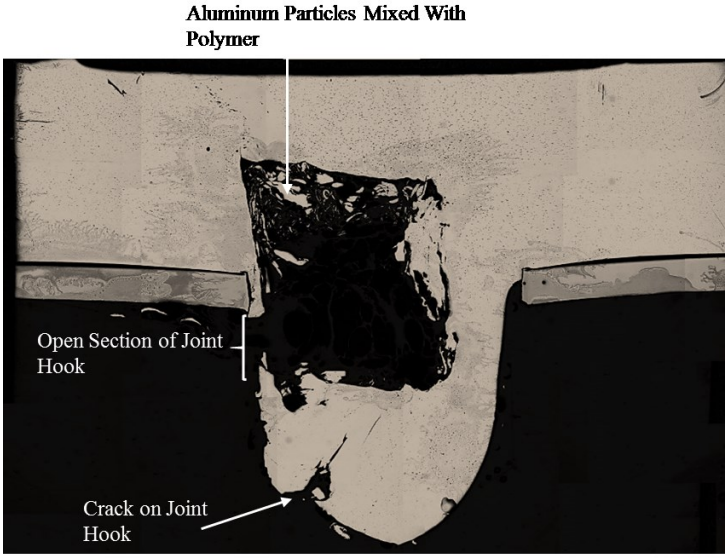

Sample 1

The larger joint hook geometry at the initial position (sample 1) is due to the presence of a blind hole into the polymer at the tool plunging point, which creates a larger area to accommodate the Vico-plasticized aluminium. There is a significant mixture of the aluminium particles and polymer in between the aluminium ceiling and top surface of the joint hook. The opening section of the joint hook is due to the offset length given initially perpendicular to the tool travel direction. The figures also reveal the presence of the crack at

a various section of the joint hook which is due to the intrusion of the molten polymer into the joint hook.

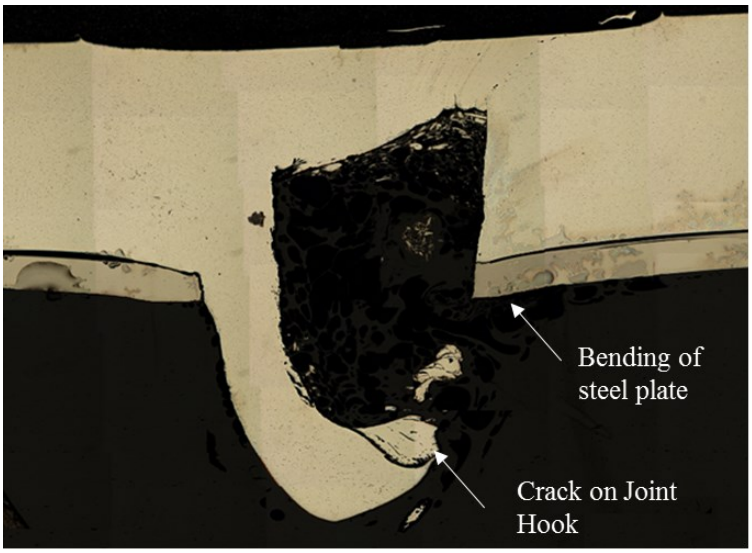

Sample 2

(Sample 2) Reveals the decrease in the joint hook geometry compare to (sample 1). Although there is the presence of proper 'joint hook.' The presence of a crack in the joint hook and the presence of mixture aluminium/polymer particles is due to the intrusion of the molten polymer into the joint hook.

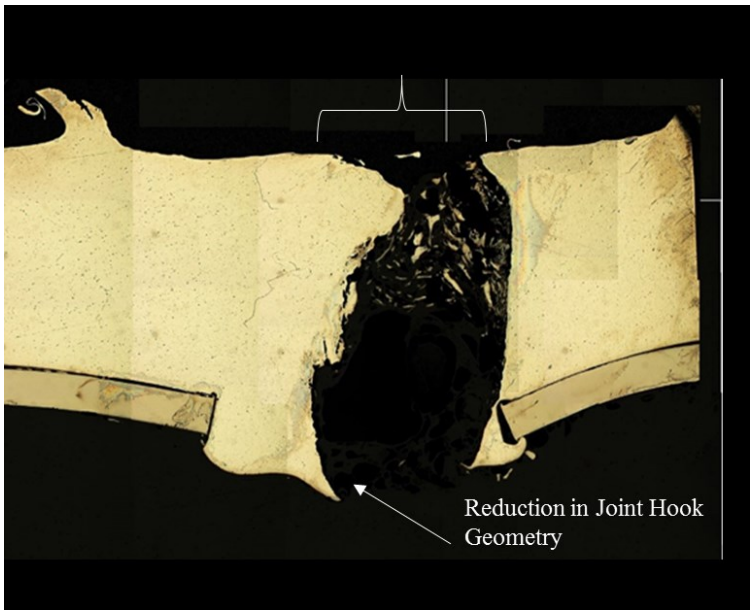

(sample3) Reveals no presence of the joint hook and opening of the aluminium ceiling due to the pressurized outward flow of the molten polymer. A multilayer mixture of aluminium particles suspended in the polymer can be observed.

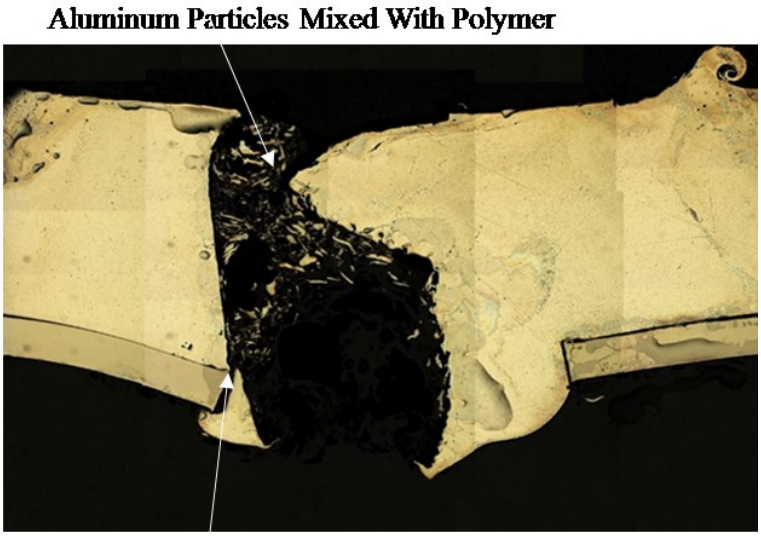

Sample 4

(sample 4) structure resembles (sample 3). It reveals the significant bending of the stainless steel plate. The bending of stainless steel plate is due to its movement during the joining process when the polymer surface where it rests, soften due to the high temperature. This also explains the occurrence of varying flash amount during the joining process while the same optimal parameter and experimental condition are used.

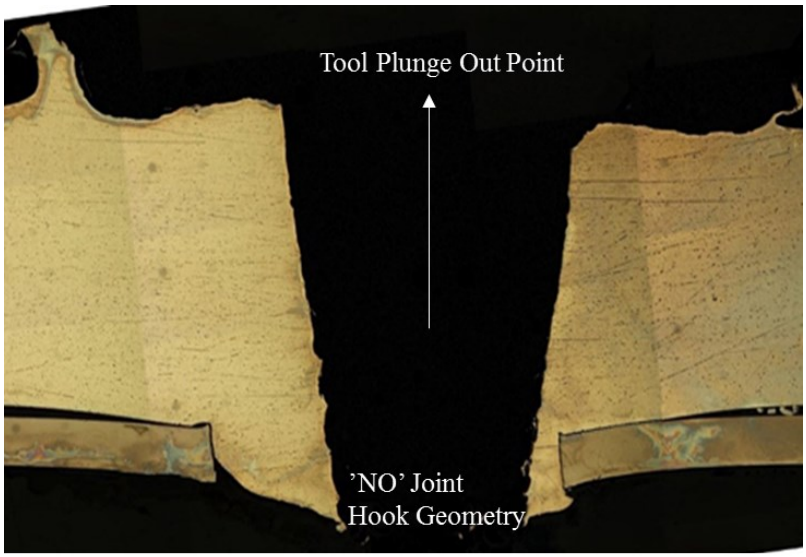

Sample 5

Figure 59: Geometry of The Joint Hook at 5 Different Section in Transverse Direction (Aluminium Focused)

(sample5) reveals there is minimum deposition of visco plasticized aluminium on polymer surface with complete loss of joint hook geometry at the end of the weld where tool plunges out.

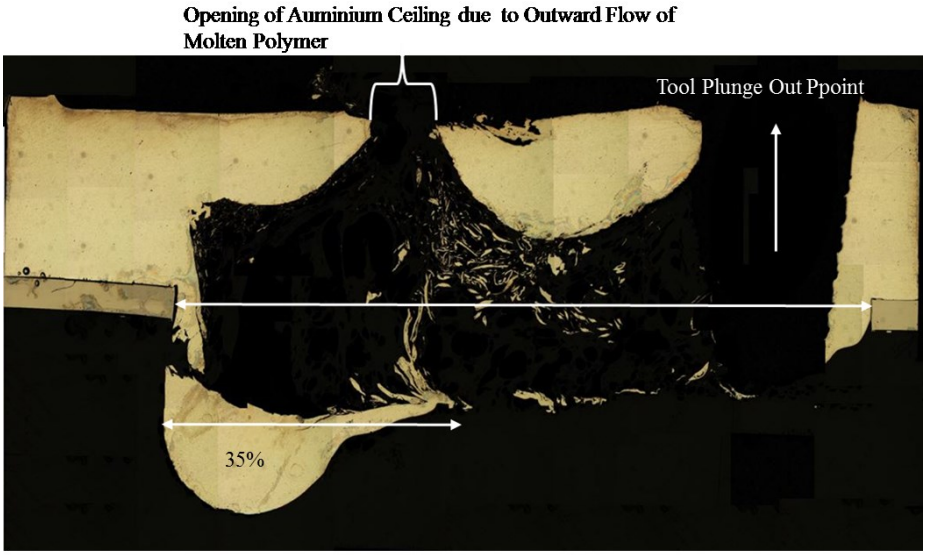

Figure 60: Geometry of the Joint Hook in Longitudinal Direction (Aluminium Focused)

The geometry of the joint hook was also studied in the longitudinal direction to see the consistency of the joint hook. The initial massive deposition of aluminium material on the polymer surface is due to the pre-drilled hole on the surface of polymer which accommodates substantial aluminium deposition during the plunging of the tool. The joint hook is consistent approximately to 35% of total weld length as in (Figure 60). The crack in the geometry is due to the intrusion of molten polymer into the joint hook geometry.

- **Polymer Focused**

The micrograph was taken with polymer in focus, to see the effect of high temperature on the polymer surface and polymer degradation at the overlapping area at the aluminium/stainless steel/polymer interfaces

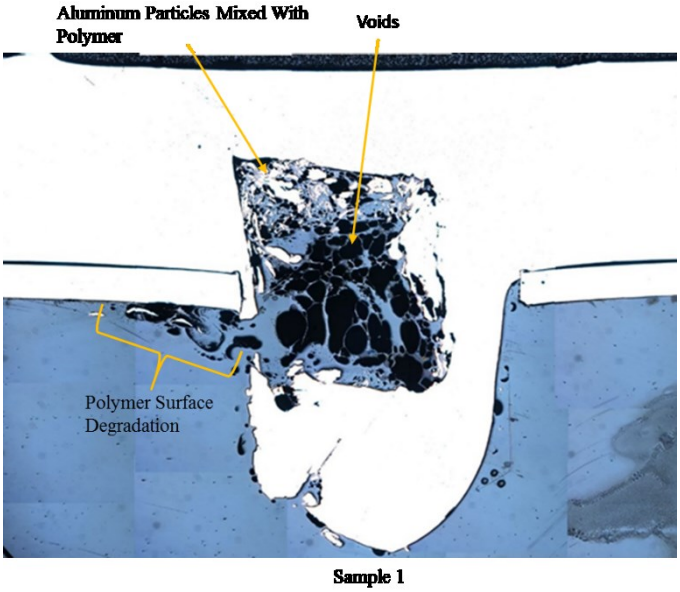

(smaple1) reveals the black dots, which are the voids introduced there due to the vaporization of the polymer by the high-temperature condition during the joining process. The sponge-like structure over the top of the joint hook is a combination of voids and polymer (molten during the joining process and solidified after at room temperature). It can be seen more aluminium particles suspended in the polymer and polymer surface degradation at aluminium/stainless steel/polymer interfaces.

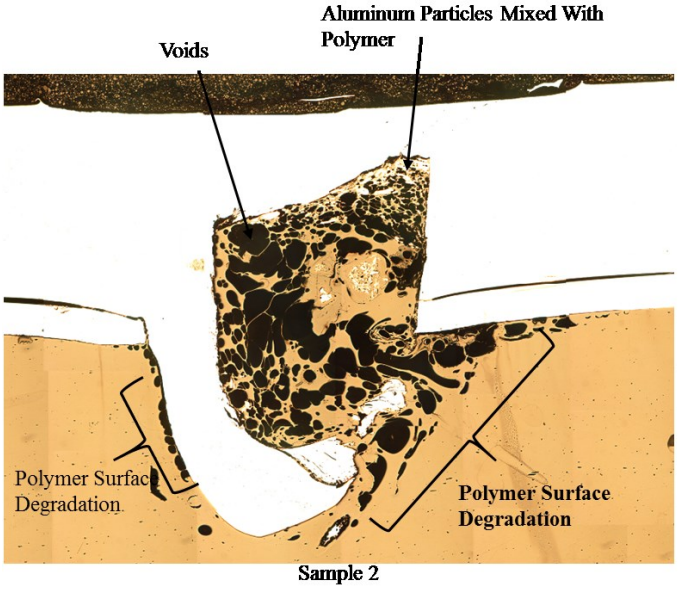

Sample 2

(Sample 2) Reveals polymer surface degradation at aluminium/stainless steel/ polymer interfaces. The sponge-like structure can be seen in between the aluminium ceiling and the joint hook top surface. Larger aluminium particles are seen suspended in the polymer.

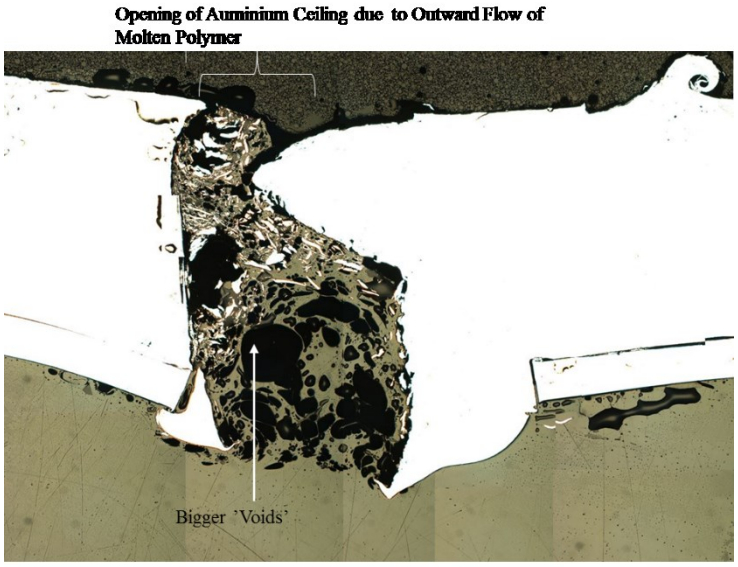

Sample 3

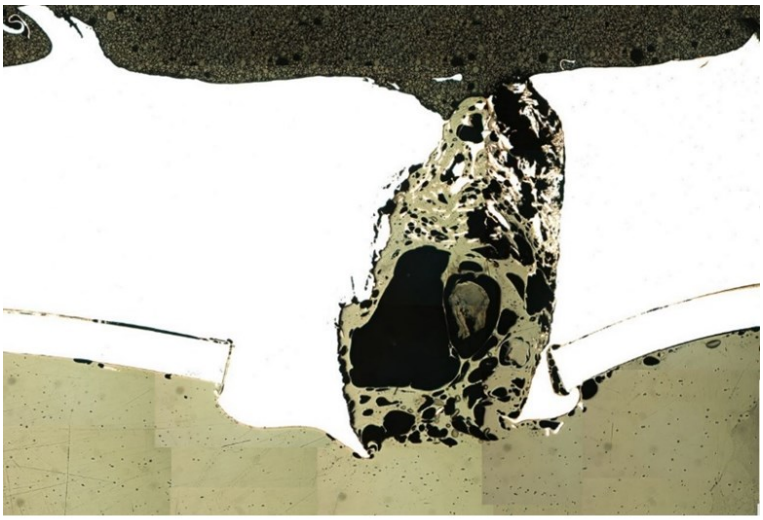

Sample 4

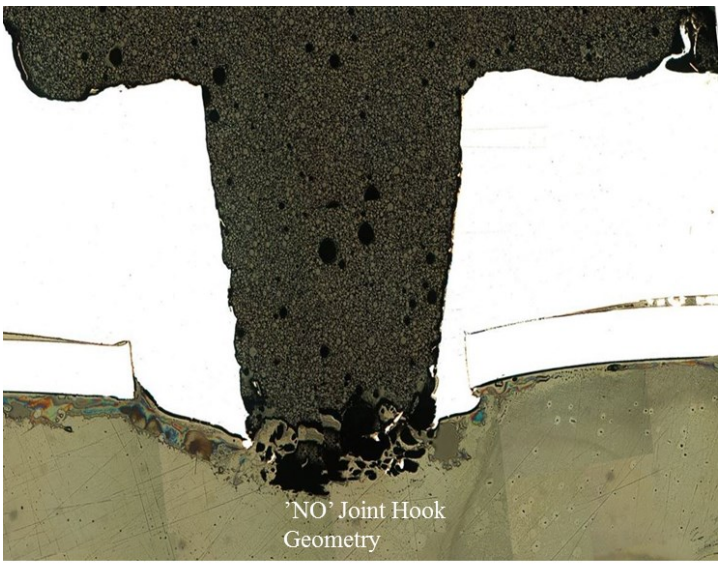

Sample 5

Figure 61: Geometry of the Joint Hook at 5 Different Section in Transverse Direction (PEEK Focused)

(sample 3), (sample4) and (sample5) has similar polymer surface condition as explained for (sample1) and (sample 2).

(Sample 6) (Figure 62)Reveals the polymer condition in the longitudinal direction. It has the similar polymer surface condition in the various positions as explained for the sample cut in the transverse direction.

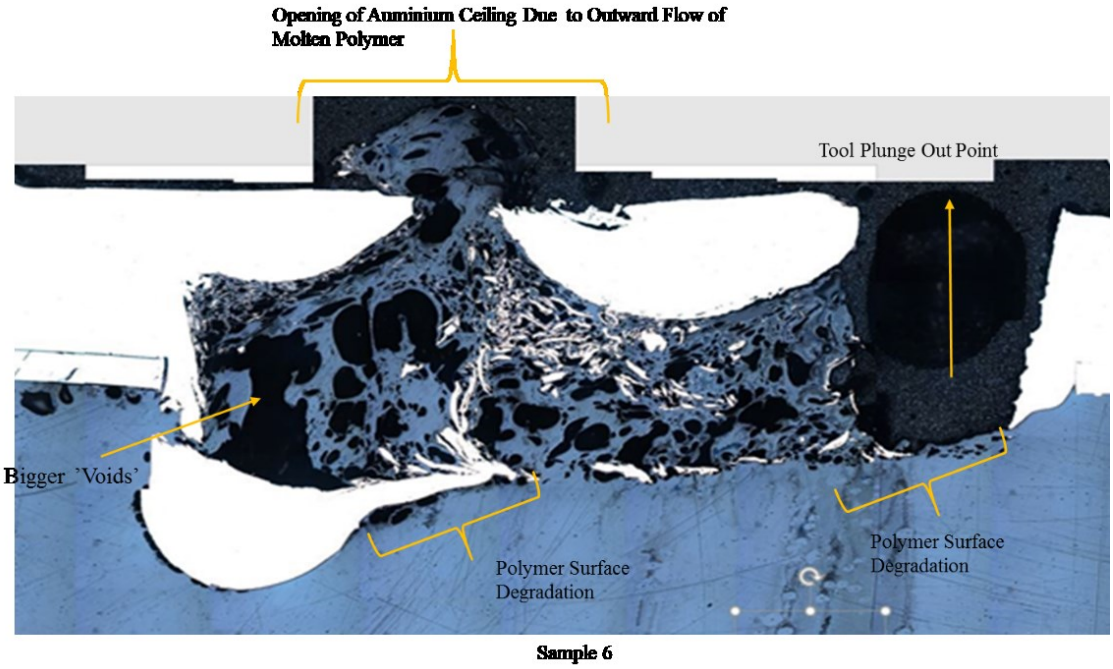

Figure 62: Geometry of the Joint Hook in Longitudinal Direction (PEEK Focused)

8.3.2 After Etching

All the sample were then etched using the 10% hydrofluoric acid for about 25-30 seconds to see the material grain structure and flow direction on aluminium. Since the etchant used is specific for aluminium material, the third set of micrograph was taken with aluminium in focus only(Figure 63) (five sample in the transverse direction) and in (Figure 64) (sample in the longitudinal direction). The grain structure orientation and flow direction can be observed which reveals significant recrystallization and grain refinement. Etching of (smaple1) reveals the thin opening of the aluminium ceiling (circled part) through which polymer is squeezing out to the surface. A similar condition is observed in (sample2). Micrographs of all sample are below.

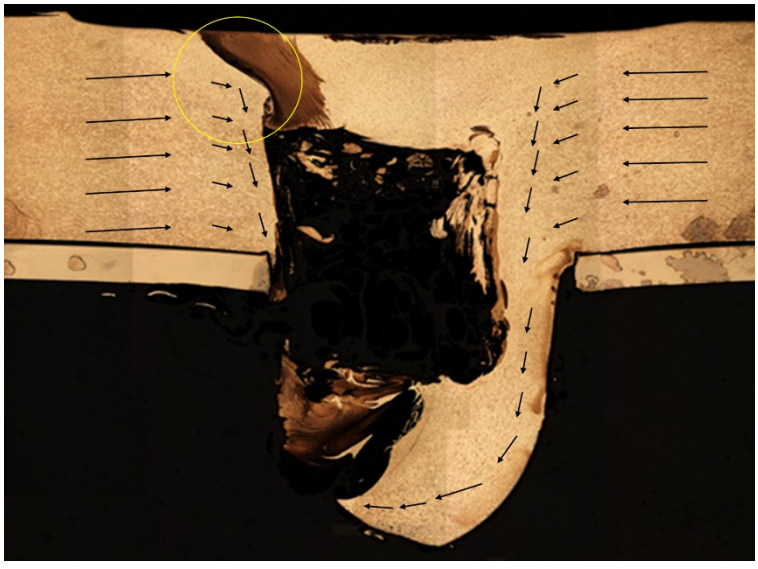

Sample 1

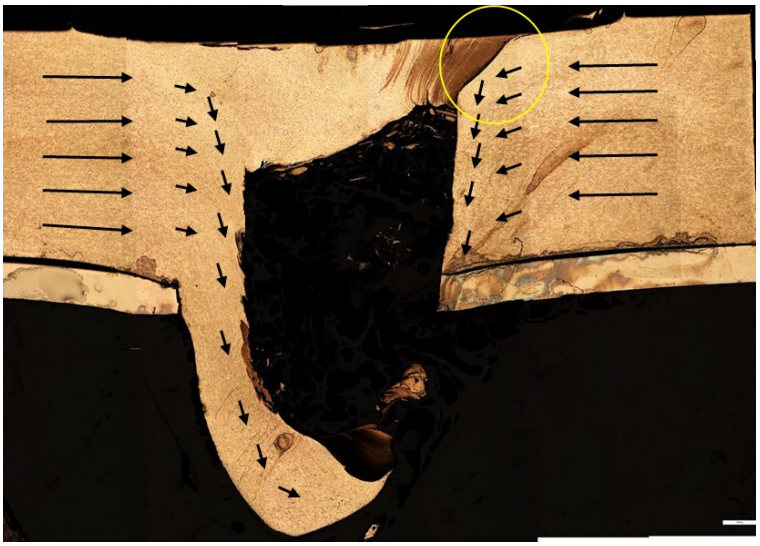

Sample 2

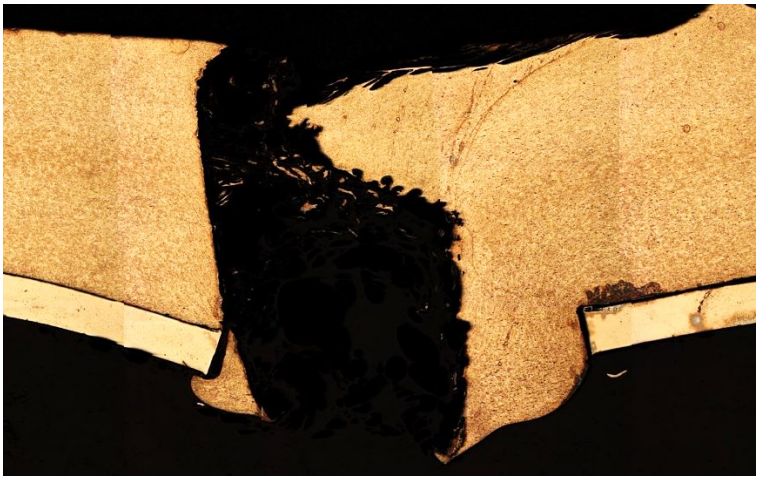

Sample 3

Sample 4

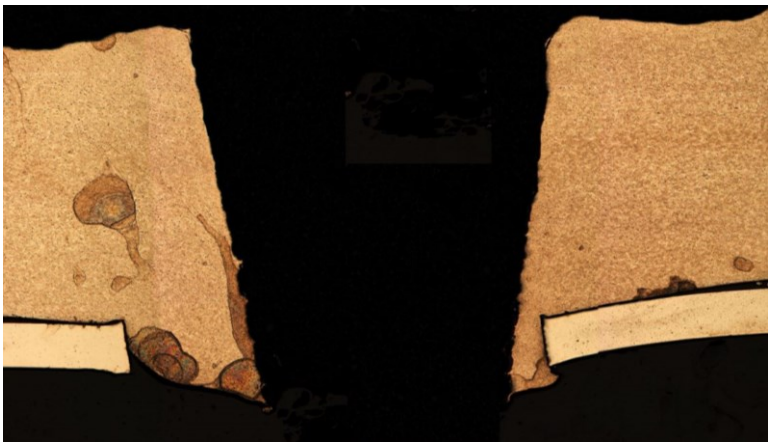

Sample 5

Figure 63: Geometry of the Joint Hook after Etching, at 5 Different Section in Transverse Direction

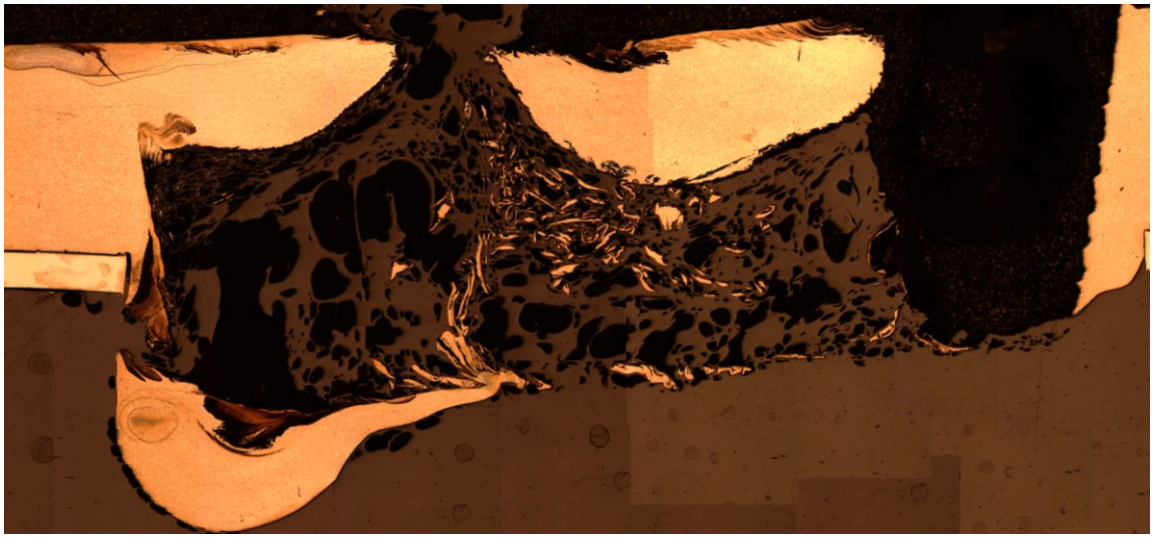

Sample 6

Figure 64: Geometry of the Joint Hook After Etching in Longitudinal Direction

8.4 Microstructure Analysis

8.4.1 Microstructure of THE-FSpW Sample

The number designated on the picture (Figure 65) are the position where microstructure was studied. The detailed micrograph picture at those positions is discussed further below. Micrograph was taken in 10X and 20X amplifications.

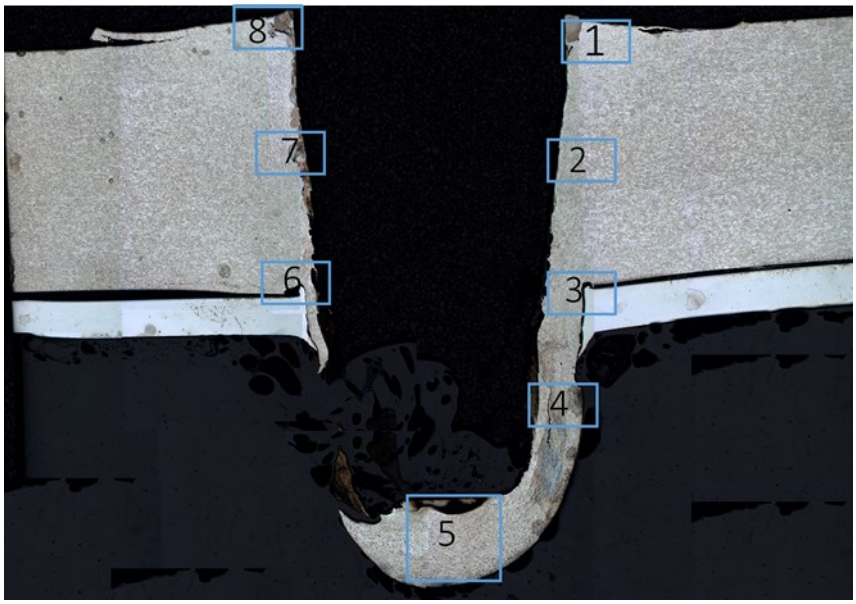

Figure 65: Various Section On Joint Hook Selected for Microstructure Analysis

In general in all micrograph below reveals fine grains and distinctive grain boundaries, which is due to the dynamic recrystallization and grain refinement at the stir zone (SZ). The black particle structure present in the micrograph is the iron (Fe), and manganese (Mn) based second phase particles.

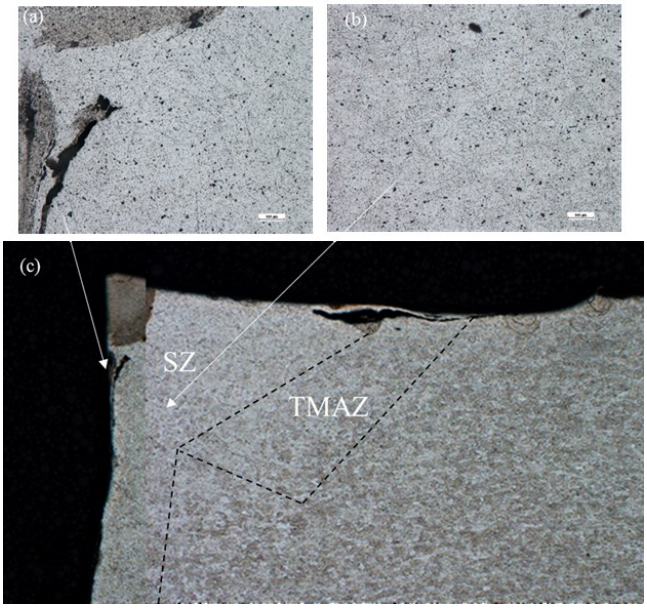

Figure 66: OM at point 1;(a) 2.5 X; (b and c) 20X

In (Figure 66a) reveals a crack on the surfaces. (Figure 66 b and c) reveals fine grain, which is common in the SZ. Also in TMAZ, severely deformed grains can be observed The upper surface of weld area consists of material that is stirred by shoulder resulting on the deformed surface with flash attached to it.

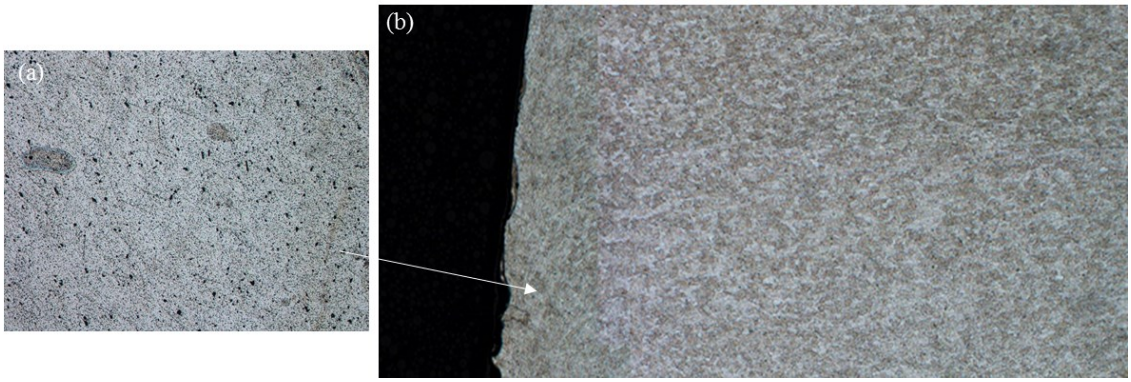

Figure 67: OM at point 2;(a) 20 X; (b) 2.5X

(Figure 67) Is a micrograph taken at the position 2 (Figure 65) reveals the general characteristics as explained initially. The irregular rough surface is due to its contact with the rotating tool during the joining process.

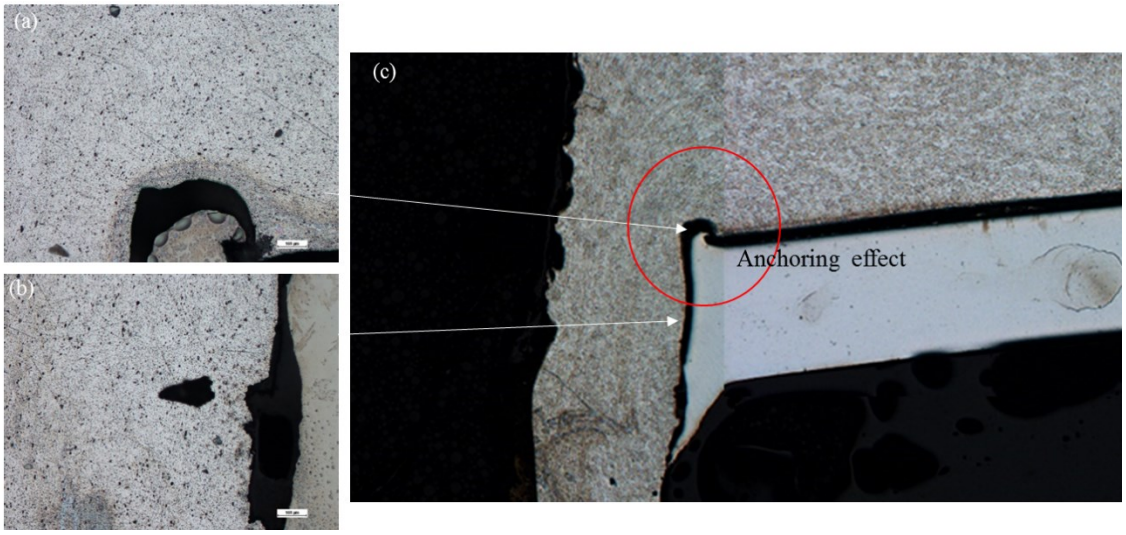

Figure 68: OM at point 3;(a and b) 20 X; (c) 2.5X

(Figure 68a) and (Figure 68b) reveals a gap between the aluminium/stainless steel interface. There is an 'anchoring effect'(marked by a red circle in Figure 68c) achieved from the flash on stainless steel plate surface resulted there while pre-drilling the hole on the stainless steel plate.

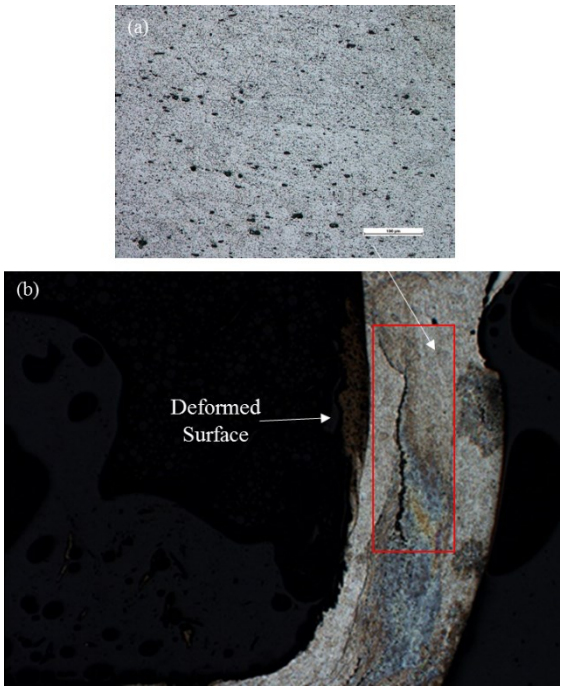

Figure 69: OM at point 4;(a) 20 X; (b) 2.5X

(Figure 69) Moreover, reveals a long crack in to join hook surface. It also revels deformation and irregularities on the surface and the inconsistency in the thickness of the joint hook.

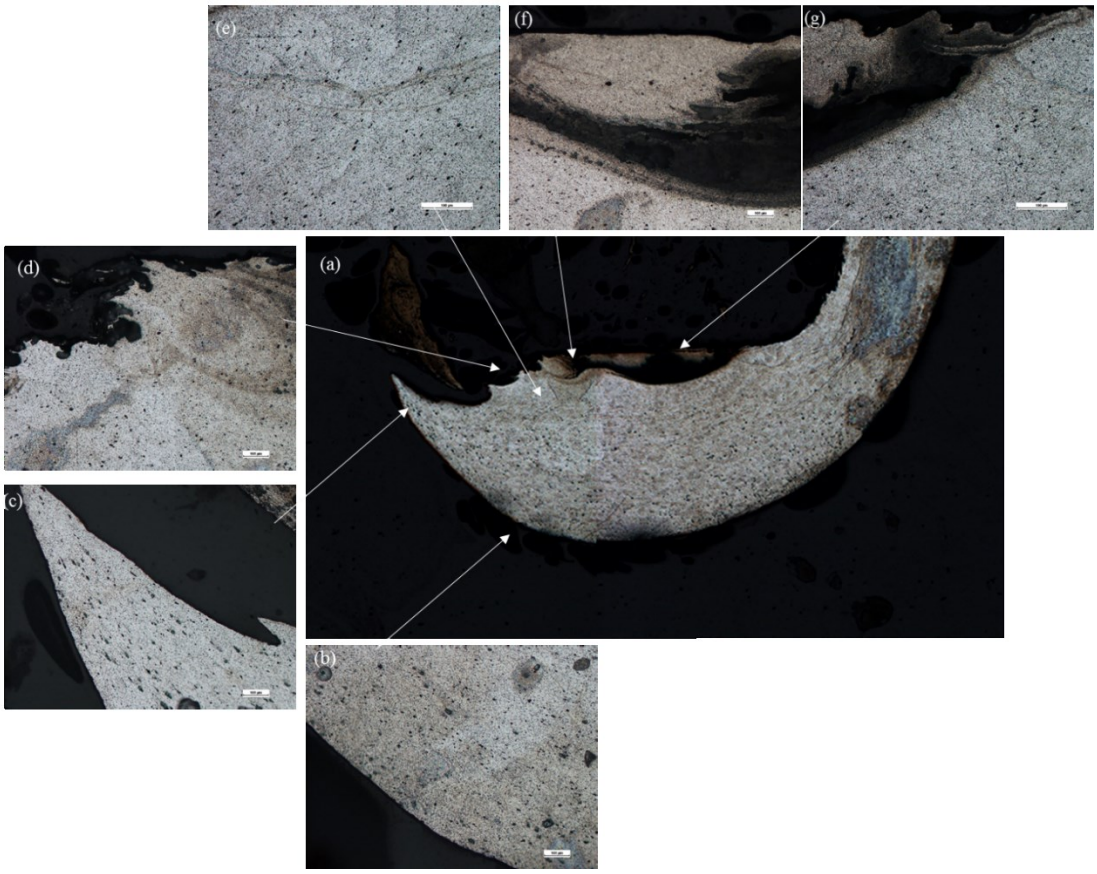

Figure 70: OM at point 5;(a) 2.5 X; (b-g) 20X

(Figure 70 b and c) reveals the unidirectional elongated grains flow.(Figure 70d) shows the large irregularities on the surface with detached aluminium particles around it. (Figure 70´a,f, and g) reveals the detached aluminium particles with the polymer in between the suspended particles and the joint hook. (Figure 71 a) reveals the geometry of the bottom section of the joint hook which creates anchoring effect on the polymer.

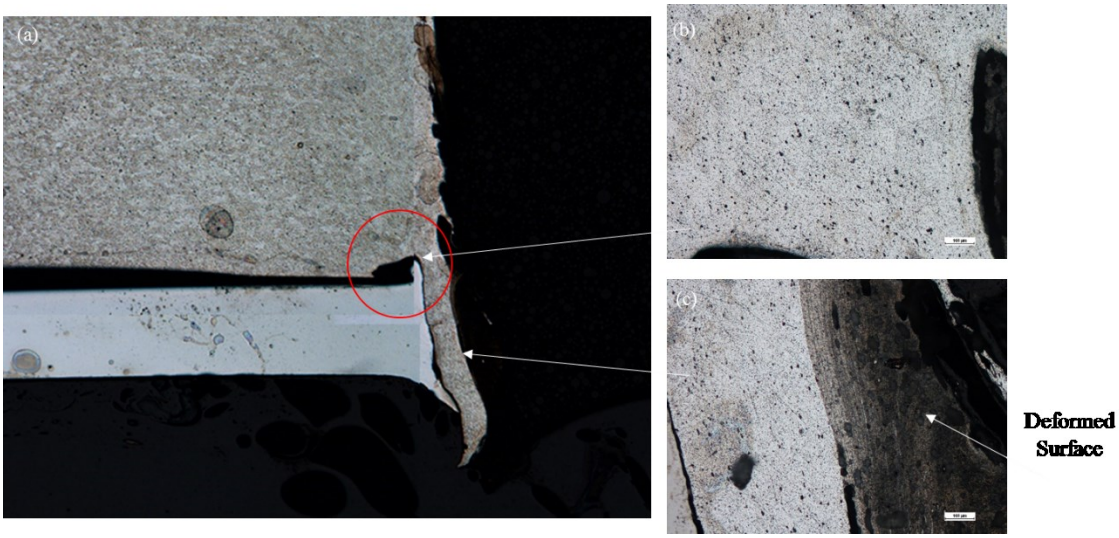

Figure 72: OM at point 6;(a) 2.5 X; (b and c) 20X

(Figure 72a) also reveals ‘anchoring effect’(marked by a red circle in the figure, from the flash on stainless steel plate surface resulted in their while pre-drilling the hole on the stainless steel plate. A gap between the aluminium and stainless steel plate interface can be seen. (Figure 72c) reveals a surface deformation.

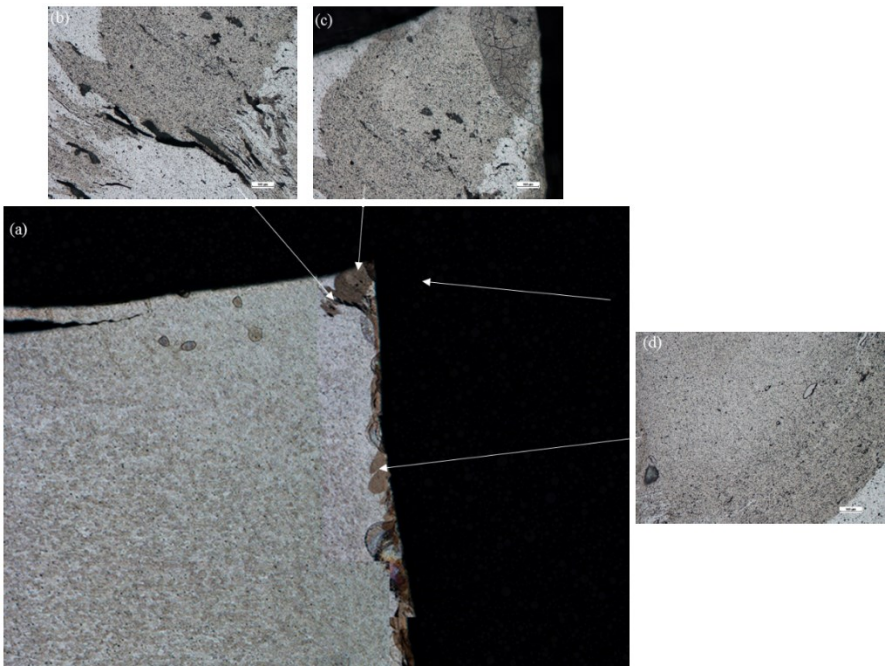

Figure 73: OM at point 7and 8,;(a) 2.5 X; (b-d) 20X

In (Figure 73a) the upper surface of weld area consists of material that is stirred by shoulder resulting on the deformed surface with flash attached to it. (Figure 73b and c) reveals a series of cracks on the surface edges where tool penetrates during the joining process.

8.4.2 **Microstructure of The-FSSpW Sample**

The number designated on the pictures (Figure 74) is the position where microstructure was studied. The detailed micrograph at those positions is discussed in this section below. Micrograph was taken in 10X and 20X amplifications.

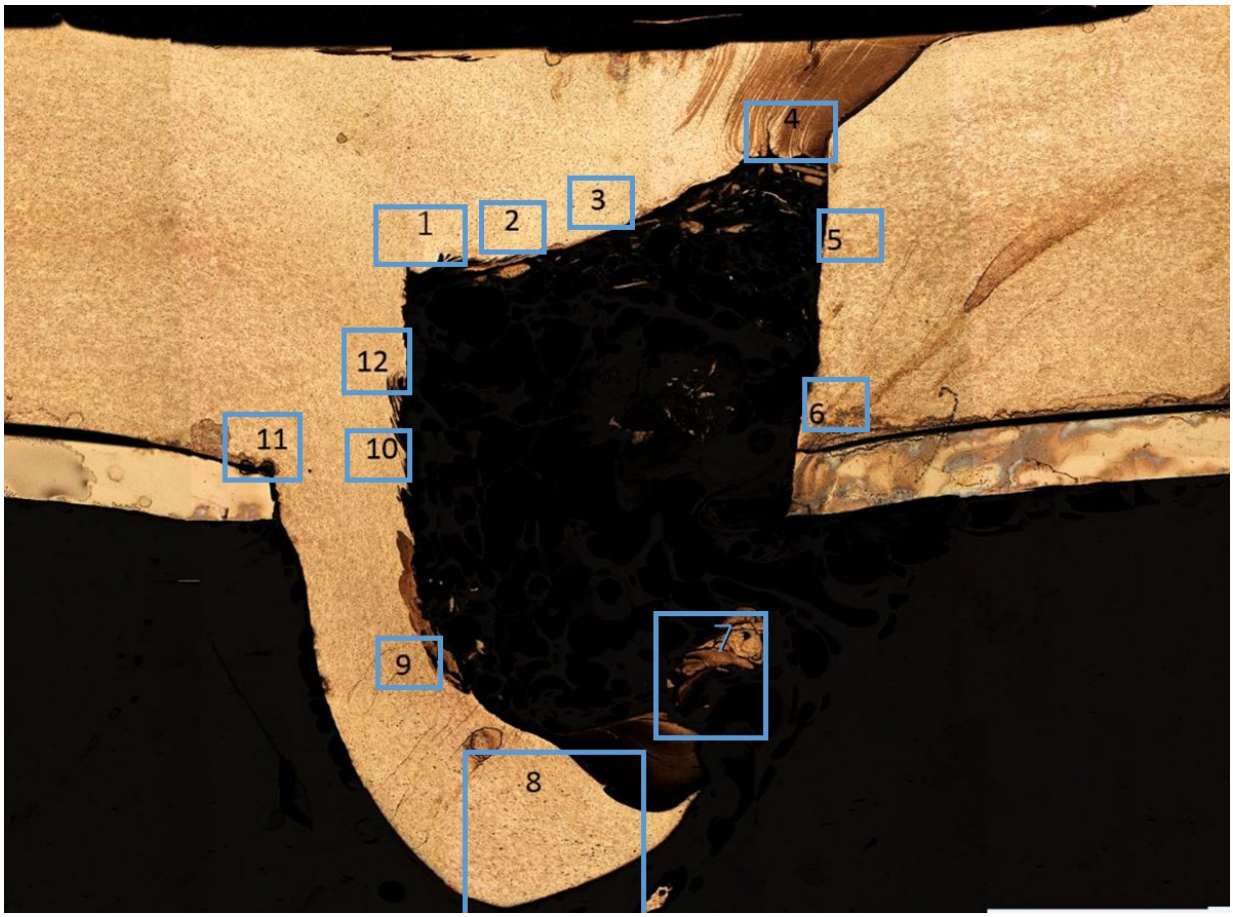

Figure 74: Various Section On Joint Hook Selected for Microstructure Analysis

In general in all micrograph below reveals fine grains and distinctive grain boundaries, which is due to the dynamic recrystallization and grain refinement at the stir zone (SZ). The black particle structure present in the micrograph is the iron (Fe), and manganese (Mn) based second phase particles.

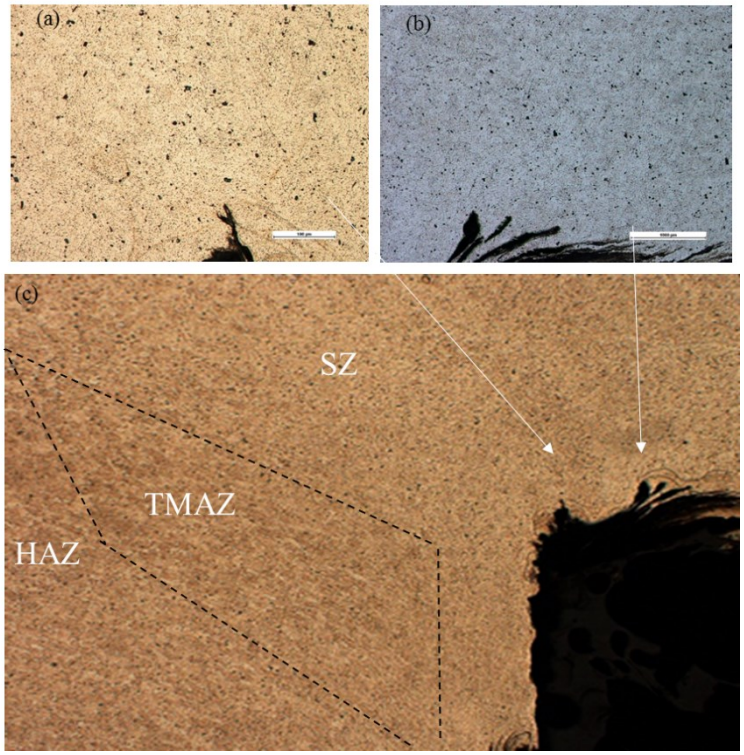

Figure 75: OM at point 1;(a and b) 20 X; (c) 2.5X

In (Figure 75) reveals three distinctive zones, i.e., SZ, TMAZ, and HAZ. The figure also reveals flakes like structure advancing out from the aluminium ceiling and presence of surface irregularities.

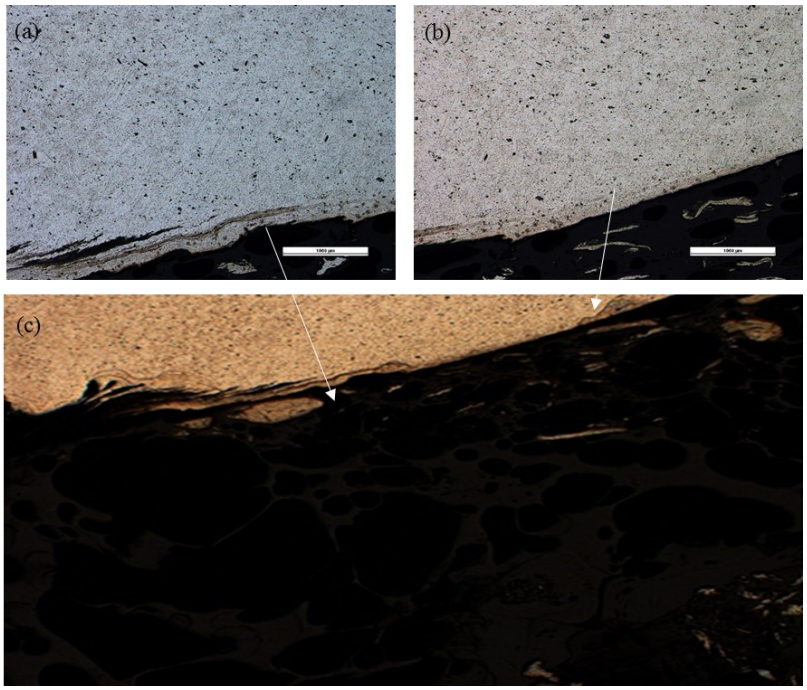

Figure 76: OM at point 2 and 3;(a and b) 20 X; (c) 2.5X

(Figure 77) reveals many aluminium particles suspended in polymer and flakes like structure coming out from the aluminium ceiling and presence of surface irregularities. It also reveals a crack initiated at ceiling advancing toward the top surface.

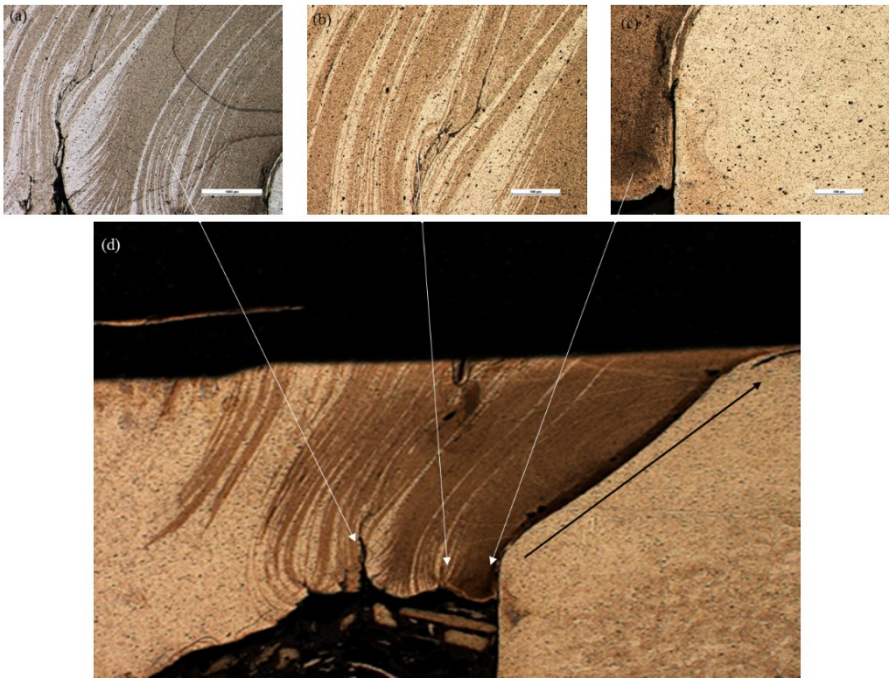

Figure 78: OM at point 4;(a-c) 20 X; (d) 2.5X

(Figure 79 d) reveals a channel (shown by the arrow) through which polymer is escaping out to top surface from the aluminium ceiling. It also reveals the dark and light stripes which are a multilayer of mixed material piling up. There is the presence of small and large crack propagating from the aluminium ceiling and on the top surface.

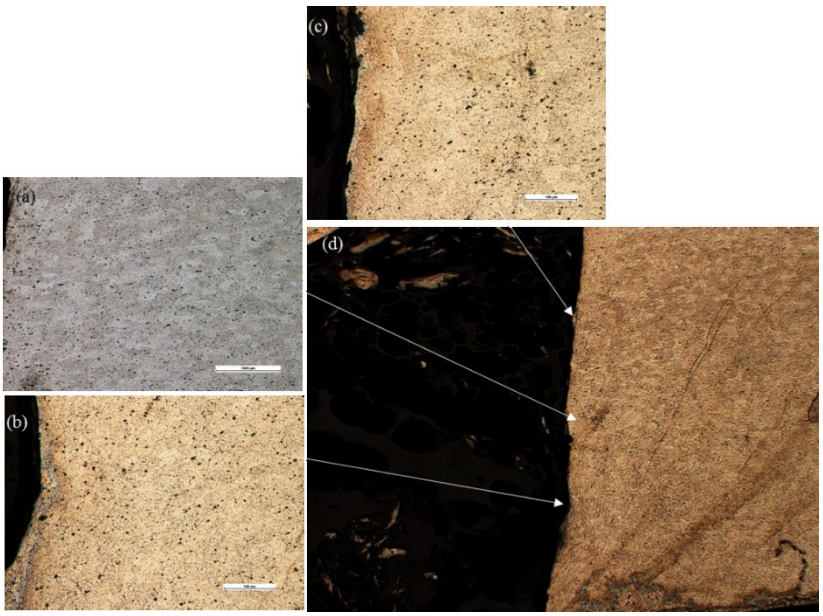

Figure 80: OM at point 5;(a-c) 20 X; (d) 2.5X

(Figure 74) reveals suspended aluminium particles in the polymer. In (Figure 80 a) the grain with distinctive grain boundaries can be observed. The irregular rough surface is due to its contact with the rotating tool during the joining process.

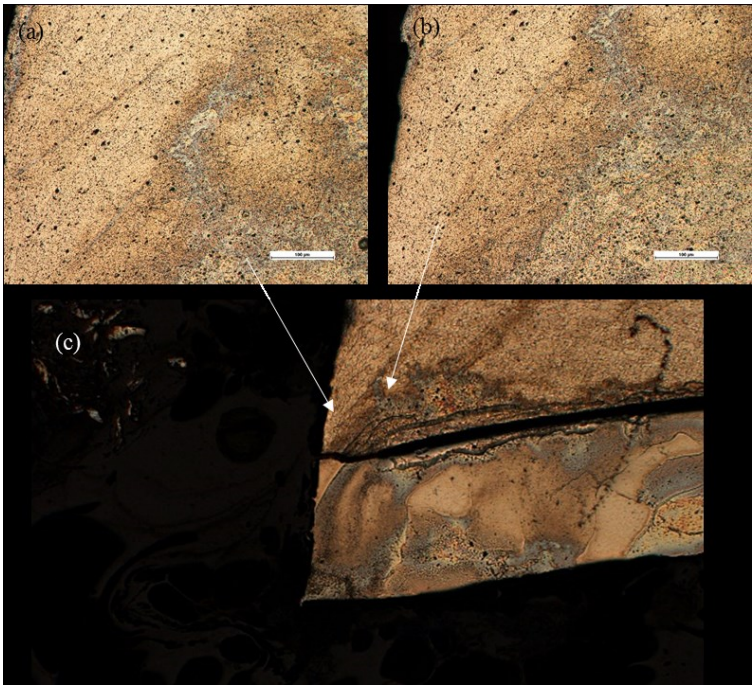

Figure 81: OM at point 6;(a and b) 20 X; (c) 2.5X

(Figure 82)reveals the gap between the aluminium/stainless steel plate interface. It also reveals the aluminium particles suspended in the polymer.

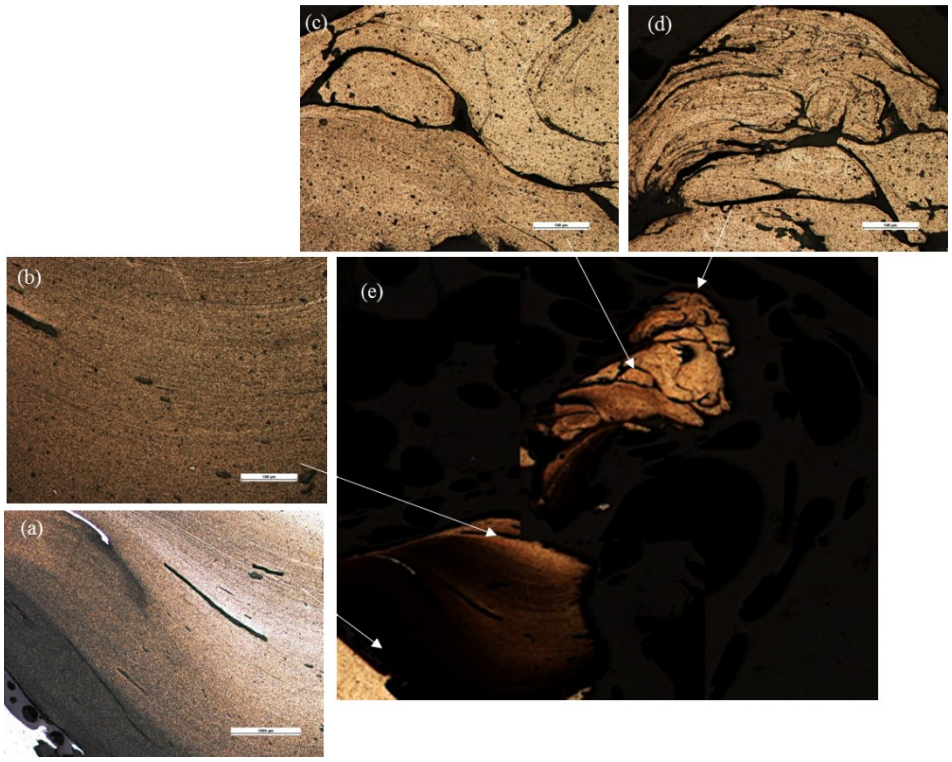

Figure 83: OM at point 7;(a-d) 20 X; (e) 2.5X

(Figure 83) It reveals the multilayer piling up polymer and aluminium.(Figure 81 a and b) is a highly overetched zone highly sensitive to the etchant is due to the presence of a mixture of the heat affected polymer and aluminium particles.

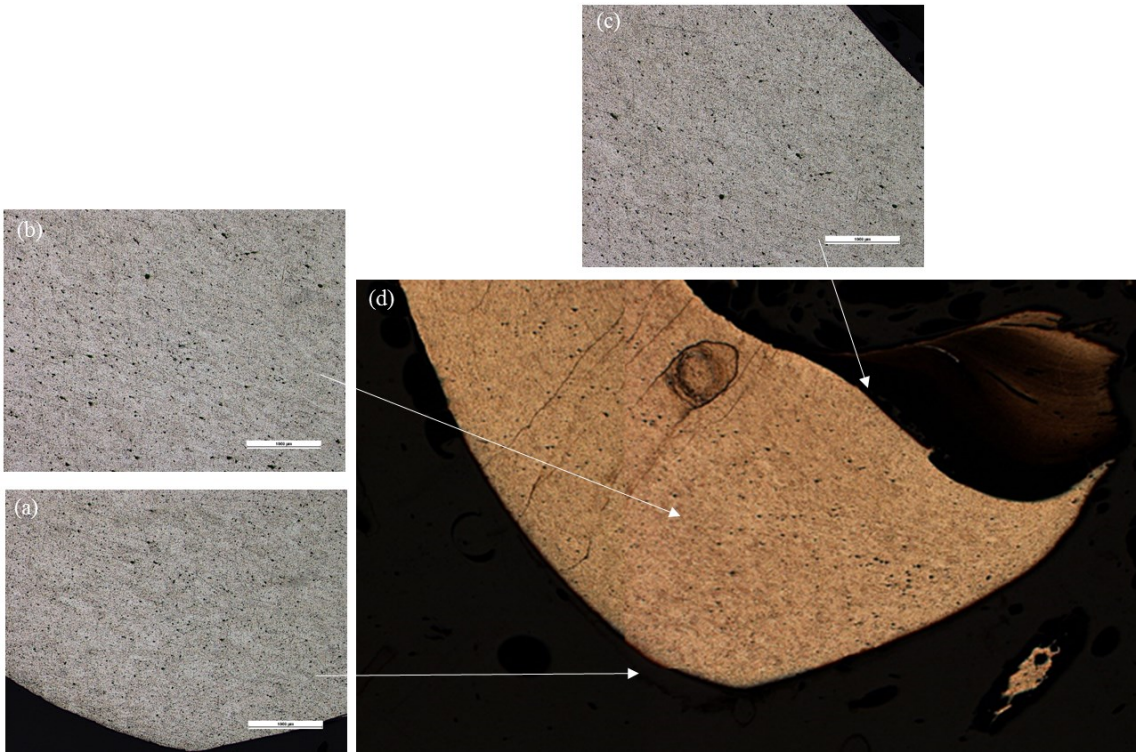

Figure 84: OM at point 8;(a-c) 20 X; (d) 2.5X

(Figure 85) It reveals the unidirectional elongated grains flow and a large particle of aluminium suspended into the polymer. (Figure 86 d) reveals the geometry of the bottom section of the joint hook which creates anchoring effect on the polymer.

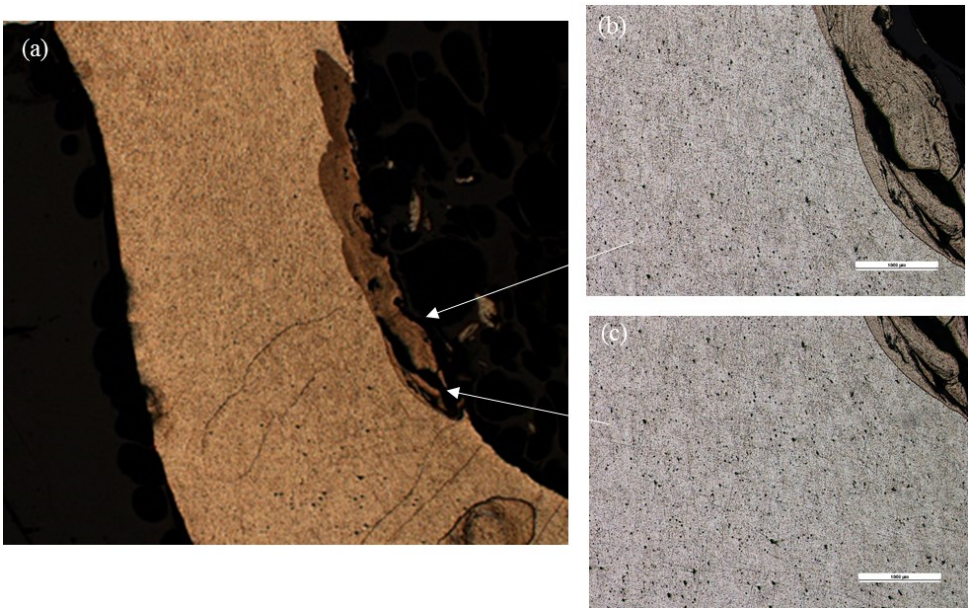

Figure 87: OM at point 9;(a) 2.5 X; (b-c) 20X

(Figure 87) reveals the presence of deformed surfaces and irregularities on the aluminium surface and also inconsistency in the thickness of this section of joint hook. The detachment of aluminium particles from the surface and the irregular rough surface can be observed. A visible polymer intrusion can be seen in (Figure 87 b and c).

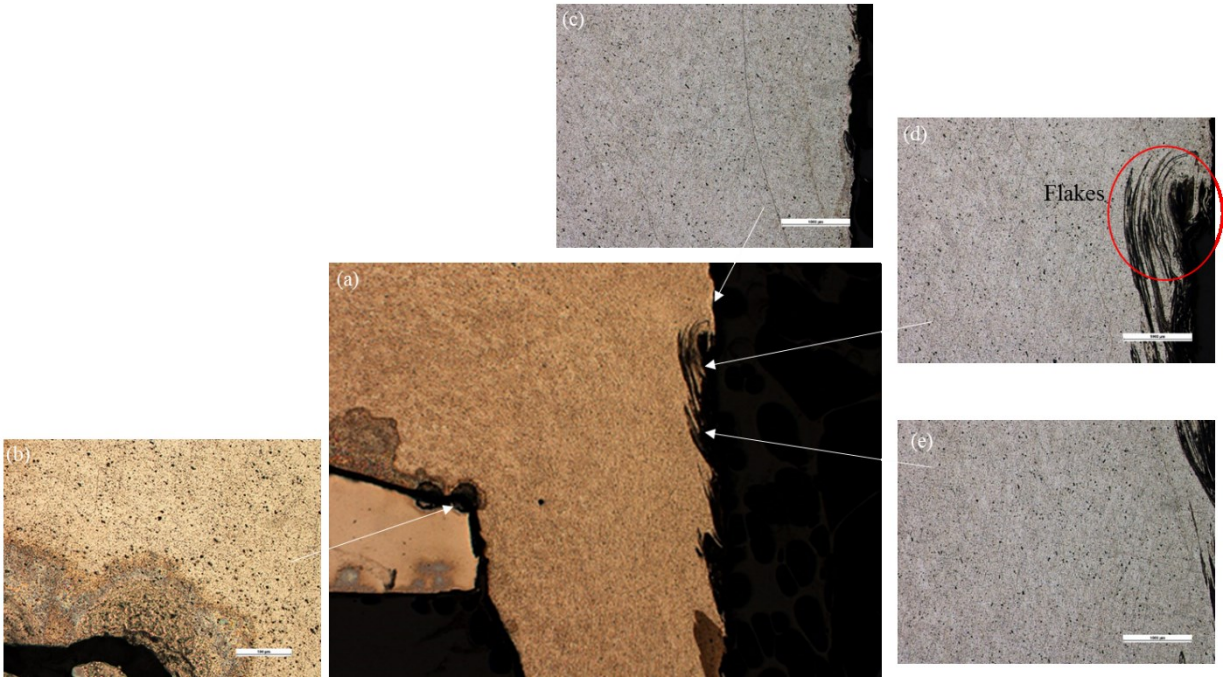

Figure 88: OM at point 10,11 and 12,;(a) 2.5 X; (b-e) 20X

(Figure 88) reveals flakes like structure hanging from the aluminium surface, the presence of deformed surfaces and irregularities on the aluminium surface. It also reveals the gap between the aluminium and stainless steel plate interface.

8.5 Geometrical Parameterization of Joint Hook

8.5.1 THE-FSpW Sample

The hook geometry was studied for one of the samples produced from the THE-FSpW process using the optimum set of parameters. The geometry of the hook was measured at the different section as shown in the (Figure 89). The obtained dimension for the corresponding sections is tabulated in (Table 18).

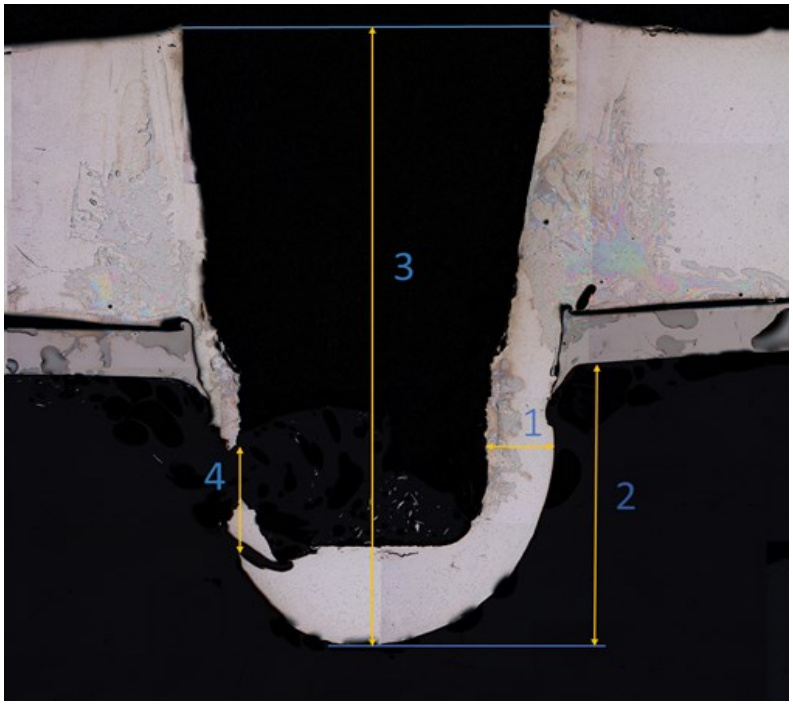

Figure 89: Joint Hook Geometry Measuremént for THE-FSpW sample

Table 18 Joint Hook Geometry Dimension

Point in Picture	Geometry	Dimension (mm)
1	Thickness of AA Hook	1.345
2	Penetration of AA Hook into Polymer	5.940
3	AA Ceiling	13.003
4	Open Throat of AA Hook	2.202

8.5.2 THE-FSSpW Sample

A hook geometry was studied for one of the samples produced from the THE-FSSpW process using the optimum set of parameters sample was taken from a section which has similar joint hook shape as obtained from the THE-FSpW process. The geometry of the hook was measured at the different section as shown in the (Figure 90). The obtained dimension for the corresponding sections is tabulated in (Table 19).

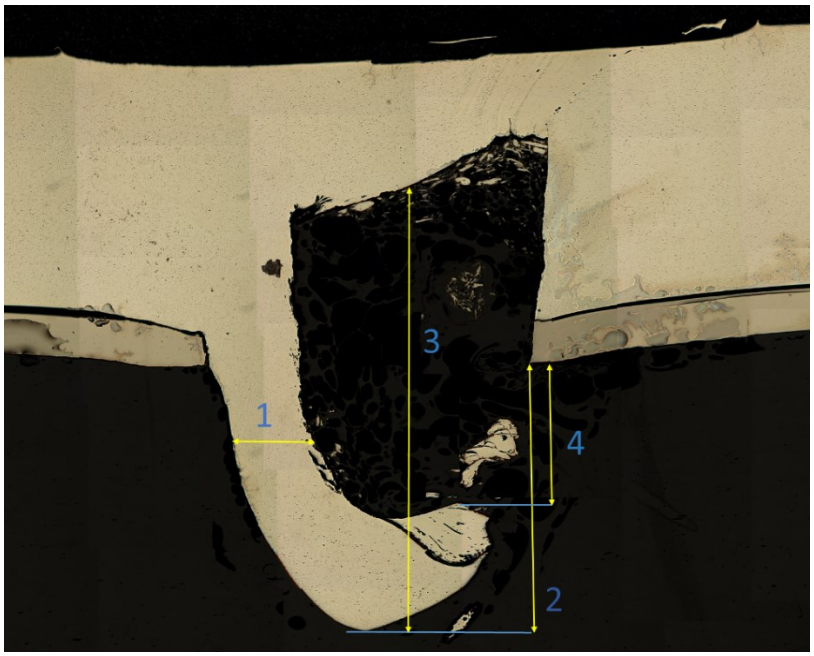

Figure 90: Hook geometry measuremént for THE-FSSpW sample

Table 19: Joint Hook Geometry Dimension

S.N	Geometry	Dimension (mm)
1	Thickness of AA Hook	1.892
2	Penetration of AA Hook into Polymer	6.452
3	AA Ceiling	10.714
4	Open Throat of AA Hook	3.416

9 Mechanical Testing

9.1 Introduction

In this chapter, mechanical test, and analysis of weld joints produced from the THE-FSpW process and the THE-FSSpW process are presented. The test is carried out to assess the maximum failure load that the joint can withstand. Tensile shear test and the cross tension test were the major standard test performed.

In section 9.2, the result and analysis of mechanical test performed for the joint produced from the THE-FSpW process are presented. The tensile shear test and cross tension test were conducted on the several specimens of the metal-polymer joint. An overlap joints between the selected set of base material were made for the testing. The tensile-shear test was carried out to understand the joint behavior during the shear loading. The aim was to determine the maximum shear load that joint can withstand. A set of the optimal parameter was used to prepare the test specimen. Similarly, Cross-tension test was carried out to test the behavior of join in the tensile load. The test aimed to determine the maximum tensile load that the joint can withstand. The failure mechanism for both the test is also studied.

Similarly, in section 9.3, the result and analysis of the standard mechanical test performed for the joint produced from the THE-FSSpW process are presented.

9.2 Mechanical Test of THE-FSpW Joint

The section presents the mechanical test and microscopic characterization of weld joints produced from THE-FSpW for the various material combination.

9.2.1 Tensile Shear Test of AA5754-H111/PA6 Joint

The (Figure 91) shows the force-displacement plot for the tensile shear test carried out on the THE-FSpW weld joint between aluminium AA5754-H111 and polyamide 6. All the test specimen are prepared using the same set of optimal parameters and conditions.

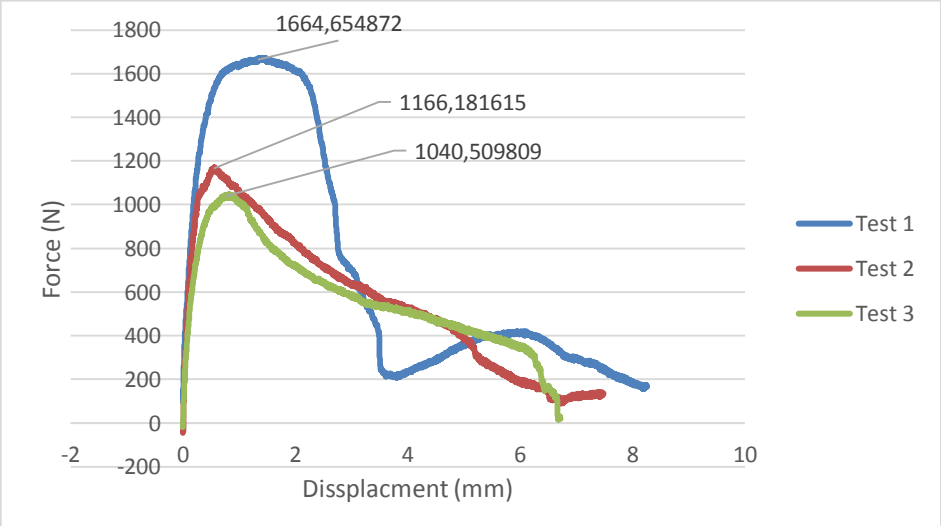

Figure 91: Load-Dispalcment Plot (AA5754-H111/PA6)

From (Figure 91), the joint initially start to deform elastically with an almost linear increase in load, when the maximum load is reached the curve linearity deviates as yielding takes place, the yielding region are not so distinctive. Then the joint start to deform plastically and the load start decreasing. For test specimen 1 the load decreases suddenly to a lower point unlike for test specimen 2 and 3. The plastic deformation occurred for a long time before the fracture of the joint occurred. The specimen failed by the detachment of the aluminium plate and the polymer plate. The stainless steel plate was still attached to the aluminium plate side, which also explains the adhesive bonding (from the molten polymer at the interfaces) failure between the polymer and stainless steel plate interface.

The failure load obtained for the joint test 1 is 1664.6N, was the highest compare the other two test that has almost similar failure load. All the specimen showed similar fracture modes (Figure 92) such that the tearing of joint hook at the common junction between stainless steel and polyamide. The possible cause of this is due to the stress concentration created by the hole that is present in the stainless steel plate. The failure of the joint was due to the fracture of the hook geometry. The fracture initiated from the open part of the circumference of the round joint hook area formed by the deposition of aluminium at the stainless steel-polymer interface zone and propagated towards the other end until the joint failed.

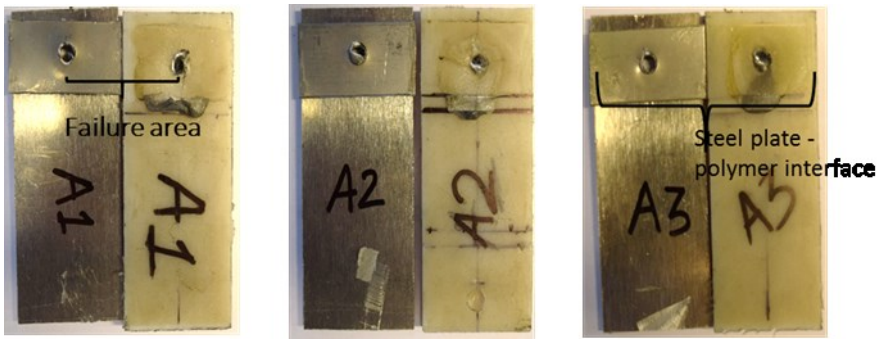

Figure 92: Specimen After Test

9.2.2 Tensile Shear Test of AA5754-H111/PEEK Joint

The (Figure 93) shows the force-displacement plot for the tensile shear test carried out on the THE-FSpW joint between AA5754-H111 and PEEK. All the test specimen are prepared using the same set of optimal parameters and conditions.

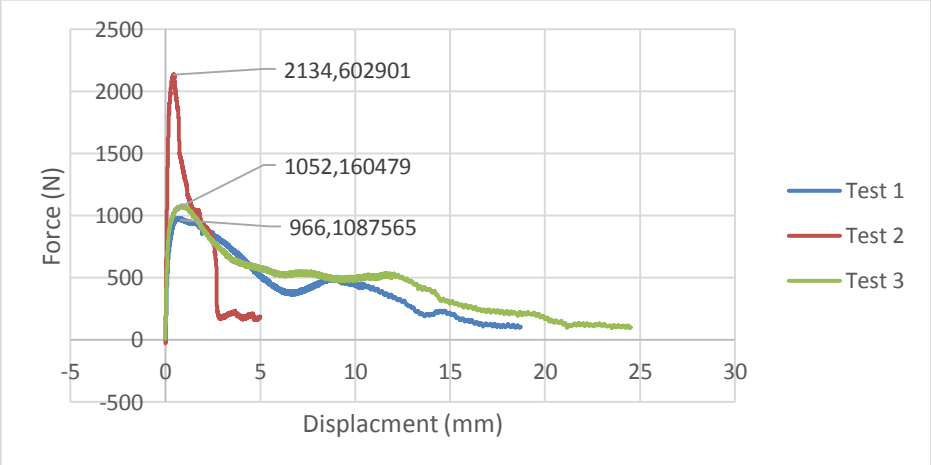

Figure 93: Load-Displacement Plot (AA5754-H111/PEEK)

From (Figure 93) the joint initially start to deform elastically with an almost linear increase in load, when the maximum load is reached the curve linearity deviates as yielding takes place, the yielding region are not so distinctive. Then the joint start to deform plastically and the load start decreasing with a sudden decrease of load to a certain point initially. For test specimen 2 the load decreases suddenly to a lower point unlike for test specimen 1 and 3. The plastic deformation for test 1 and 3 occurred for a long time before the fracture of the joint took place. The large plastic deformation was because of the two modes of failure that occurred at the joint, such that the tearing of the hook at the stainless steel polymer interface and the continuous decrease in the adhesive bonding at the joint hook and polymer interface. The specimen finally failed by the detachment of the aluminium plate and the polymer plate. The stainless steel plate was still attached to the aluminium plate side, which also explains the adhesive bonding failure between the polymer and stainless steel plate interface.

The failure load for the joint test 2 is 2134.6N, was the highest compare the other two test that has almost similar failure load. The specimen showed two different fracture modes (Figure 94) The test specimen 2 that has the maximum failure load compare to other two test fractured by the tearing of joint hook at the junction between stainless steel and PEEK polymer. The fracture initiated from the open part of the circumference of the round joint hook area formed by the deposition of aluminium at the stainless steel-polymer interface zone and propagated towards the other end until the joint failed. The second type of failure for test specimen 1 and 3 was a combination of the failure mode explained above but without complete hook fracture and addition to that the ejection of the joint hook from the polymer.

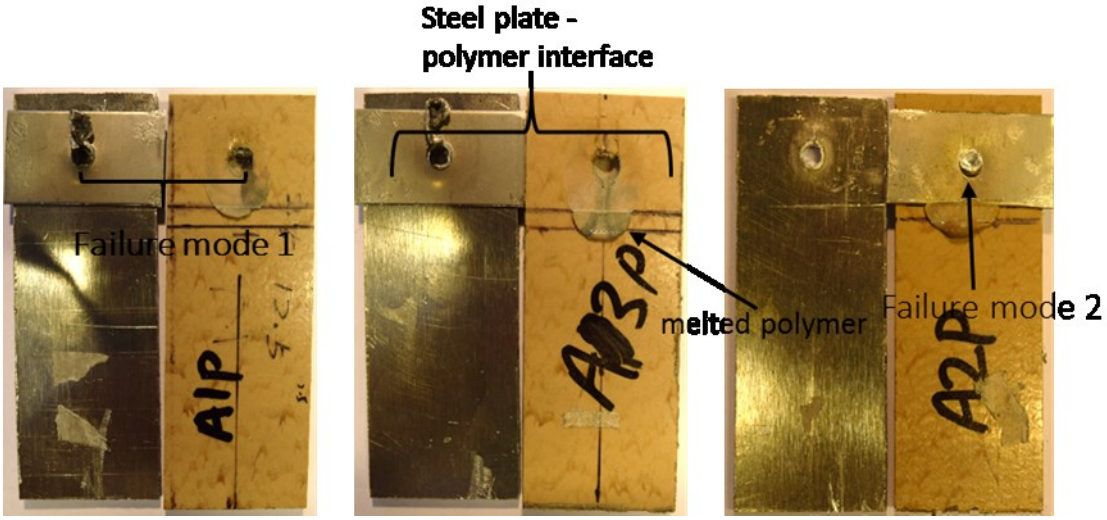

Figure 94: Specimen After Test

9.2.3 Tensile Shear Test of AA2024-T351/PA6 Joint

The (Figure 95) shows the force-displacement plot for the tensile shear test carried out on the THE-FSpW joint between aluminium AA2024-T351 and polyamide 6. All the test specimen are prepared using the same set of optimal parameters and conditions.

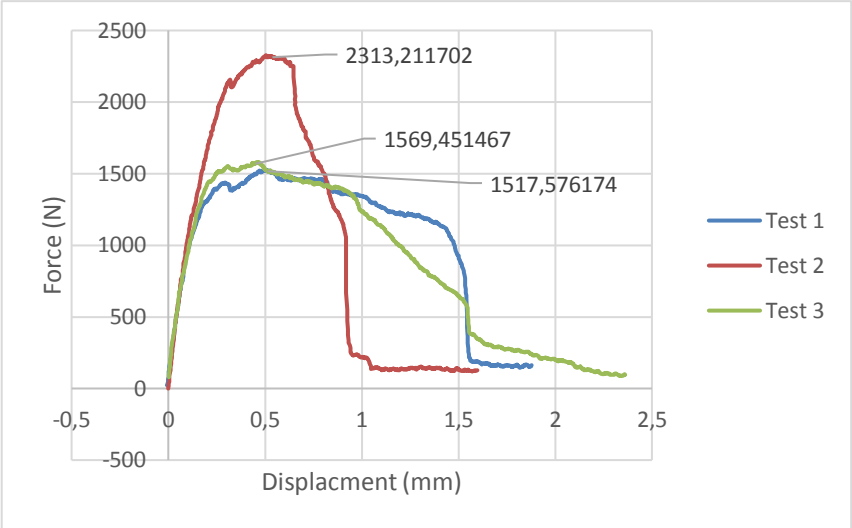

Figure 95: Load-Dispalcment Plot (AA2024-T351/PA6)

From (Figure 95), the joint initially start to deform elastically with an almost linear increase in load, when the maximum load is reached the curve linearity deviates as yielding takes place, the yielding region are not so distinctive. Then the joint start to deform plastically and the load start decreasing. For test specimen 2 the load decreases suddenly to a lower point unlike for test specimen 1 and 3 for which the decrease in load occur slowly to a certain point, and there is sudden decrease after that. The failure was instant and brittle, but the longer plastic deformation was from the adhesive bonding between the aluminium-stainless steel plate and polymer plate, due to the deposition of the molten polymer between their interfaces during the spot weld. The specimen finally failed by the detachment of the aluminium plate and the polymer plate. The stainless steel plate attached to the polymer plate side for test 1 and 2, which explain the existence of higher adhesive bonding between the polymer and stainless steel plate interface.

The failure load for the joint test 2 is 2313.2N, was the highest compare the other two test that has almost similar failure load. All the specimen showed similar fracture modes (Figure 96), similar to the joint test for AA5754-PA6. However, the failure load was higher compared to AA5754-PA6 joint test. That was likely due to the high strength of the aluminium AA2024 compare to the AA5754. The failure was due to the tearing of joint hook at the junction between stainless steel and polyamide. The failure of the joint was due to the fracture of the hook geometry. The fracture initiated from the open part of the circumference of the round joint hook area formed by the deposition of aluminium at the stainless steel-polymer interface zone and propagated towards the other end until the joint failed.

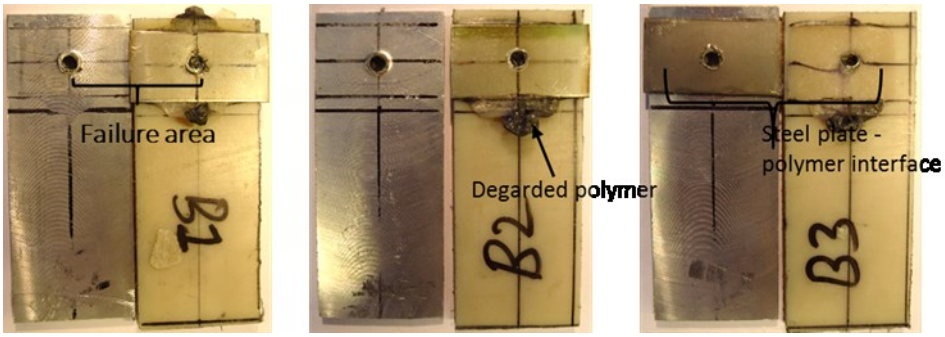

Figure 96: Specimen After Test

9.2.4 **Tensile Shear Test of AA2024-T351/PEEK Joint**

The (Figure 97) shows the force-displacement plot for the tensile shear test carried out on the THE-FSpW joint between AA2024-T351 and PEEK. All the test specimen are prepared using the same set of optimal parameters and conditions.

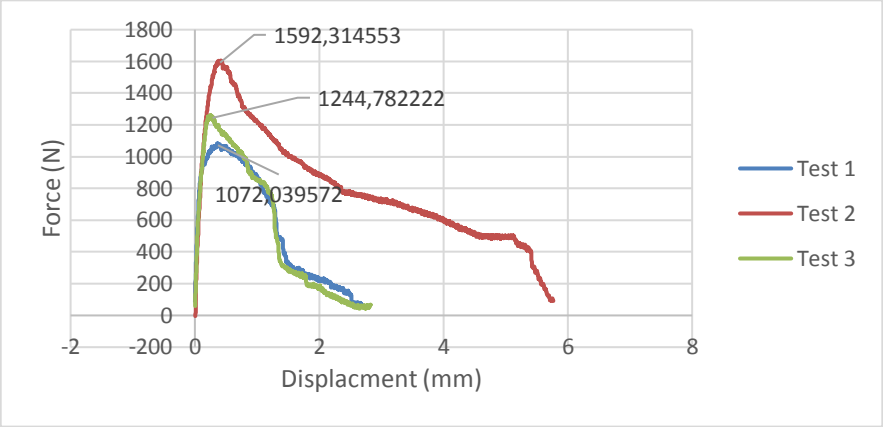

Figure 97: Load-Displacement Plot (AA2024-T351/PEEK)

From (Figure 97) the joint initially start to deform elastically with an almost linear increase in load, when the maximum load is reached the curve linearity deviates as yielding takes place, the yielding region are not so distinctive. Then the joint start to deform plastically and the load start decreasing. Al the test shows similar load decrease pattern. The plastic deformation region for test 2 was long compared to the other two test because of the two modes of failure that occurred at the joint, such that the tearing off the hook at the stainless steel polymer interface and the continuous decrease in the adhesive bonding at the joint hook and polymer interface. The specimen finally failed by the detachment of the aluminium plate and the polymer plate. The stainless steel plate was still attached to the aluminium plate side, which here also explain the adhesive bonding failure between the polymer and stainless steel plate interface.

The failure load for the joint test 2 is 1592.3N, was the highest compare the other two test that has almost similar failure load. All the specimen showed similar fracture modes (Figure 98) such that the tearing of joint hook at the junction between stainless steel and PEEK. The failure of the joint was due to the fracture of the hook geometry. The fracture initiated from the open part of the circumference of the round joint hook area formed by the deposition of aluminium at the stainless steel-polymer interface zone and propagated towards the other end until the joint failed.

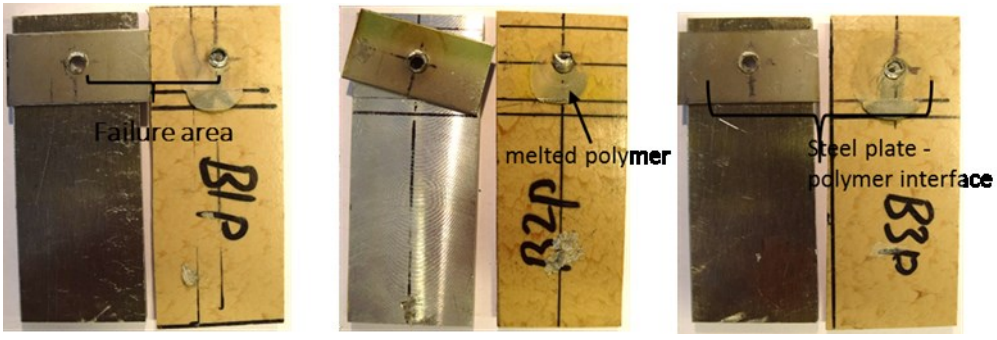

Figure 98: Specimen After Test

9.2.5 Cross-Tension Test of AA5754-H111/PA6 Joint

The (Figure 99) shows the force-displacement plot for the cross-tension test carried out on the THE-FSpW joint between AA5754-H111 and polyamide 6. All the test specimen are prepared using the same set of optimal parameters and conditions.

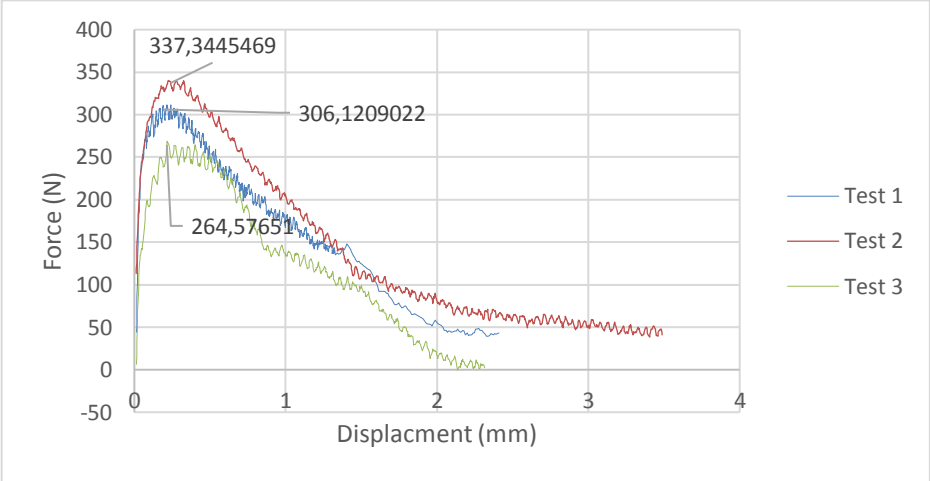

Figure 99: Load-Displacement Plot (AA5754-H111/PA6)

From (Figure 99) the load-displacement path followed is similar for all the test with initial plastic deformation with an almost linear increase in load when the maximum load is reached the curve linearity deviates as yielding takes place, the yielding region is not so distinctive. Then the joint start to deform plastically and the load start decreasing. Finally, the specimen fails with the detachment of the aluminium plate and polymer plate.

The failure load for the all the joint tested were almost similar with maximum failure load of 337,3N. All the specimen showed similar fracture (Figure 100) such that the ejection of the joint hook from polyamide 6. The failure was due to the adhesive bonding failure between the aluminium/polymer interfaces.

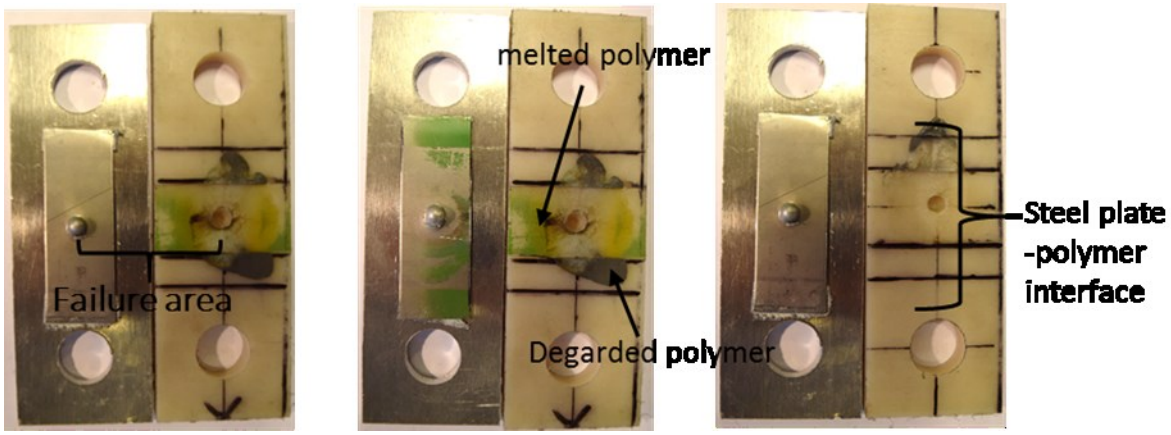

Figure 100: Specimen After Test

9.2.6 **Cross-Tension Test of AA5754-H111/PEEK Joint**

The (Figure 101) shows the force-displacement plot for the tensile shear test carried out on the THE-FSpW joint between AA5754-H111 and PEEK. All the test specimen are prepared using the same set of optimal parameters and conditions.

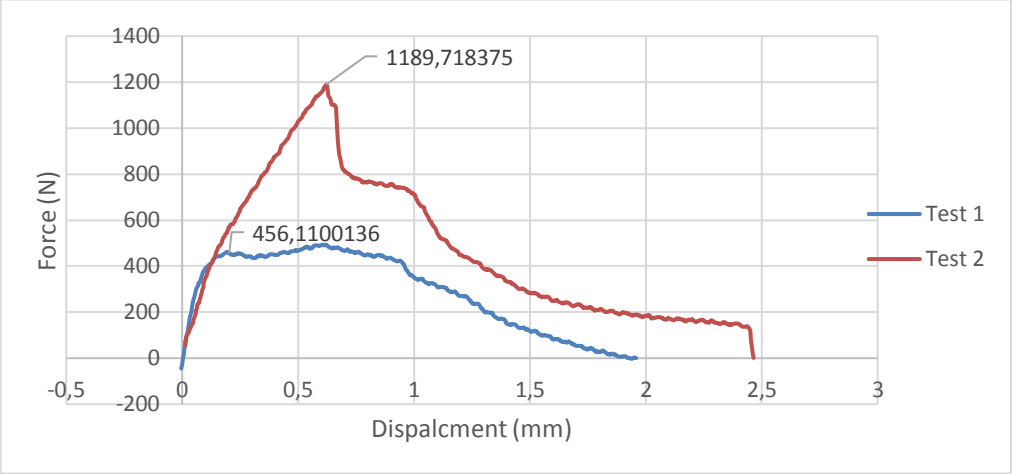

Figure 101: load-Displacement plot (AA5754-H111/ PEEK)

The load-displacement path followed is similar for all the test with initial plastic deformation with an almost linear increase in load, when the maximum load is reached the curve linearity deviates as yielding takes place, the yielding region is not so distinctive. The maximum load peak was quite sharp for the test 2 with a sudden decrease in load after the peak point. Then the joint start to deform plastically and the load start decreasing. Finally, the specimen fails with the detachment of the aluminium plate and polymer plate. The fracture of the joint hook was instant and brittle for test 1.

The failure load for the all the joint tested were almost similar with maximum failure load of 1189, 7N. The specimen showed two distinctive fracture (Figure 102) such that the test 1 failed due to brittle fracture of the joint hook failed at the stainless steel and polymer interface and test 2 failed by ejection of the joint hook from PEEK surface. The failure was due to the adhesive bonding failure between the aluminium/polymer interfaces.

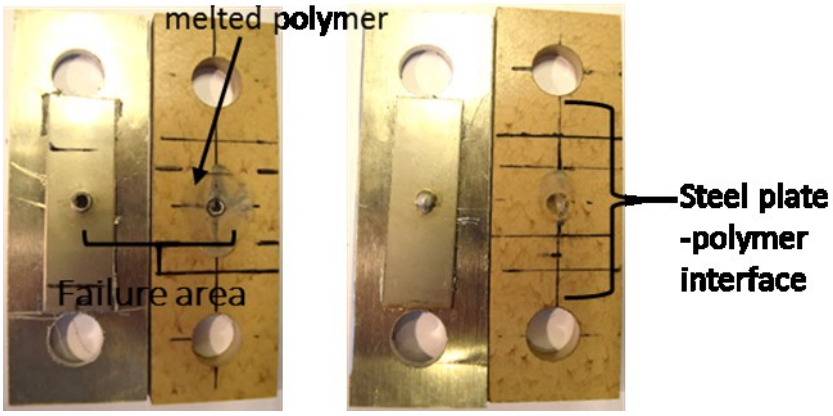

Figure 102: Specimen After Test

9.2.7 Analysis of Results for THE-FSpW

As per the objective of the whole work, which is to develop and characterize a new friction spot joining process THE-FSpW, to join aluminium alloy to the polymer. The various selected combination of the base materials was used for testing the joint, by the tensile-shear testing and the cross-tension testing. The material combination, AA2024-T351/PA6, AA2024-T351/PEEK, AA5754-H111/PA6, and AA5754-H111/PEEK were successfully joint by the THE-FSpW process. The range of failure load from the test is listed in (Table 20).

Table 20: Failure Load Range THE-FSpW Joint

Material Combination	Failure Load (lowest) (N)	Failure Load (Highest) (N)
	Tensile-shear Test	
AA2024-T351/PA6	1517	2313
AA2024-T351/PEEK	1072	1592
AA5754-H111/PA6	1040	1664
AA5754-H111/PEEK	966	2134
	Cross-Tension Test	
AA5754-H111/PA6	264	337
AA5754-H111/PEEK	456	1189

The analysis of joint and its various mode of a failure condition, following conclusion is made: the maximum failure of the joint was due to the tearing of the joint hook geometry in the junction at the stainless steel/polymer plate interface. The two possible reason for the failure at that point is, the minimum thickness of the joint hook geometry due to minimal volume of aluminium deposited into the polymer and the second is the hole present on the stainless steel plate which acts as stress concentration zone.

The above test result gave some vital information that can help to improve the joint strength: by increasing the joint hook geometry such that larger deposition of visco-plasticized aluminium into the polymer and to change the hole geometry in the stainless steel plate to reduce the stress concentration. The finding from the result for the THE-FSPW process was utilized to develop an improved process to join aluminium to the polymer, termed as the THE-FSSpW- Through hole extruded friction stir spot weld joining, which test result is discussed in next section.

9.3 Mechanical testing of THE-FSSpW Joint

Both tensile shear and cross tension test are carried out on the weld made in two directions, longitudinal direction and transverse direction (in reference to the aluminium plate). This test in two directions was performed to identify the influence of weld direction on the maximum joint failure load.

9.3.1 Tensile Shear Test of AA5754-H111/PEEK Joint

- **Transverse Direction Weld**

The (Figure 103) shows the force-displacement plot for the tensile shear test carried out on the THE-FSSpW joint between AA5754-H111 and PEEK. All the test specimen are prepared using the same set of optimal parameters and conditions.

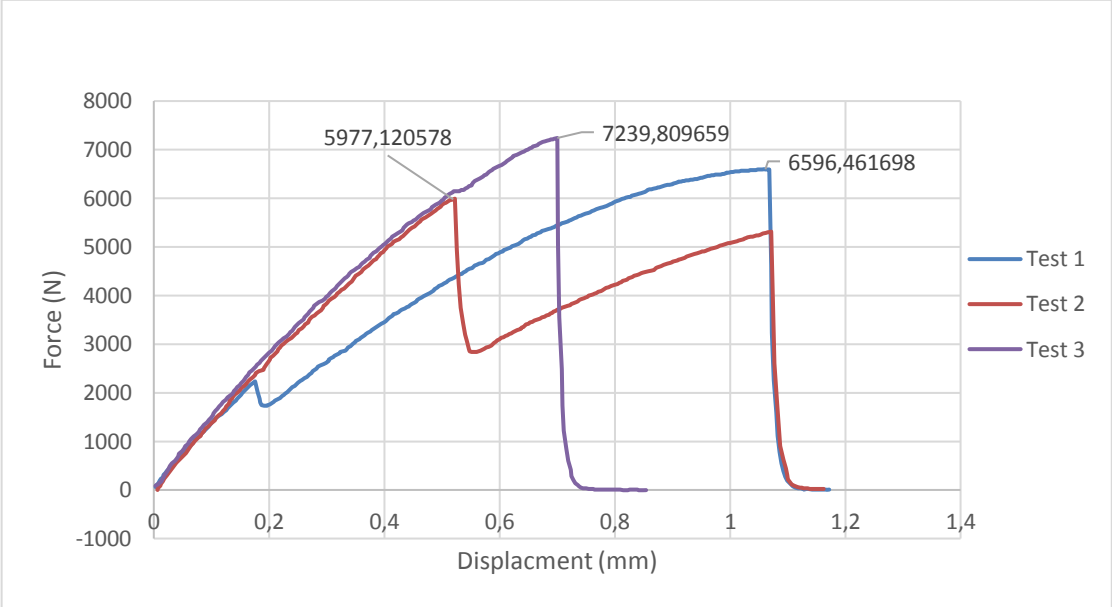

Figure 103: Load-Displacement Plot (AA5754-H111/PEEK) Transverse Direction

In the load-displacement curve (Figure 103) test 1 and test 2 has two peaks. The joint initially start to deform elastically with an almost linear increase in load, after a particular load the curve linearity deviates and a small drop in load for test 1 and a significant drop in load for test 2 as shown in the curve. However, the load starts to increase again almost linearly until it reaches the second peak where it fractures instantly. There is no any distinctive yielding and plastic deformation region. Although for test 3 the load increases linearly and reach maximum and fractures instantly. A maximum failure load of 7239N was for test 3.

The failure mode for the entire test specimen was similar (Figure 104). The failure was a material failure near the weld area. The failure initiated with the crack in the PEEK material near weld area and fracture occurred in the same plane almost straight. The failure of the PEEK at adjacent weld area is due to the increased brittleness of the molten polymer deposited around the weld area. The crack initiation is from the degraded polymer deposition due to high temperature during the joining process. Although the material failure was around the weld area, the joint was still intact and in place after the failure. The load measured were very concentrated on the load-bearing capacity of the polymeric plate since the failure was

on PEEK material. Due to this failure mode, the joint strength was not explored thoroughly and can be far stronger.

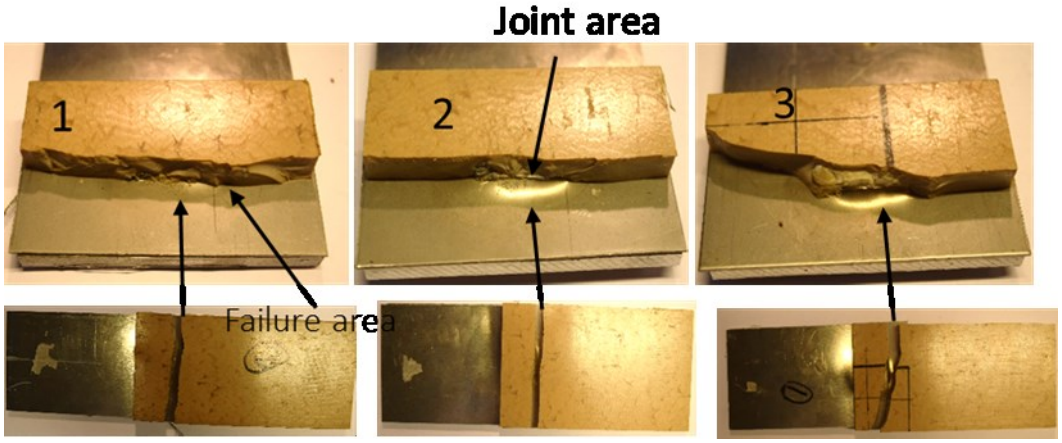

Figure 104:Specimen After Test

- **Longitudinal Direction Weld**

The (Figure 105) shows the force-displacement plot for the tensile shear test carried out on the THE-FSSpW joint between aluminium AA5754-H111 and PEEK. All the test specimen are prepared using the same set of optimal parameters and conditions

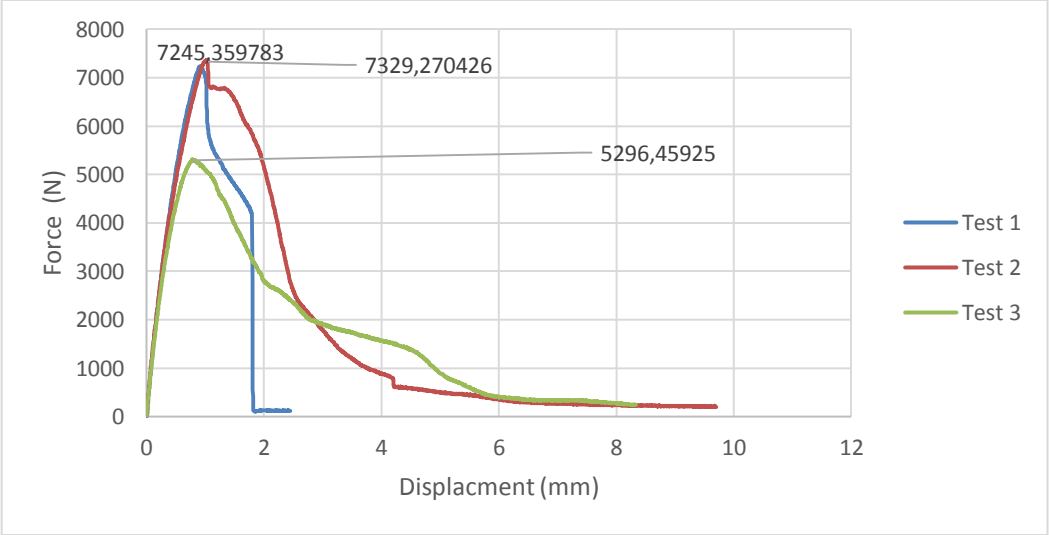

Figure 105: Load-Displacement Plot (AA5754-H111/PEEK) Longitudinal Direction

In the load-displacement curve (Figure 105), the joint initially start to deform elastically with an almost linear increase in load, after a particular load the curve linearity deviates and yielding starts, the plastic deformation starts with sharp decrease in the load and continues until the joint fails. A maximum failure load obtained was of 7329N for test 2.

There was two kind of failure mode observed during the test (Figure 106). For test specimen 1 it was a material failure near the weld area. The failure initiated with the crack in the PEEK material near weld area and fracture occurred in the same plane at an angle. The test 2 and 3

failed differently. When the maximum load for those test was obtained, the load started decreasing fast, with the tearing sound of the polymer in the weld area and failure occurred when the deposited aluminium geometry was detached from the polymer surface.

Figure 106: Specimen After Test

9.3.2 Cross-Tension Test of AA5754-H111/ PEEK Joint

- **Transverse Direction Weld**

The (Figure 107) shows the force-displacement plot for the cross-tension test carried out on the THE-FSSpW joint between aluminium AA5754-H111 and PEEK. All the test specimen are prepared using the same set of optimal parameters and conditions.

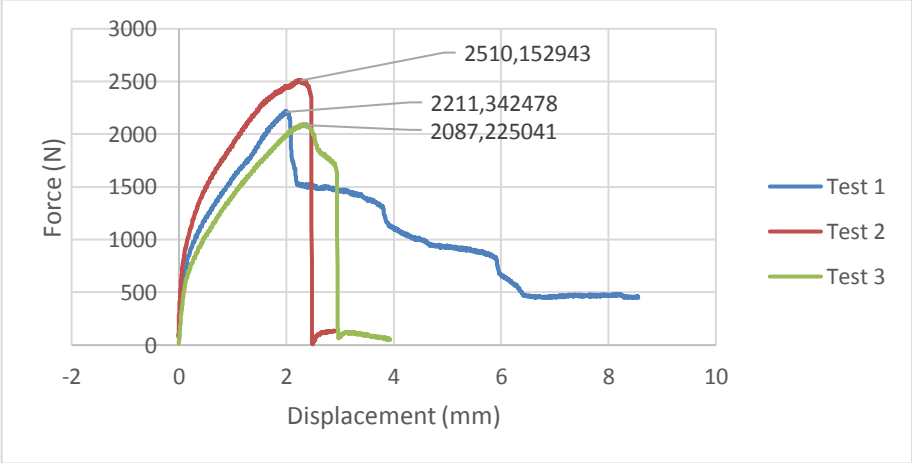

Figure 107: Load-Displacement Plot (AA5754 and PEEK)Transverse Direction

In the load-displacement curve (Figure 107), the joint initially start to deform elastically with an almost linear increase in load, after a particular load the curve linearity deviates and yielding starts, the plastic deformation starts with sharp decrease in the load and continues until the joint fails. A maximum failure load obtained was of 2510N for test 2.

The failure mode for the entire specimen was similar (Figure 108), when the maximum load for the test was obtained, the load started decreasing fast, with the tearing sound of the polymer in the weld area and failure occurred when the deposited aluminium geometry was detached from the polymer surface. The reason for failure is similar to that explained for the tensile shear test.

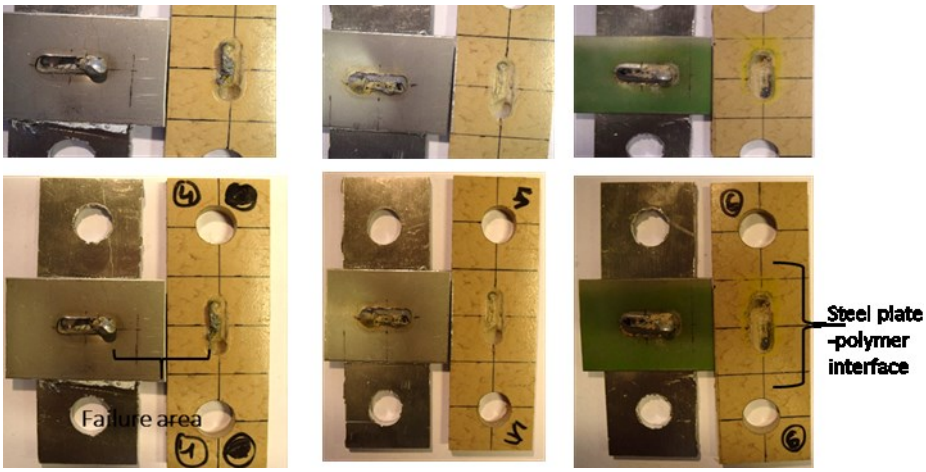

Figure 108: Specimen After Test

- **Longitudinal Direction Weld**

The (Figure 109) shows the force-displacement plot for the cross-tension test carried out on the THE-FSSpW joint between aluminium AA5754-H111 and PEEK. All the test specimen are prepared using the same set of optimal parameters and conditions.

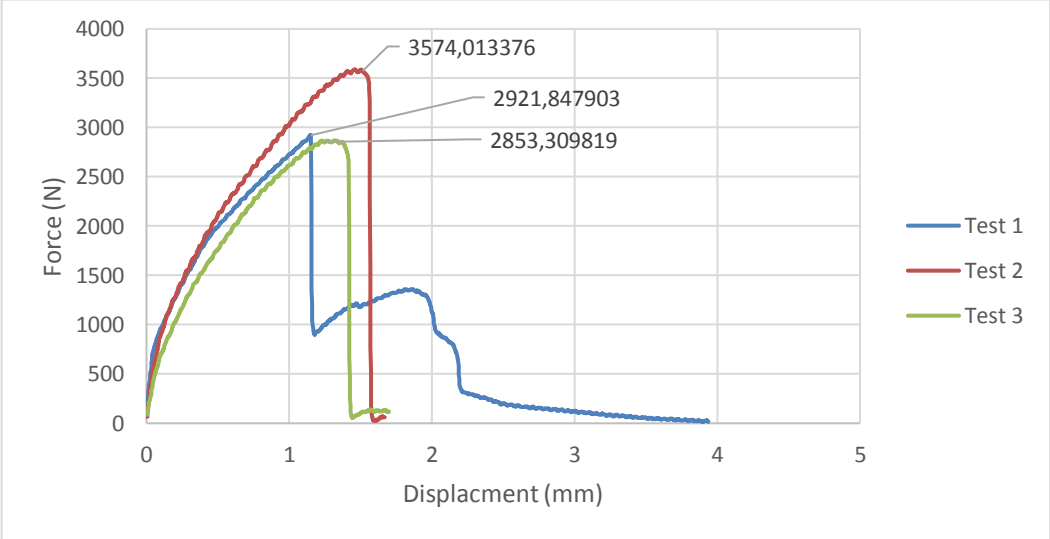

Figure 109: Load-Displacement Plot (AA5754 and PEEK) Longitudinal Direction

In the load-displacement curve (Figure 109), the joint initially start to deform elastically with an almost linear increase in load, after a particular load the curve linearity deviates and yielding starts, the plastic deformation starts with sharp decrease in the load and continues until the joint fails. A maximum failure load obtained was of 3574N for test 2.

There was two kind of failure mode observed during the test (Figure 110). For test specimen 1 it was a material failure near the weld area. The more extended plastic region for test 1 is due to the adhesive bond from the molten polymer in stainless steel-polymer. Such that after the maximum load reached the material cracked and failed, but the existing adhesive bond was still holding the joint. The test 2 and 3 failed differently. When the maximum load for

those test was obtained, the load started decreasing fast, with the tearing sound of the polymer in the weld area and failure occurred when the deposited aluminium geometry was detached from the polymer. The reason for failure is similar to that explained for the tensile shear test.

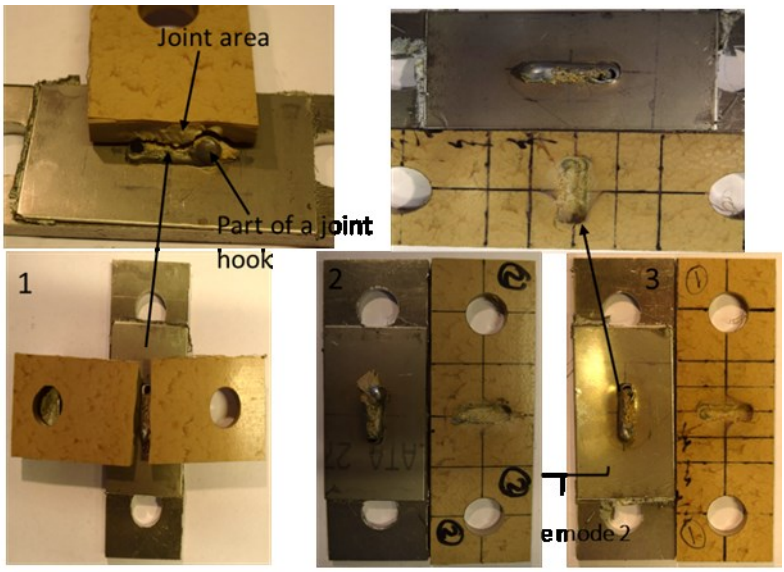

Figure 110: Specimen After Test

9.3.3 Analysis of Results for THE-FSSpW

The material combination AA5754-H111/PEEK were successfully joined by the THE-FSSpW process. The joint mechanical strength was improved, i.e., tensile shear load for the same material combination was increased by 658% compared to the joint produced by the THE-FSpW process and similarly cross tension load was increased by 669%.The summary of the mechanical test result of the joint produced by the THE-FSSpW process is listed in (Table 21).

Table 21: Failure Load Range for THE-FSSpW Joint.

Material Combination	Failure Load (lowest) (N)	Failure Load (Highest) (N)
	Tensile-Shear Test	
	Transverse Weld	
AA5754-H111/PEEK	5977.12	7239.80
	Longitudinal Weld	
AA5754-H111/PEEK	5296.45	7329.27
	Cross-Tension Test	
	Transverse Weld	
AA5754-H111/PEEK	2087.15	2510.15
	Longitudinal Weld	
AA5754-H111/PEEK	2853.30	3574.01

There was two kind of failure mode observed during both the test. Failure mode one was a material failure in the polymeric material near the weld area. The failure initiated with the crack in the PEEK material near weld area and failure mode two was by the tearing of the polymer surface in the weld area, and failure occurred when the deposited aluminium geometry was detached from the polymer.

From the above test carried out, and the analysis of joint and its various mode of a failure condition, following conclusion are made, during the test, both the failure mode of the joint was related to the polymer material strength (base material and processed material). In failure mode one the polymer material fractured at the weld area and in the second mode of failure the tearing of polymer surface was observed. The reason for the fracture at the weld area is due to the increased brittleness of the polymer surface at the processed area. This explains the instant fracture which is brittle in nature for failure mode 1. In the second mode of failure, the tearing of polymer surface is observed which is due to the stress concentration area created by the sharp edges of the joint hook. In both, the test the longitudinal direction weld yielded higher failure load compared to the transverse direction weld. This confirms the influence of the geometry of the samples to be joined on the weld strength.

10 Summary

10.1 Discussion and Conclusion

The first objective of the work was to develop, demonstrate and characterize the two new processes for joining aluminium alloy to polymer. The results and analysis of the work carried out yield the conclusions compiled in this chapter.

Feasibility test of the THE-FSpW concept for joining aluminium alloy to polymer was carried out initially on 5000 series aluminium alloy and polycarbonate. The initial test findings led us to understand the various peculiarities of the process with the indication that it could be developed into a new joining process for aluminium alloy to polymer. The findings helped to establish the guidelines and requirement for new tool design, clamping system, and material selection. These initial tests for joining the aluminium alloy to polycarbonate led us to change the polymeric material into one with higher melting temperature (such as PEEK and PA6). Further developments of the joining process was done on joining aluminium alloy to PEEK. The findings from feasibility test also helped to establish the set of performance assessment parameters, process parameters, and key monitoring issues (e.g., polymer degradation).

Design and development of new tool especially the shoulder and probe were done to eliminate the problem encountered while using the initial tool. A new improved tool body, shoulder and 8 different probe designs were developed and manufactured. Several probe geometry were tested, and selection of the best probe for THE-FSpW process was made. A new design of probe termed as 'Hybrid probe' which is a combination of the conical and cylindrical probe was selected due to its positive effect on deposition of visco-plasticized aluminium into the polymer and also in the joint hook geometry. All the test for the THE-FSpW process utilizes hybrid probe. For the THE-FSSpW process, the new conical probe was tested and used further because of the acceptable result obtained from the use of it, regarding its effect on visco-plasticized aluminium deposition into the polymer and joint hook geometry.

New clamping system was developed in order eliminate the problem of the initial clamping system. The process requires positioning of the three layer of materials (aluminium/stainless steel plate/polymer) in proper alignment, such that the plunging point for the tool is accurately at the center of the hole made in the stainless steel plate. The use of offset travel of 0.50 mm to 1 mm for the THE-FSpW process for maintaining joint hook thickness is one more reason why the accuracy for positioning the plunging point is important. Similarly, the improved cooling system to prevent excessive thermal degradation of the polymer surface was required. The new system consists of the table vice along with a cooling bed for the polymer and utilizes the FSW machine to position the plunging point. The polymer and stainless steel plate were initially clamped using a table vice; then the FSW machine with drilling tool was used to drill a through hole in the stainless steel plate and the blind hole of 3mm deep in the polymer. The drill position is saved in the FSW machine and later used for THE-FSpW process after adding the aluminium plate and the THE-FSpW tool. This helped to eliminate the problem of inconsistent joint hook thickness and enabled to make controllable and repeatable joints.

With the growing maturity of using THE-FSpW process, optimization of process parameters for the selected base materials was done. And a set of optimal process parameters were established for the selected base materials. AA5754-H111, AA2024-T351, PEEK and polyamide 6 were selected as the base materials to be joined using the THE-FSpW process. The selected combination of base material (AA5754-H111/PEEK, AA5754-H1116/ polyamide 6, AA2024-T351/PEEK AA2024-T351/ polyamide 6) were joined successfully.

The specimens produced from the THE-FSpW process were subjected to the mechanical test, i.e., tensile shear test and cross-tension test. The maximum failure loads obtained for various material combination subjected to tensile shear and cross tension test are tabulated below:

Material Combination	Failure Load (Highest) (N)
Tensile-Shear Test	
AA2024-T351/PA6	2313
AA2024-T351/PEEK	1592
AA5754-H111/PA6	1664
AA5754-H111/PEEK	2134
Cross-Tension Test	
AA5754-H111/PA6	337
AA5754-H111/PEEK	1189

Two joint failure mechanisms were observed in both the test. Failure mode one was by the tearing of joint hook at the common junction between stainless steel and polymer. The fracture initiated from the open section of the circumference of the round joint hook area formed by the deposition of visco-plasticized aluminium at the interface zone and propagated towards the other end until the joint failed. The second type of failure mode was a combination of the failure mode 1 but without complete hook fracture, such that the ejection of the joint hook from the polymer surface before complete fracture occurred at the stainless steel/polymer common junction. The primary reasons for the joint failure were the insufficient joint hook geometry regarding thickness and insufficient volume of aluminium deposition in the polymer surface. For eliminating this problem, a new improved process termed as THE-FSSpW was developed.

The problems encountered in the THE-FSpW process were eliminated by the development of the THE-FSSpW process. This process involves a slot of 8mm diameter and 26 mm length in the stainless steel plate differently from the 7 mm hole in the THE-FSpW process. The use of slot increased the material deposition and reinforced the joint hook geometry. The testing of the THE-FSSpW process was done joining AA5754-H111/PEEK material combination. This material combination was successfully joined, and a set of optimal process parameters was established.

Due to the unsymmetrical shape of the joint in relation to the test specimens, two direction were tested for mechanical resistance characterization: transverse weld and longitudinal weld. The mechanical strength of the THE-FSSpW produced joints was improved. Tensile shear load for the same material combination was increased by 658% compared to the joint produced by the THE-FSpW process and similarly cross tension load was increased by 669%. The results for maximum failure load obtained from the mechanical tests are listed in the table below:

Material combination	Failure Load (Highest) (N)
Tensile Shear Test	
Transverse weld	
AA5754-H111/PEEK	7239.80
Longitudinal Weld	
AA5754-H111/PEEK	7329.27
Cross-Tension Test	
Transverse Weld	
AA5754-H111/PEEK	2510.15
Longitudinal Weld	
AA5754-H111/PEEK	3574.01

There was two kind of failure mode observed during the test. Failure mode one was a material failure near the weld area. The failure initiated with the crack in the PEEK material near weld area. The failure mode two was by the tearing of the polymer surface in the weld area, and failure occurred when the deposited aluminium geometry was detached from the polymer. The joint hook geometry over the weld length was consistent only for over 35% of the weld length, and the joint hook geometry starts declining over the remaining 65 % of weld length with no joint hook at the tool plunging out position. By further improving the consistency of the joint hook geometry over the weld length, the load capacity can be further improved.

Microstructural analysis was carried out to understand and observe the joint hook geometry, bonding mechanism, to analyze the polymer surface degradation at stirred zone and heat affected zone and to parameterize the joint hook geometry. For both the process, in aluminium it revealed the finer grains in the processed zone due to the dynamic recrystallization and the distinctive TMAZ and HAZ. It also revealed the significant mixture of aluminium particles suspended in the polymer at the stirred zone. There was polymer surface degradation at aluminium alloy/stainless steel/polymer interfaces and the presence of small and large voids in the stirred zone where polymer and aluminium overlap. The joint hook from both the process was parametrized, and the overall joint hook thickness of 1,345 mm for the THE-FSpW process and 1.892 mm for the THE-FSSpW process was obtained.

10.2 **Future Work**

The present work is an essential foundation of the THE-FSpW and the THE-FSSpW process. There is a several further investigations that is recommended and required to establish it as the best solution for joining aluminium alloy to the polymer. The next step for further development of the current work can be approached as described in the various section below:

Further optimization of process parameters:

- Optimization of the parameter further to get the best set of process parameters which can enhance the joint strength.
- Development of computer-based analytical modeling system to determine the breake-ven point for the minimum temperature that can be used to create a visco plasticized metal flow in accordance to the highest temperature up to which the polymer can retain its properties without surface degradation.
- Modeling of the process to assess the internal flow of the materials, and temperature field during the joint formation.

Further testing of joint produced:

- Further detail examination and testing of the joint produced from both the process. To perform a various non-destructive test to understand the conditions of processed material and bonding mechanisms in detail
- Further study on the effect of environmental conditions on the durability of the joint.
- Further, through testing of processed polymer zone to understand the behavior of material at heat affected zone compare to the base material.
- Study of the properties of aluminium particles and polymer mixture at the stir zone.

Steel plate geometry:

- To further improve the hole and slot geometry that is acting as a point of stress concentration.

Probe and shoulder geometry improvement for the THE-FSSpW process:

- Further improvement on the probe design to improve the joint hook geometry and its uniformity throughout the weld length.
- Further improvement on the shoulder geometry that can reduce flash and close the aluminium surface and prevent the outward flow of the polymer.
- Optimization of process parameter concerning new probe and shoulder design.

Testing of other engineering polymers and lightweight metals:

- Establish and improve the process parameters for other engineering polymers other than that were used in this work.

11 References

[1] B. D. T. M.V. Gandhi, Smart Materials and Structures. Springer Science & Business Media, 31 May 1992.

[2] J. C. Williams and E. A. Starke, "Progress in structural materials for aerospace systems," Acta Materialia, vol. 51, (19), pp. 5775-5799, 2003.

[3] T. Dursun and C. Soutis, "Recent developments in advanced aircraft aluminium alloys," Mater Des, vol. 56, pp. 862-871, 2014.

[4] S. Amancio-Filho, "Friction Riveting: development and analysis of a new joining technique for polymer-metal multi-materials structures," Technical University Hamburg-Harburg/GKSS Research Center, Germany, 2007.

[5] G. Meschut, V. Janzen and T. Olfermann, "Innovative and highly productive joining technologies for multi-material lightweight car body structures," Journal of Materials Engineering and Performance, vol. 23, (5), pp. 1515-1523, 2014.

[6] C. Rodrigues, L. Blaga, J. Dos Santos, L. Canto, E. Hage and S. Amancio-Filho, "FricRiveting of aluminium AA2024-T351 and polycarbonate: Temperature evolution, microstructure, and mechanical performance," J. Mater. Process. Technol., vol. 214, (10), pp. 2029-2039, 2014.

[7] S. T. Amancio-Filhoa and J. F. dos Santosb, "PRELIMINARY ANALYTICAL MODELING OF HEAT INPUT IN FRICTION RIVETING,."

[8] N. Z. Borba, C. R. Afonso, L. Blaga, J. F. dos Santos, L. B. Canto and S. T. Amancio-Filho, "On the Process-Related Rivet Microstructural Evolution, Material Flow and Mechanical Properties of Ti-6Al-4V/GFRP Friction-Riveted Joints," Materials, vol. 10, (2), pp. 184, 2017.

[9] P. Kah, R. Suoranta, J. Martikainen and C. Magnus, "TECHNIQUES FOR JOINING DISSIMILAR MATERIALS: METALS AND POLYMERS." Reviews on Advanced Materials Science, vol. 36, (2), 2014.

[10] S. Amancio-Filho and J. Dos Santos, "Joining of polymers and polymer–metal hybrid structures: recent developments and trends," Polymer Engineering & Science, vol. 49, (8), pp. 1461-1476, 2009.

[11] J. A. Speck, Mechanical Fastening, Joining, and Assembly. CRC Press, 2015.

[12] Mechanica Technical Solutions.

[13] C. Niu, Airframe Structural Design: Practical Design Information and Data on Aircraft Structures. Conmilit Press, 1988.

[14] R. LEAUERSUCH, "'Collar joining'method makes plastic-metal hybrids," Plastics Technology, vol. 48, (10), pp. 49-51, 2002.

[15] W. Brockmann, Paul Ludwig Gei and J. Klingen, Adhesive Bonding: Materials, Applications and Technology. Wiley Online Library, 2008.

[16] A. Baldan, "Adhesively-bonded joints in metallic alloys, polymers and composite materials: mechanical and environmental durability performance," J. Mater. Sci., vol. 39, (15), pp. 4729-4797, 2004.

[17] A. Higgins, "Adhesive bonding of aircraft structures," Int J Adhes Adhes, vol. 20, (5), pp. 367-376, 2000.

[18] G. Scarselli, C. Corcione, F. Nicassio and A. Maffezzoli, "Adhesive joints with improved mechanical properties for aerospace applications," Int J Adhes Adhes, vol. 75, pp. 174-180, 2017.

[19] A. Baker, "Bonded composite repair of fatigue-cracked primary aircraft structure," Composite Structures, vol. 47, (1), pp. 431-443, 1999.

[20] W. Brockmann, P. L. Geiß, J. Klingen and K. B. Schröder, Adhesive Bonding: Adhesives, Applications and Processes. John Wiley & Sons, 2008.

[21] T. Barnes and I. Pashby, "Joining techniques for aluminium spaceframes used in automobiles: Part I—solid and liquid phase welding," J. Mater. Process. Technol., vol. 99, (1), pp. 62-71, 2000.

[22] M. Grujicic, V. Sellappan, M. Omar, N. Seyr, A. Obieglo, M. Erdmann and J. Holzleitner, "An overview of the polymer-to-metal direct-adhesion hybrid technologies for load-bearing automotive components," J. Mater. Process. Technol., vol. 197, (1), pp. 363-373, 2008.

[23] Fundamentals of adhesive bonding.

[24] C. V. Katsiropoulos, A. Chamos, K. Tserpes and S. G. Pantelakis, "Fracture toughness and shear behavior of composite bonded joints based on a novel aerospace adhesive," Composites Part B: Engineering, vol. 43, (2), pp. 240-248, 2012.

[25] ADHESIVES. Available: https://nzic.org.nz/ChemProcesses/polymers/10H.pdf.

[26] M. A. Butt, A. Chughtai, J. Ahmad, R. Ahmad, U. Majeed and I. Khan, "Theory of adhesion and its practical implications," Journal of Faculty of Engineering & Technology, vol. 2007, pp. 21-45, 2008.

[27] B. Chang, Y. Shi and S. Dong, "Comparative studies on stresses in weld-bonded, spot-welded and adhesive-bonded joints," J. Mater. Process. Technol., vol. 87, (1), pp. 230-236, 1999.

[28] O. A. Daniel and K. L. DeVries, "Durability of Adhesively Bonded Joints For Aircraft, Daniel O. Adams, K. L. DeVries, Clint Child, Department of Mechanical Engineering, University of Utah, Salt Lake City, UT 84112," .

[29] Adhesive bonding of composites.

[30] S. Amancio-Filho and J. Dos Santos, "Joining of polymers and polymer–metal hybrid structures: recent developments and trends," Polymer Engineering & Science, vol. 49, (8), pp. 1461-1476, 2009.

[31] K. Sato, Y. Kurosaki, T. Saito and I. Satoh, "Laser welding of plastics transparent to near-infrared radiation," in Photon Processing in Microelectronics and Photonics, 2002, pp. 528-537.

[32] T. Kim, J. Yum, S. Hu, J. Spicer and J. Abell, "Process robustness of single lap ultrasonic welding of thin, dissimilar materials," CIRP Annals-Manufacturing Technology, vol. 60, (1), pp. 17-20, 2011.

[33] S. Matsuoka, "Ultrasonic welding of ceramics/metals using inserts," J. Mater. Process. Technol., vol. 75, (1), pp. 259-265, 1998.

[34] S. Matsuoka and H. Imai, "Direct welding of different metals used ultrasonic vibration," J. Mater. Process. Technol., vol. 209, (2), pp. 954-960, 2009.

[35] F. Balle, G. Wagner and D. Eifler, "Ultrasonic metal welding of aluminium sheets to carbon fibre reinforced thermoplastic composites," Advanced Engineering Materials, vol. 11, (1-2), pp. 35-39, 2009.

[36] N. Amanat, N. L. James and D. R. McKenzie, "Welding methods for joining thermoplastic polymers for the hermetic enclosure of medical devices," Med. Eng. Phys., vol. 32, (7), pp. 690-699, 2010.

[37] R. Borrisutthekul, Y. Miyashita and Y. Mutoh, "Dissimilar material laser welding between magnesium alloy AZ31B and aluminium alloy A5052-O," Science and Technology of Advanced Materials, vol. 6, (2), pp. 199-204, 2005.

[38] E. Schubert, M. Klassen, I. Zerner, C. Walz and G. Sepold, "Light-weight structures produced by laser beam joining for future applications in automobile and aerospace industry," J. Mater. Process. Technol., vol. 115, (1), pp. 2-8, 2001.

[39] T. Mai and A. Spowage, "Characterisation of dissimilar joints in laser welding of steel–kovar, copper–steel and copper–aluminium," Materials Science and Engineering: A, vol. 374, (1), pp. 224-233, 2004.

[40] A. Fortunato, G. Cuccolini, A. Ascari, L. Orazi, G. Campana and G. Tani, "Hybrid metal-plastic joining by means of laser," International Journal of Material Forming, vol. 3, (1), pp. 1131-1134, 2010.

[41] J. Holtkamp, A. Roesner and A. Gillner, "Advances in hybrid laser joining," The International Journal of Advanced Manufacturing Technology, vol. 47, (9), pp. 923-930, 2010.

[42] W. Tillmann, A. Elrefaey and L. Wojarski, "Toward process optimization in laser welding of metal to polymer. Prozessoptimierung beim Laserstrahlschweißen von Metall mit Kunststoff," Materialwissenschaft Und Werkstofftechnik, vol. 41, (10), pp. 879-883, 2010.

[43] S. Amancio-Filho, C. Bueno, J. Dos Santos, N. Huber and E. Hage, "On the feasibility of friction spot joining in magnesium/fiber-reinforced polymer composite hybrid structures," Materials Science and Engineering: A, vol. 528, (10), pp. 3841-3848, 2011.

[44] J. Esteves, S. Goushegir, J. Dos Santos, L. Canto, E. Hage and S. Amancio-Filho, "Friction spot joining of aluminium AA6181-T4 and carbon fiber-reinforced poly (phenylene sulfide): effects of process parameters on the microstructure and mechanical strength," Mater Des, vol. 66, pp. 437-445, 2015.

[45] S. Goushegir, J. Dos Santos and S. Amancio-Filho, "Friction spot joining of aluminium AA2024/carbon-fiber reinforced poly (phenylene sulfide) composite single lap joints: microstructure and mechanical performance," Mater Des, vol. 54, pp. 196-206, 2014.

[46] F. Yusof, Y. Miyashita, N. Seo, Y. Mutoh and R. Moshwan, "Utilising friction spot joining for dissimilar joint between aluminium alloy (A5052) and polyethylene terephthalate," Science and Technology of Welding and Joining, vol. 17, (7), pp. 544-549, 2012.

[47] K. Nagatsuka, S. Yoshida, A. Tsuchiya and K. Nakata, "Direct joining of carbon-fiber–reinforced plastic to an aluminium alloy using friction lap joining," Composites Part B: Engineering, vol. 73, pp. 82-88, 2015.

[48] K. Nagatsuka, T. Onoda, T. Okada and K. Nakata, "Direct dissimilar joining of aluminium alloys and polyamide 6 by friction lap joining," Welding International, vol. 31, (1), pp. 9-16, 2017.

[49] F. Liu, J. Liao and K. Nakata, "Joining of metal to plastic using friction lap welding," Materials & Design (1980-2015), vol. 54, pp. 236-244, 2014.

[50] J. Altmeyer, J. dos Santos and S. Amancio-Filho, "Effect of the friction riveting process parameters on the joint formation and performance of Ti alloy/short-fibre reinforced polyether ether ketone joints," Mater Des, vol. 60, pp. 164-176, 2014.

[51] C. Rodrigues, L. Blaga, J. Dos Santos, L. Canto, E. Hage and S. Amancio-Filho, "FricRiveting of aluminium AA2024-T351 and polycarbonate: Temperature evolution, microstructure and mechanical performance," J. Mater. Process. Technol., vol. 214, (10), pp. 2029-2039, 2014.

[52] B. Proenca, L. Blaga, J. Santos, L. B. Canto and S. T. Amancio-Filho, "Force controlled friction riveting of glass fiber reinforced polyamide 6 and aluminium alloy 6056 hybrid joints," in Society of Plastics Engineers. Proceedings of the Technical Conference Exhibition–ANTEC, 2015, pp. 23-25.

[53] I. S. Amancio, "Friction spot joining of lightweight metals and fiber reinforced polymer hybrid structures," Institute of Materials Research, Material Mechanics, Solid State Joining Process and Advanced Polymer-Metal Hybrid Structures Germany, .

[54] D. Radakovic and M. Tumuluru, "An evaluation of the cross-tension test of resistance spot welds in high-strength dual-phase steels," Welding Journal, vol. 91, (1), pp. 8-15, 2012.

[55] R. Joseph, V. Kliman and J. Jelemenska, "Aluminium and aluminium alloys. ASM Specialty Handbook," 1993.

[56] Aluminium AA 5757-H111 data sheet from supplier, https://alumeco.com/sheets/en-aw-5754/platevariant-6-1000x2000h111/p/415/5813.

[57]"CES Edu pack 2017," 2017.

[58] Aluminium AA AA2024-T351 data sheet from supplier, http://www.thyssenkruppaer-ospace.com/materials/aluminium/aluminium-technical-data.html.

[59] AISI 316 stainless steel data sheet from AK Steel.

[60] A. B. Strong, Plastics: Materials and Processing. Prentice Hall, 2006.

[61] R. B. Seymour, Reinforced Plastics: Properties & Applications. Asm Intl, 1991.

[62] L. B. Nohara, M. L. Costa, M. A. Alves, M. F. K. Takahashi, E. L. Nohara and M. C. Rezende, "Processing of high performance composites based on peek by aqueous suspension prepregging," Materials Research, vol. 13, (2), pp. 245-252, 2010.

[63] PEEK datasheet from supplier, http://en.chinapeek.com/Product/Wear-Resistant-Peek-Plate-Peek-Sheet.html.

[64] Polyamide- PA6 datasheet from supplier, https://akro-plastic.com/fileadmin/data-base_akro-plastic/en/TDS-B3_natural_-1024.pdf.

[65] ESAB (2014). LEGIO FSW 5U friction welding machine. Gothenburg, Sweden.

[66] MTS landmark.

[67] "MTS landmark. (2006). MTS 810 material testing system [manual]. eden prairie, MN." .

[68] "Nikon(1997). inverted metallographic microscope epiphot 200.[manual]. melville, NY." .

[69] Resistance welding. Destructive testing of welds. Specimen dimensions and procedure for tensile shear testing resistance spot and embossed projection welds (ISO 14273:2016) ".

[70] Resistance welding. Destructive testing of welds. Specimen dimensions and procedure for cross tension testing of resistance spot and embossed projection welds (ISO 14272:2016)”

[71] Bohler-Uddeholm H13 TOOL STEEL.

12 Appendix

Appendix 1: Tool Design and Drawings for THE-FSpW and THE-FSSpW

1. Tool Assembly.

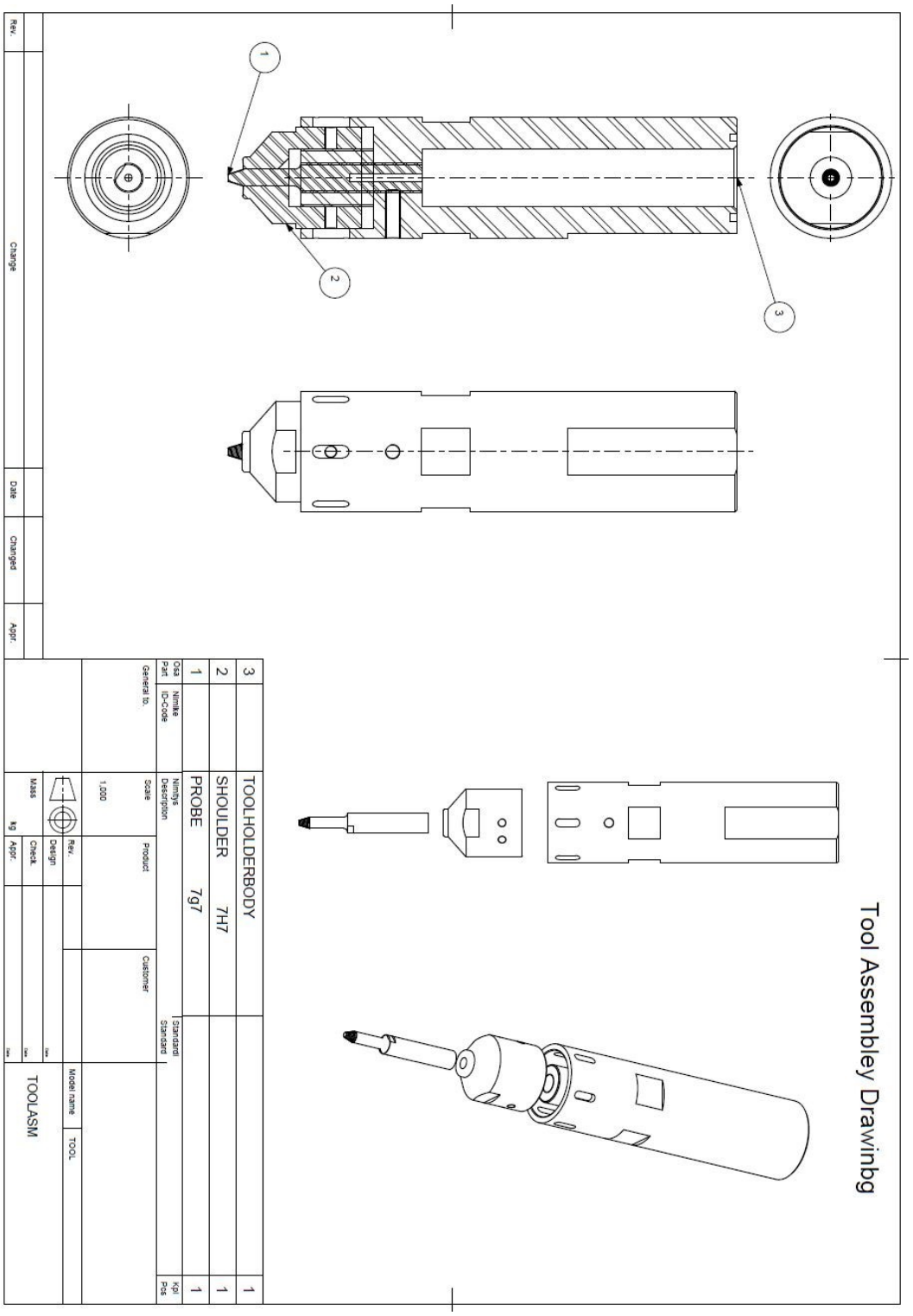

2. Tool Holder

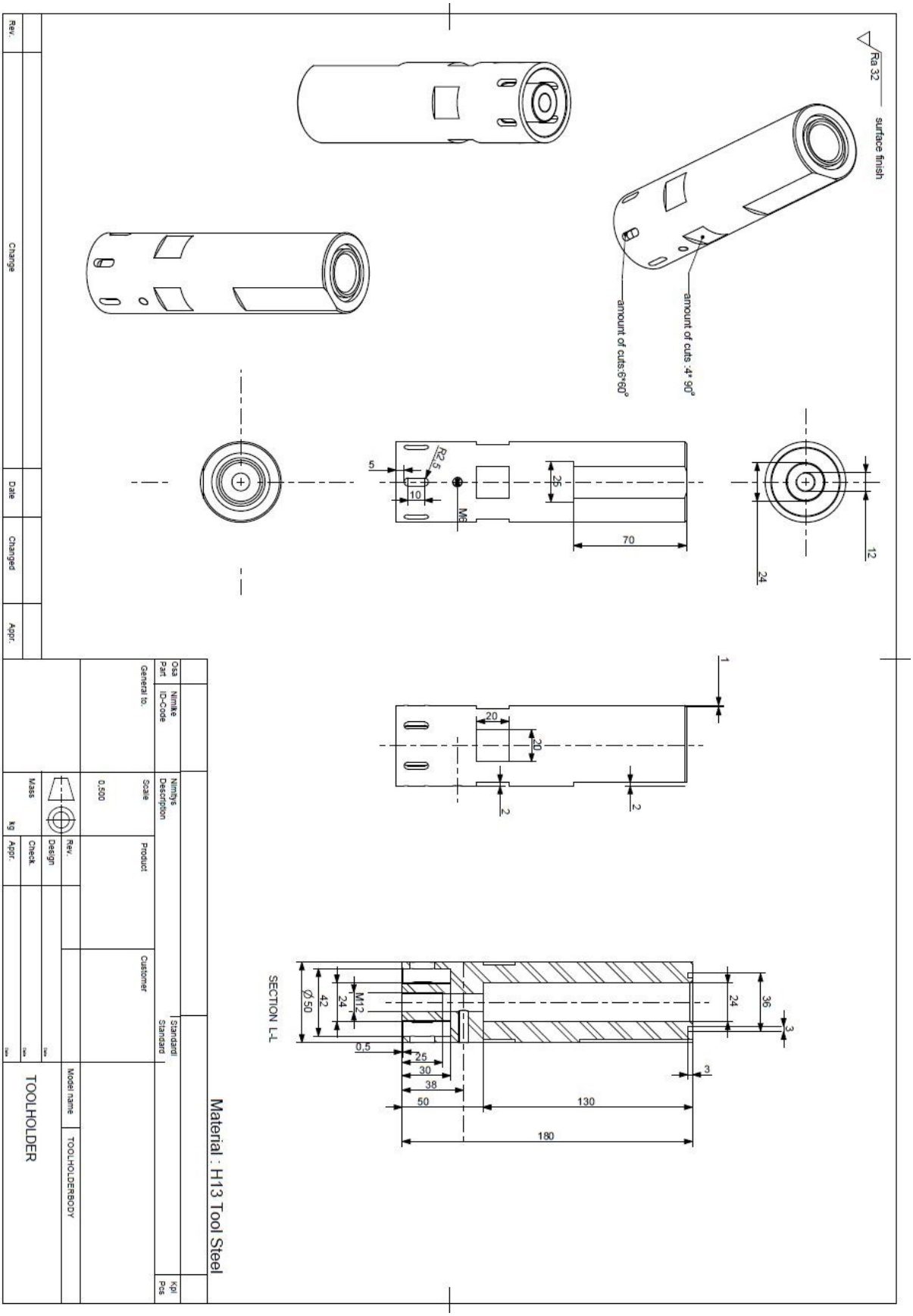
Ra 32
surface finish
amount of cuts:6*60°
amount of cuts :4* 90°
R2,5
5
10
M6
25
70
12
24
1
20
20
2
2
SECTION L-L
Ø50
42
24
M12
24
36
3
0,5
25
30
38
50
130
180
3
Material : H13 Tool Steel
TOOLHOLDER
TOOLHOLDERBODY
Model name
Standard
Standard
Customer
Product
Scale
0,500
Mass
kg
Design
Check
Appr.
Rev.
Osa
Part
Nimike
ID-Code
General to.
Nimitys
Description
Kpl
Pos
Rev.
Change
Date
Changed
Appr.

3. Shoulder

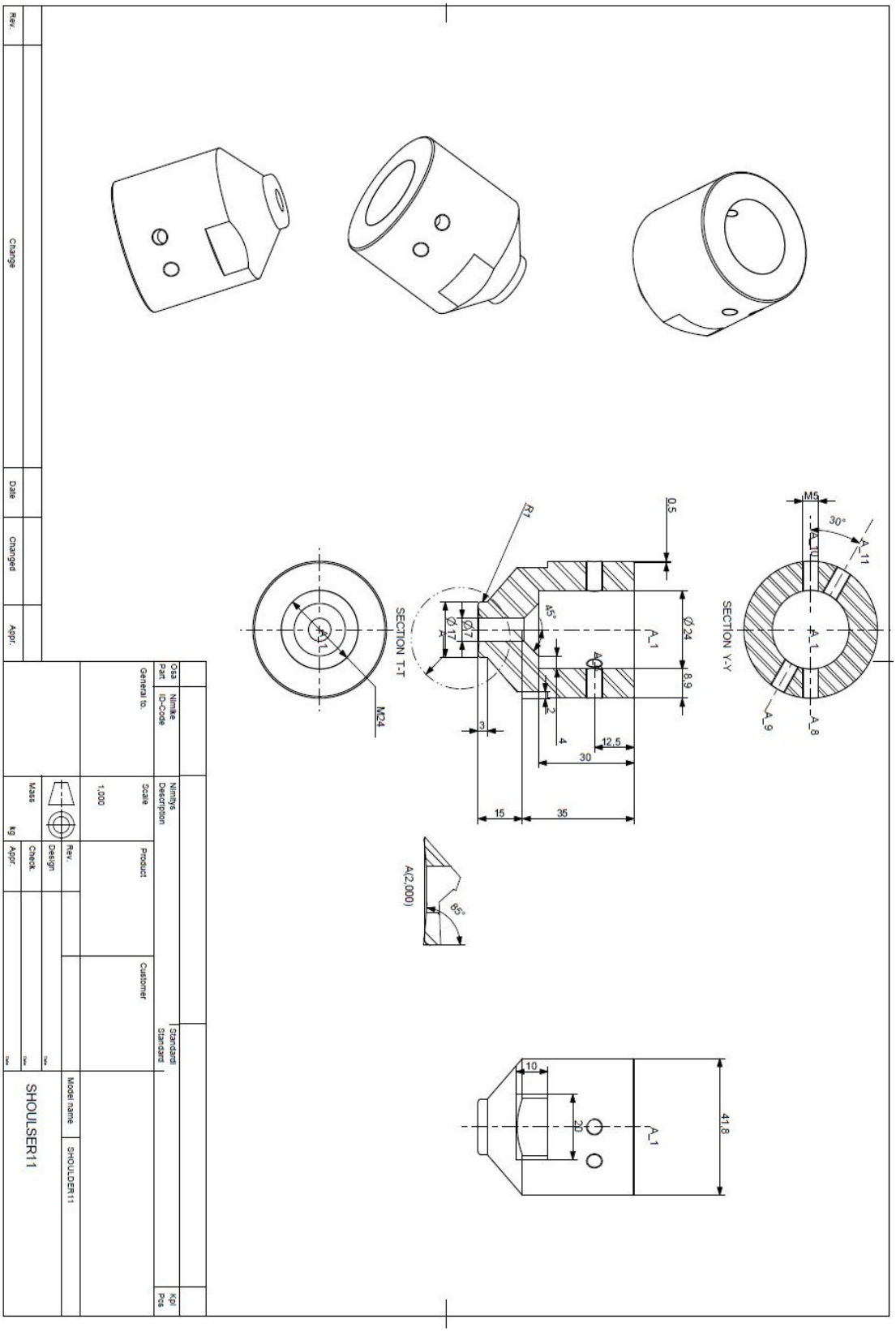
Rev.
Change
Date
Changed
Appr.
SECTION T-T
SECTION Y-Y
M24
M5
R1
0.5
Ø24
8.9
Ø17
Ø7
45°
30°
12,5
30
15
35
A(2.000)
65°
10
20
41.8
A_1
A_8
A_9
A_10
A_11
Osa
Part
Nimike
ID-Code
Nimitys
Description
Standard
Standard
General tol.
Scale
1.000
Product
Customer
Mass
kg
Rev.
Design
Check
Appr.
Model name
SHOULDER11
SHOULSER11
Kpl
Pcs

4. Probes

- Probe1

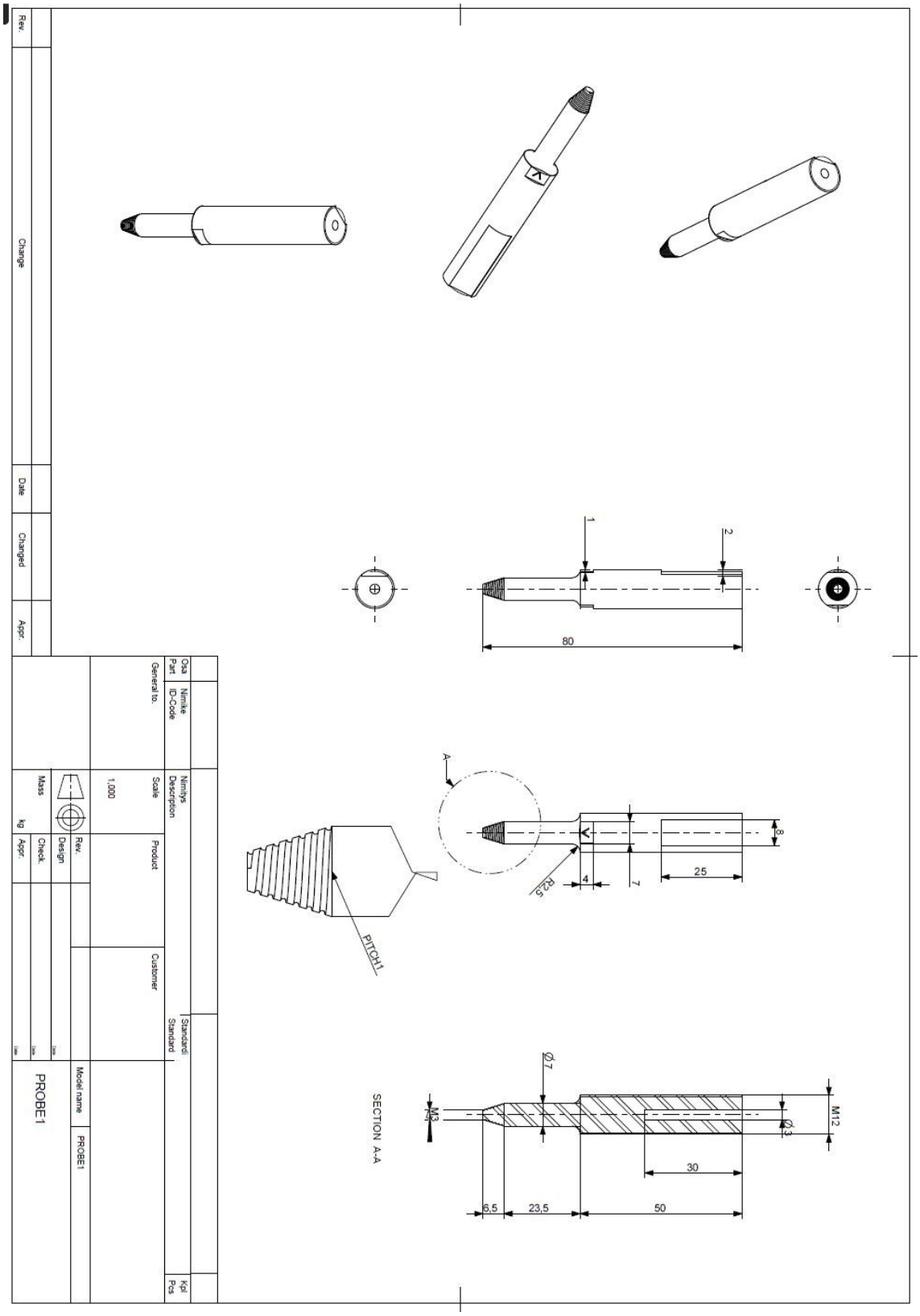

- Probe 2

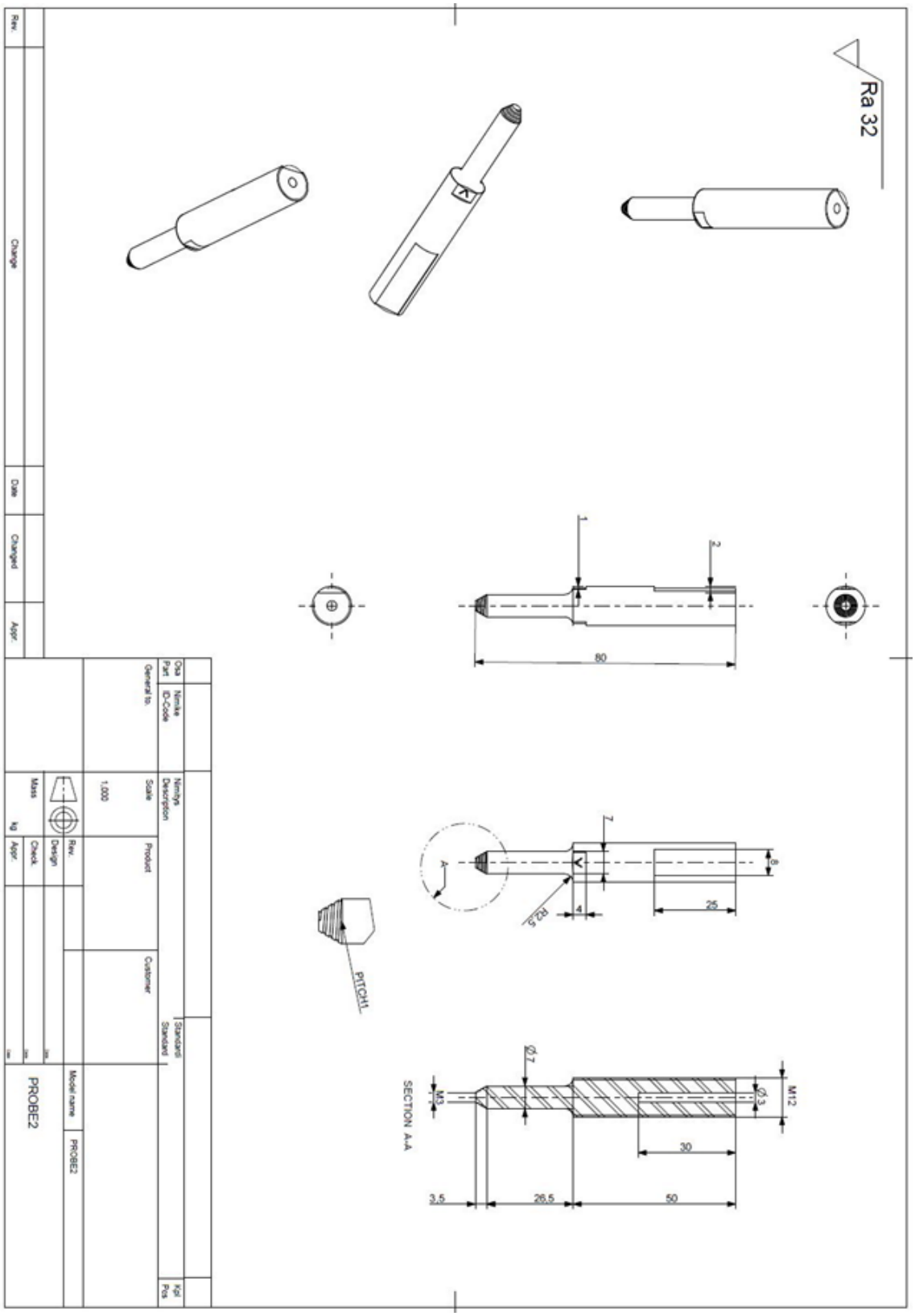
Ra 32
80
25
4
7
8
PITCH1
SECTION A-A
M12
M3
30
3,5
26,5
50
PROBE2
PROBE2

- Probe 3

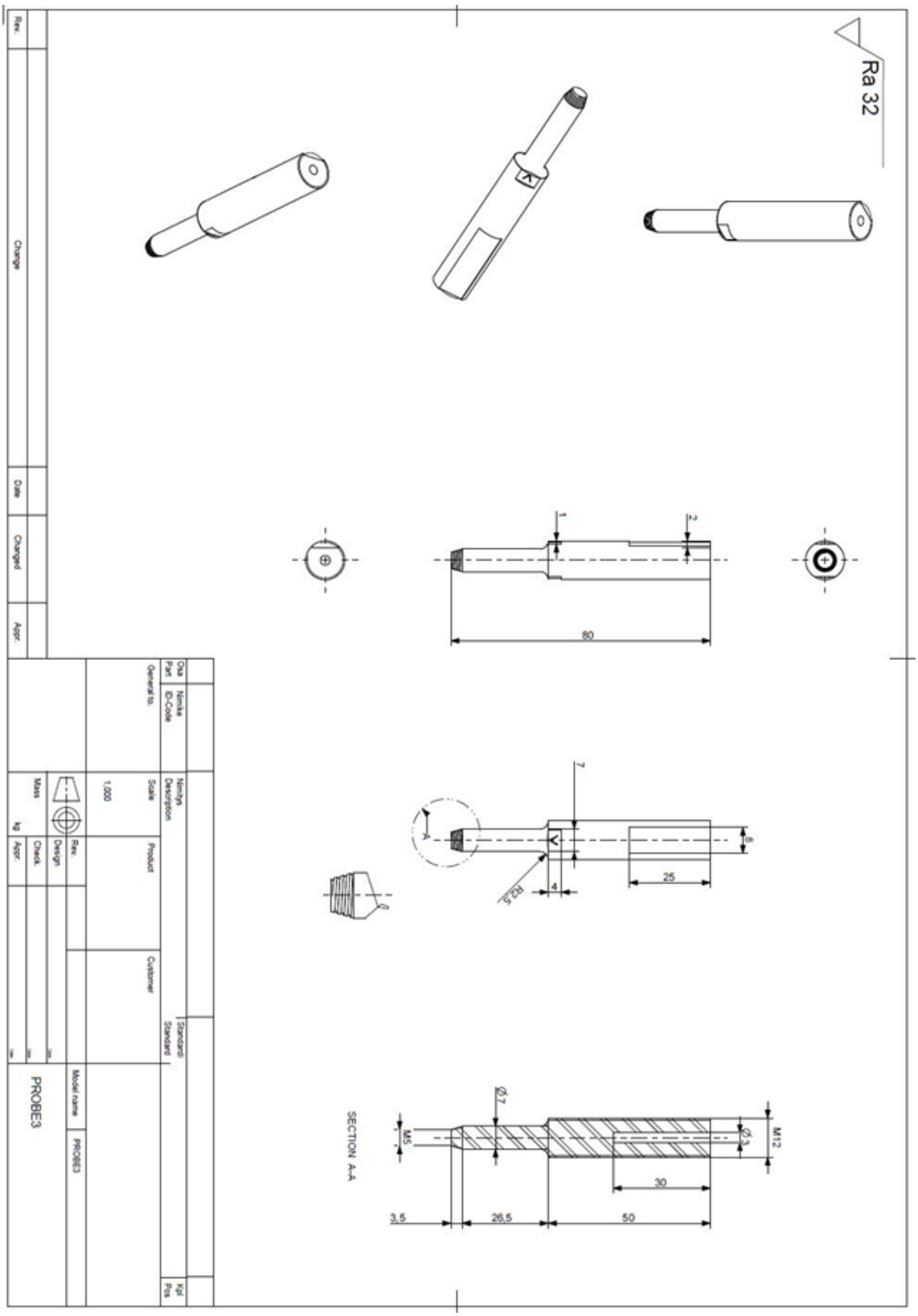

- Probe 4 (Selected for THE-FSSpW Development)

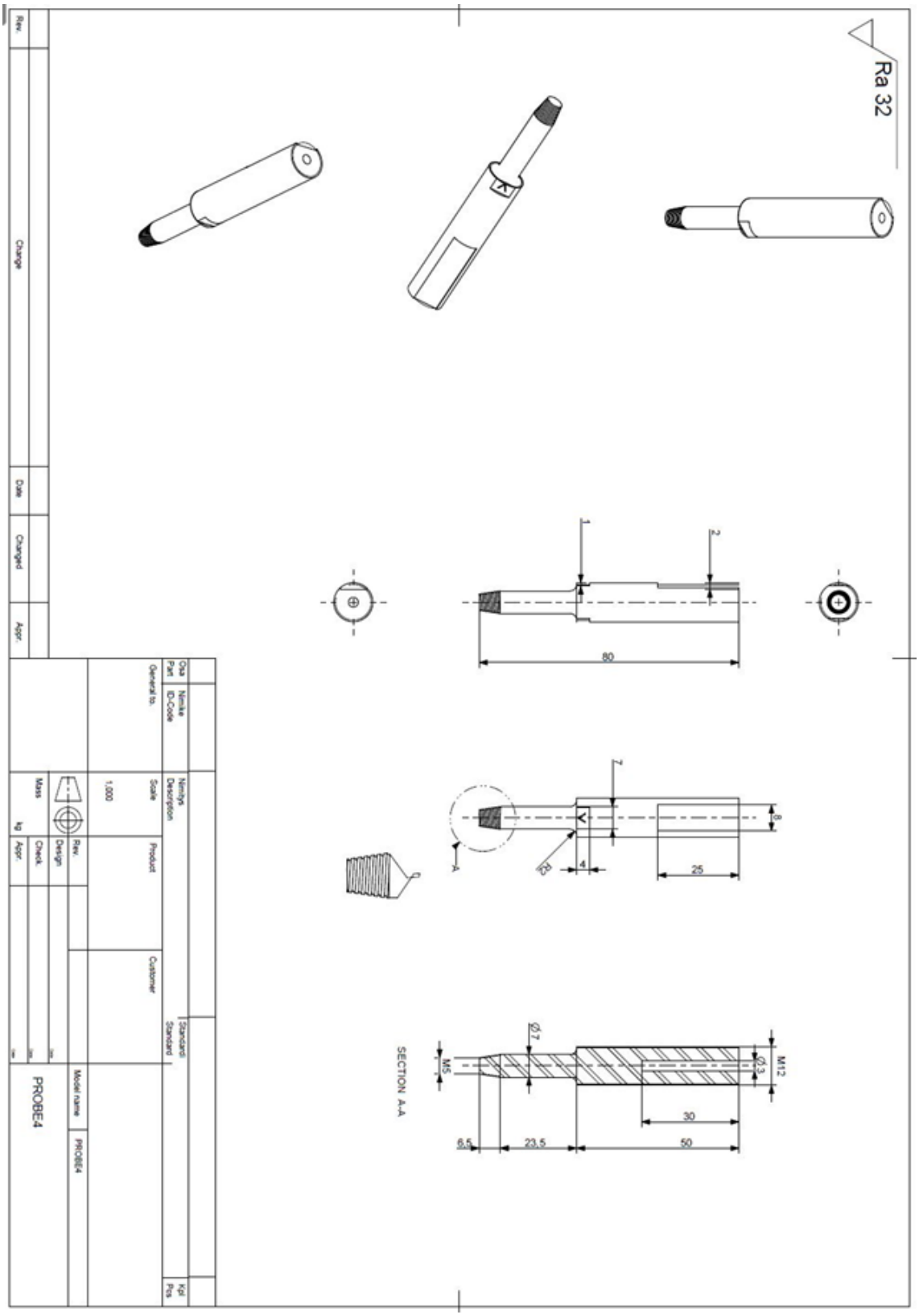

- Probe 5

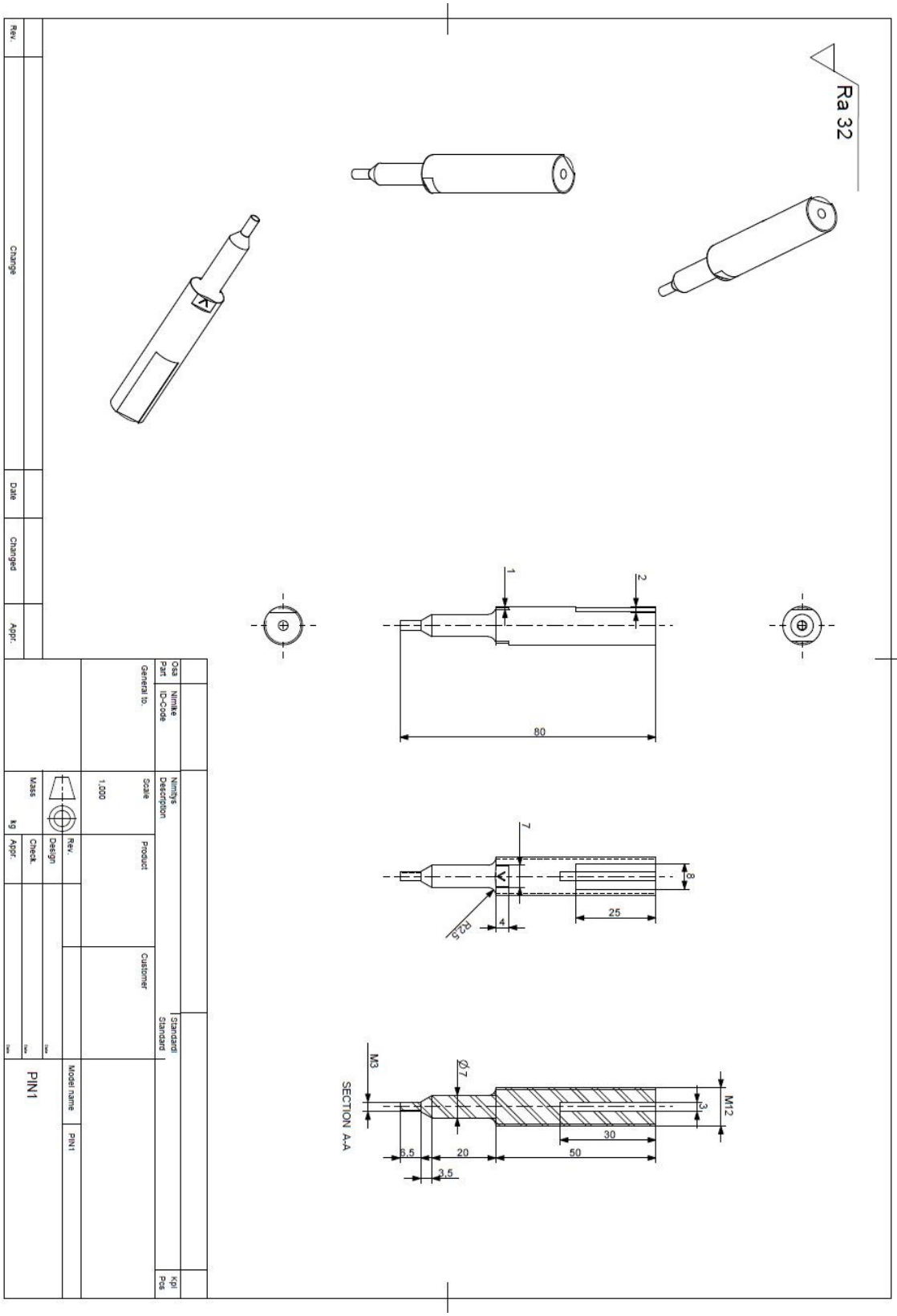

- Probe 6

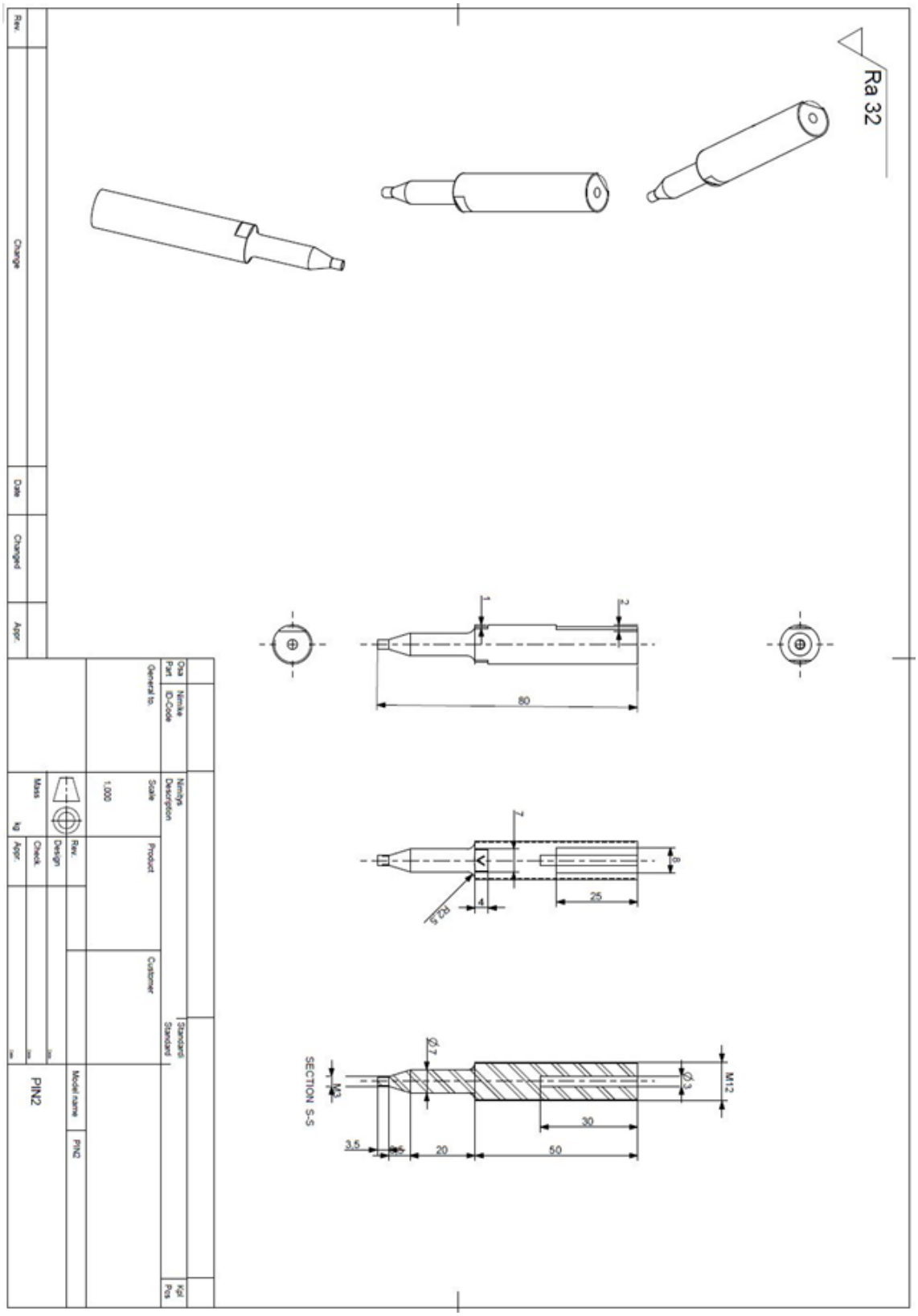

- Probe 7

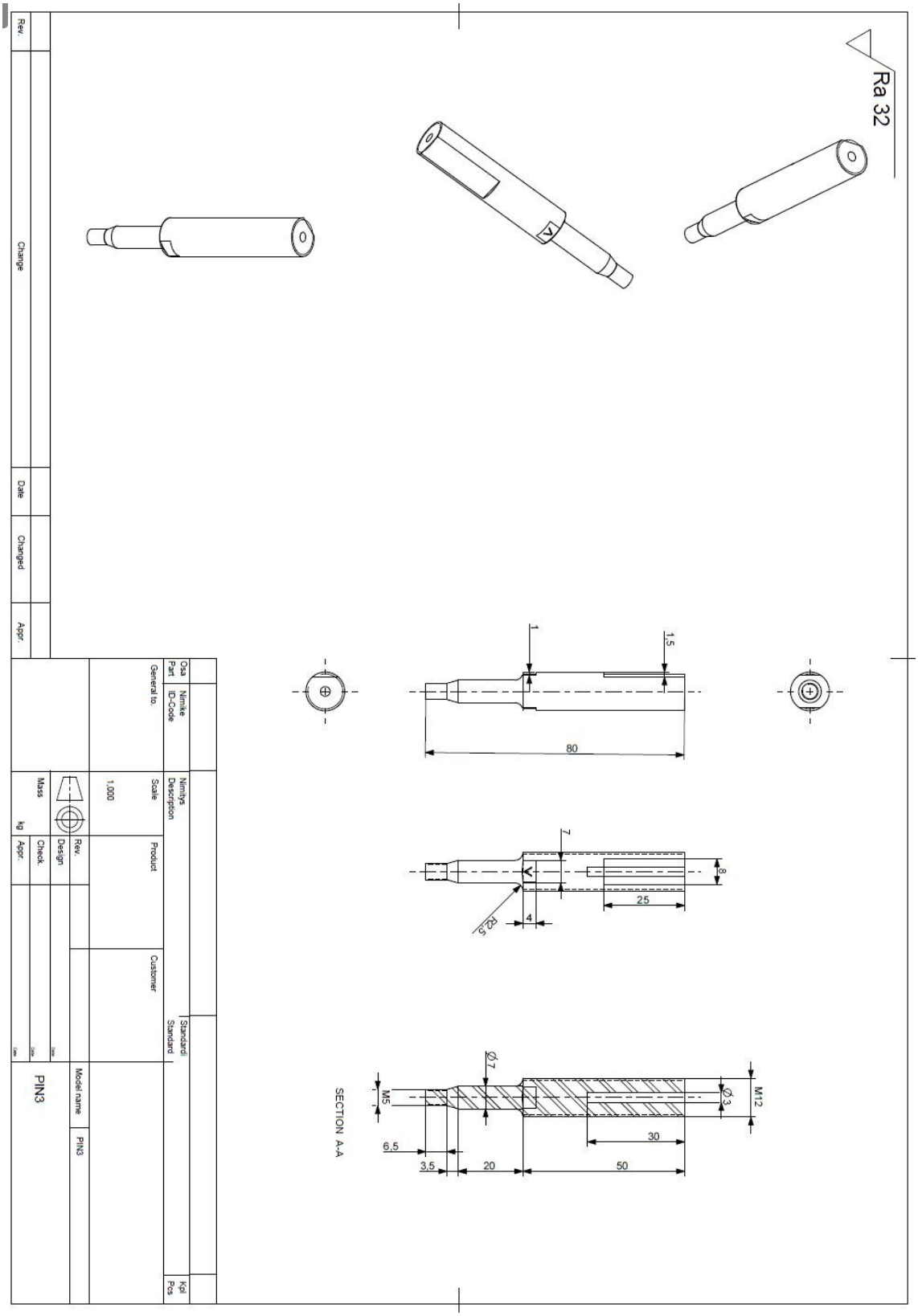

- Probe 8(Selected for THE-FSpW Development)

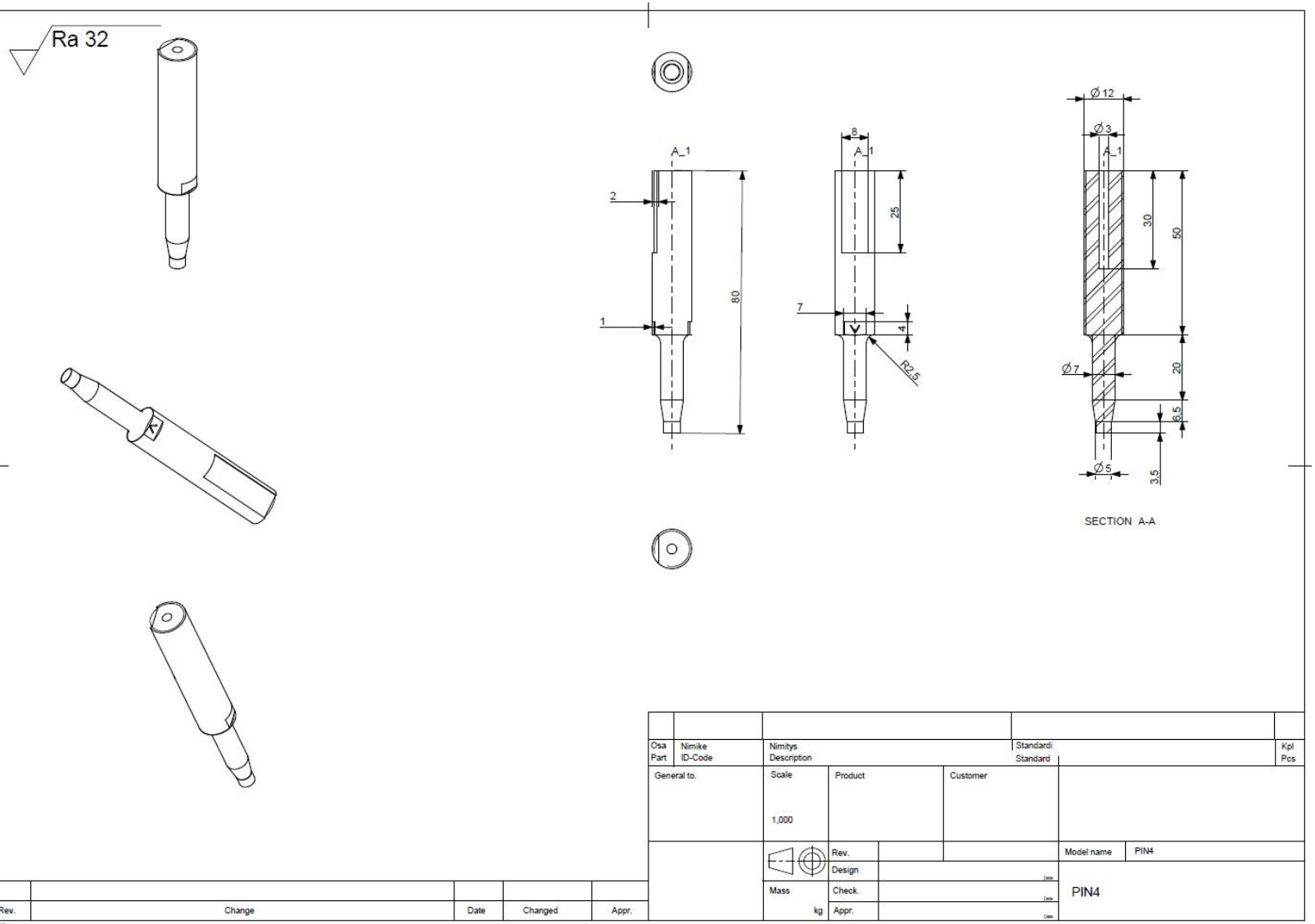

Osa Part	Nimike ID-Code	Nimitys Description	Standardi Standard	Kpl Pcs
General to.	Scale 1,000	Product	Customer	
		Rev.	Model name	PIN4
		Design		
	Mass kg	Check.	PIN4	
		Appr.		

Rev.	Change	Date	Changed	Appr.